

NASA CR 112-778  
Paper

TR- 3720293



# Viking'75 Project

BALLOON LAUNCHED DECELERATOR TEST PROGRAM  
POST- FLIGHT TEST REPORT  
BLDT VEHICLE AV-3

(NASA-CR-112178) BALLOON LAUNCHER  
DECELERATOR TEST PROGRAM: POST-FLIGHT  
TEST REPORT, BLDT VEHICLE AV-3, VIKING  
1975 PROJECT (Martin Marietta Corp.)

CSCI 01B

63/02

Unclass  
66599

N73-20012

NAS1-9000

MARTIN MARIETTA

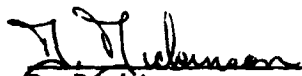
TR-3720293

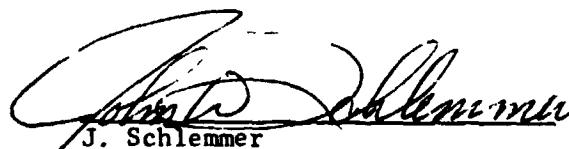
January 1973

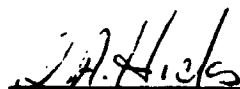
DRL Line Item No.: N3-T040

BALLOON LAUNCHED DECELERATOR  
TEST PROGRAM  
POST-TEST TEST REPORT  
(45 day)  
BLDT VEHICLE AV-3

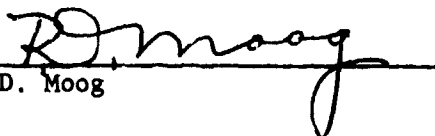
prepared by:

  
D. Dickinson

  
J. Schlemmer

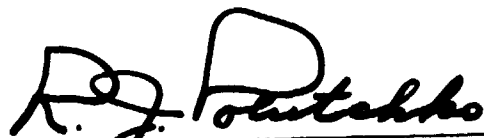
  
F. Hicks

  
F. Michel

  
R. D. Moog

PREPARED UNDER CONTRACT NAS1-9000 BY  
MARTIN MARIETTA CORPORATION  
DENVER DIVISION  
P. O. Box 179  
DENVER, COLORADO 80201

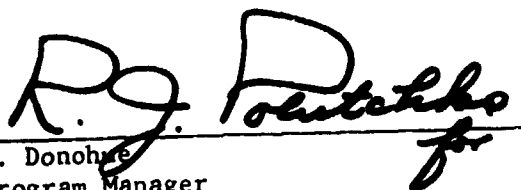
## APPROVAL SHEET



Robert Polutchko  
Project Engineer  
Viking Vehicle Engineering



Date



P. Donohue  
Program Manager  
BLDT Program



Date

TABLE OF CONTENTS

	<u>PAGE</u>
APPROVAL SHEET	ii
TABLE OF CONTENTS	iii
SECTION	TITLE
I.	PURPOSE OF REPORT I-1
II.	MISSION OBJECTIVES II-1
III.	DECELERATOR QUALIFICATION SUMMARY III-1
	A. Operations Summary III-1
	B. Vehicle Performance Summary III-2
	C. Decelerator System Summary III-2
IV.	MISSION OPERATIONS IV-1
	A. Flight Readiness Test and Launch IV-1
	B. Ascent and Float IV-1
	C. Vehicle Flight IV-3
	D. Recovery Operations IV-3
V.	DECELERATOR SYSTEM ANALYSIS V-1
	A. System Description V-1
	B. Mortar Fire Conditions V-2
	C. Mortar Performance V-3
	D. Decelerator Inflation Sequence V-4
	E. Opening Load V-6
	F. Vehicle Stability V-7
	G. Parachute Drag Performance V-8
	H. Aeroshell Separation V-10
	I. Parachute Recovery Assessment V-12

## TABLE OF CONTENTS (CONTINUED)

	<u>PAGE</u>
VI. VEHICLE PERFORMANCE ANALYSIS	VI-1
A. Flight Dynamics	VI-1
B. Capsule Aerodynamic Characteristics	VI-9
C. Thermal Control Subsystem	VI-10
D. Structural Subsystem	VI-12
E. Propulsion, Azimuth Pointing and Ordnance Subsystems	VI-13
F. Electrical Subsystem	VI-13
G. Instrumentation Subsystem	VI-14
H. RF Subsystem	VI-15
I. TSE/OSE	VI-15
J. Mass Properties	VI-15
VII. CONCLUSIONS	VII-1
VIII. REFERENCES AND OTHER DATA SOURCES	VIII-1
A. References	VIII-1
B. Abbreviations	VIII-2
APPENDIX A - Description of Balloon Launched Decelerator Test Vehicle	A-1
APPENDIX B - Description of BLDT System Mission	B-1
APPENDIX C - GAC Post-Test Inspection	C-1
APPENDIX D - Parachute Dimensional Survey	D-1
APPENDIX E - BLDT Computer Software	E-1

LIST OF ILLUSTRATIONS

<u>FIGURE</u>	<u>TITLE</u>	<u>PAGE</u>
II - 1	BLDT AV-3 Test Conditions	II-3
IV - 1	Balloon Altitude Profile	IV-7
IV - 2	Mission Ground Track AV-3	IV-8
V - 1	Viking Decelerator System	V-15
V - 2	Ejected Weight Distribution	V-16
V - 3	Canopy Growth Parameter	V-17
V - 4	Canopy Area Oscillations	V-18
V - 5	Parachute Filling Time from Line Stretch	V-19
V - 6	Parachute Opening Load	V-20
V - 7	Tensiometer Reading, Bridle Leg No. 1	V-21
V - 8	Tensiometer Reading, Bridle Leg No. 2	V-22
V - 9	Tensiometer Reading, Bridle Leg No. 3	V-23
V - 10	Parachute Pull Angle, Pitch Plane	V-24
V - 11	Parachute Pull Angle, Yaw Plane	V-25
V - 12	Parachute Total Pull Angle	V-26
V - 13	Longitudinal Acceleration	V-27
V - 14	Transverse Acceleration	V-28
V - 15	Normal Acceleration	V-29
V - 16	Vehicle Pitch Rate	V-30
V - 17	Vehicle Yaw Rate	V-31
V - 18	Vehicle Roll Rate	V-32
V - 19	Parachute Force Coefficient (Accelerometer Data)	V-33
V - 20	Parachute Force Coefficient (Tensiometer Data)	V-34

## LIST OF ILLUSTRATIONS (CONTINUED)

<u>FIGURE</u>	<u>TITLE</u>	<u>PAGE</u>
V - 21	Parachute Force Coefficient Time History (Acceleration Data)	V-35
V - 22	Parachute Force Coefficient Time History (Tensiometer Data)	V-36
V - 23	Dynamic Pressure Time History	V-37
V - 24	Mach Number Time History	V-38
V - 25	Aeroshell Separation Distance - 0-3 Seconds	V-39
V - 26	Extensiometer Separation Distance	V-40
V - 27	Extensiometer and Guide Rail Location	V-41
V - 28	Relative Angular Motion Between Aeroshell and Lander	V-42
VI - 1	BLDT AV-3 Test Conditions	VI-21
VI - 2	WSMR Map Showing Telemetry and Radar Sites	VI-22
VI - 3	Gyro Data Prior to Drop	VI-23
VI - 4	Accelerometer Data Prior to Drop	VI-24
VI - 5	Gyro Data During Powered Flight	VI-25
VI - 6	Accelerometer Data During Powered Flight	VI-26
VI - 7	Comparison Between Radar Data (R122 Transformed to R113)	VI-27
VI - 8	Radar (R122) Velocity vs. Flight Time	VI-28
VI - 9	Radar (R122) Altitude (MSL) vs. Flight Time	VI-29
VI - 10	Step Trajectory Reconstruction of Altitude and Velocity	VI-30
VI - 11	Step Trajectory Reconstruction of Mach Number	VI-31
VI - 12	Step Trajectory Reconstruction of Angle of Attack and Sideslip	VI-32
VI - 13	Step Trajectory Reconstruction of Total Angle of Attack	VI-33

## LIST OF ILLUSTRATIONS (CONTINUED)

<u>FIGURE</u>	<u>TITLE</u>	<u>PAGE</u>
VI - 14	Angles of Attack, Sideslip and Axial Force Coefficient at Mortar Fire	VI-34
VI - 15	Mission Ascent Profile	VI-35
VI - 16	Base Cover Temperature History	VI-36
VI - 17	Rocket Motor Support Structure Temperature History	VI-37
VI - 18	Aeroshell Temperature History	VI-38
VI - 19	S-Band Transmitter Temperature History	VI-39



LIST OF TABLES

<u>TABLE</u>	<u>TITLE</u>	<u>PAGE</u>
IV - 1	AV-3 Vehicle Flight Sequence of Events	IV-5
IV - 2	Summary of Flight Parameters	IV-6
V - 1	Parachute Geometric Properties	V-14
VI - 1	BLDT AV-3 Atmospheric Properties	VI-17
VI - 2	State Vector Data - BLDT AV-3	VI-18
VI - 3	Battery Performance Data	VI-19
VI - 4	Final BLDT Mass Properties Status - AV-3	VI-20

## I. PURPOSE OF REPORT

The purpose of this report is to document the pertinent events concerned with the launch, float and flight of Balloon Launched Decelerator Test Vehicle AV-3 and the performance of the Decelerator System installed therein. The report will describe and provide data pertinent to the flight trajectory and decelerator test points at the time of decelerator deployment as well as a description of the time history of vehicle events and anomalies encountered during the mission.

The final test reports for BLDV Vehicles AV-1, AV-2 and AV-4 are contained in the following MMC documents:

AV-1 - Document number TR-3720289

AV-2 - Document number TR-3720291

AV-4 - Document number TR-3720295

## II. MISSION OBJECTIVES

The mission objective for the BLDT program is to subject the Viking Decelerator System to qualification test requirements at simulated Mars entry conditions and in the wake of a full scale blunt body which simulates the Viking Lander Capsule. The program test requirements provide for parachute qualification at simulated Mars atmospheric conditions which are consistent with parachute deployment at supersonic, transonic and subsonic conditions.

The flight of vehicle AV-3 provides for deployment of the decelerator under the simulated Mars atmospheric conditions equivalent to a subsonic case. The velocity and dynamic pressure resulting from this simulated entry condition are shown on Figure II-1. The total vehicle requirements described in paragraph 3.3 of "Parachute Test Objectives and Requirements Document for BLDT Program" (RD-3720247) are:

Angle of Attack at Mortar Fire	$\leq 17^\circ$
Residual Spin Rate	$\leq 10^\circ/\text{second}$
Parachute Temperature at Mortar Fire	$\leq 80^\circ\text{F}$
Simulated Velocity/"q" Conditions	See Figure II-1

In order to provide the velocity/atmospheric density equivalent to a subsonic Mars entry, the BLDT vehicle was lifted to high altitude (approximately 92,000 feet) beneath a balloon system. Once at the correct altitude and over the White Sands Missile Range, the flight vehicle was released from the balloon load bar and under ground computer timed control the vehicle was permitted to free fall under gravitational force until the correct velocity and atmospheric density matched the subsonic test requirement.

It was also a goal of this mission to separate the vehicle aeroshell following decelerator deployment in order to obtain a time/distance history of the separation function.

A description of the BLDT vehicle, which served as the qualification test bed, is included in Appendix A of this report. A description of the BLDT mission is provided in Appendix B.

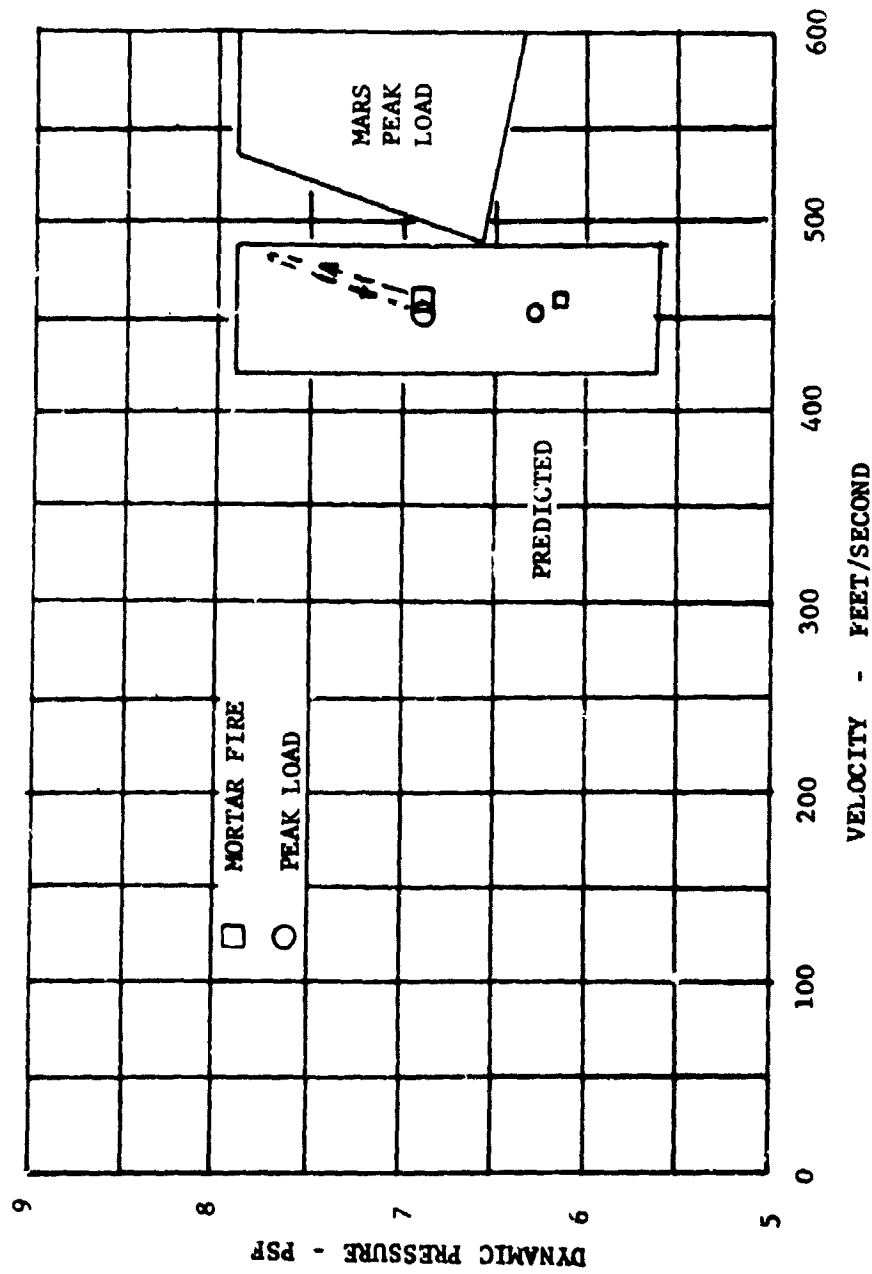


FIGURE II-1 BLDT AV-3 TEST CONDITIONS

### III. DECELERATOR QUALIFICATION SUMMARY

The following is a summary of program events, pertinent to the decelerator system, occurring from the time of decelerator system installation in the BLDT vehicle through the recovery of the decelerator system at the point of payload impact.

#### A. Operations Summary

The decelerator system was installed in the base cover of vehicle AV-3 prior to final vehicle assembly for Flight Readiness Test. The system was Martin Marietta Corporation Serial Number 0000073 (GAC System S/N 15) with a system weight of 124.34 and an ejected pack weight of 90.0 lbs.

During vehicle stand time while awaiting satisfactory meteorological conditions for launch, conditioned air was applied to the vehicle in order to maintain the vehicle interior, including the decelerator cannister, at a temperature below 80°F.

The decelerator system was subject to cooling during the ascent and float phases of the mission with pertinent decelerator temperatures just prior to release from the load bar as follows:

<u>Sensor Location</u>	<u>Spec. Req'd (°F)</u>	<u>Actual Temp. (°F)</u>
*Bridle #1	+210 to -90	0
*Bridle #2	+210 to -90	18
*Bridle #3	+210 to -90	13
Mortar Cannister #1	+80 (No Min)	25
Mortar Cannister #2	+80 (No Min)	26
Mortar Breach	+175 to +25	45 (Automatic heater controlled)
Mortar Breach Flange	+74 to +25	27

\*Temperature measured on the base cover interior beneath the bridle leg.

### B. Vehicle Performance Summary

The AV-3 Vehicle performed normally and all anticipated functions occurred. Mortar fire was commanded from the ground at the proper time for the decelerator test. The flight conditions at mortar fire were:

	<u>Target</u>	<u>Actual</u>
Mach Number	.468	.471
Velocity, fps	460	464
Dynamic Pressure, psf	6.15	6.90
Residual Spin Rate (deg/sec)	$\leq 100$	.5
Total Angle of Attack	$\leq 17$	5.7

There was no vehicle induced damage to the decelerator system.

### C. Decelerator System Summary

Test conditions at peak load fell within the envelope of Mach number and dynamic pressure shown in Figure II-1. Mortar velocity of 106 fps was lower than expected but above the minimum required for Viking. Visual evaluation of bag stripout and early canopy inflation were impaired by ice on the camera lens. Enough could be seen, however, to conclude that canopy inflation was normal with little evidence of unsymmetrical loading.

The maximum parachute opening load of 12906 lbs. occurred shortly before first full inflation. After less than 1 second of canopy area fluctuations, the canopy reached stable inflation and showed good stability for the remainder of flight. No damage, other than a few black smudges, was sustained by the parachute.

Parachute drag fell very near the middle of the expected range established from wind tunnel testing.

The parachute opening transient induced vehicle attitude rates as high as 118 degrees/second initially but these rates had damped to below 30 degrees/second in 14 seconds.

Aeroshell separation was successfully demonstrated at a dynamic pressure of 1.38 psf and Mach number of .193. These conditions approximate the lowest dynamic pressure expected at aeroshell separation on Mars and did, in fact, produce the slowest separation of any of the BLDT flights. The separation distance of 97 feet in 3 seconds was more than required to meet the minimum system requirement of 50 feet in 3 seconds. All separation hardware performed satisfactorily.



#### IV. MISSION OPERATIONS

The following is a summary of the program events occurring from the time of vehicle Flight Readiness Test through Recovery Operations.

##### A. Flight Readiness Test and Launch

BLDT Vehicle AV-3 completed Flight Readiness Test on August 16, 1972 with data review being completed on August 17, 1972. The airborne battery activation was completed on August 14 with installation in the vehicle completed prior to FRT.

Vehicle roll out for launch was completed following a 2200 hours weather briefing on August 18 for a launch attempt at 0430 hours on August 19. The vehicle was moved out during light and intermittent rain which continued through to about 0200 hours. At about 0200 hours, the balloon operations moved forward with balloon roll out and layout. It is noted that the early launch hour was prompted by a requirement to clear the range and control center by 1100 hours due to range schedule interference caused by a higher priority program.

Balloon winch up proceeded at approximately 0535 at which time a light to moderate rain storm hit the launch site. The winch up and launch continued smoothly and without incident despite the local rain shower. The winds at launch (surface to 600 feet) were very light contributing to a very smooth launch at 0545 hours.

##### B. Ascent and Float

The ascent and float phase of the mission was very eventful with the balloon ascent being very erratic and slow and with the trajectory to float

deviating from the predicted trajectory. The expected ascent rate for this mission was on the order of 1000 feet/minute. As shown on Figure IV-1, the ascent rate during the initial hour and fifteen minutes following launch was erratic probably due to added system weight of atmospheric moisture and wet balloon corn starch which would normally have shed from the balloon surfaces. The balloon was also floating in cloud layers which prevented solar heating of the helium which would have aided in system lift. It was reported that the balloon passed through a temperature inversion which would also delay the system ascent.

Because of the initial slow ascent, the trajectory to float followed ground winds in a northeasterly direction reaching approximately 55 miles NNE of the launch site before assuming a trajectory which intersected the northern range extension. The ground track is shown in Figure IV-2. This initial ground track is shown in arrows and is an estimated plot based on sightings and estimated wind velocity and time. The predicted track for this mission would have had the system float to 60,000 feet at 8 to 10 miles north of Roswell then float westerly through the middle of the range 70 mile area. The time from launch to range intersect was predicted at 3.8 hours. The actual time to range intersect was approximately 6 hours.

The range radar acquired the floating system at 1353 hours Z at an altitude of approximately 24,000 feet. The ground track shown in Figure IV-2 is radar plot from the point of radar acquisition to the end of mission.

During the ascent phase, first TM data was received at 1347 hours Z while the system float altitude was approximately 20K feet. Radar beacon track was acquired at approximately 1353 hours Z and 24K feet. The airborne command receivers were captured at approximately 1510 hours Z when the system

was at an altitude of about 85K feet. The command system operation was verified by transmitting the commands safe and safe backup and monitoring system response via the TM downlink.

Since there was no range constraint on the vehicle drop azimuth, the AV-3 vehicle did not utilize an airborne azimuth pointing system.

#### C. Vehicle Flight

The flight of vehicle AV-3 consisted of a vertical drop with no spin or main motor propulsion. Once released from the balloon load bar, the vehicle accelerated to the test velocity while dropping to the altitude (density) where the test requirement of velocity vs dynamic pressure was in accordance with the test envelope shown in Figure II-1. During the drop all vehicle functions occurred as predicted with the mortar fire function occurring on ground command when the ground computer timed out at drop +16.47 seconds. (Airborne programmer issued mortar fire at drop +18.17 seconds).

The sequence of vehicle events is provided in Table IV-1. Table IV-2 contains a summary of predicted and actual flight parameters.

#### D. Recovery

The recovery portion of the mission was completed on T+1 day with all major portions of the vehicle and decelerator being recovered. The recovery was complicated by the distance between the northern range extension impact and the L-36 recovery building. The impact also occurred on a hillside in such position that vehicle disassembly was required so that a helicopter could airlift the pieces to a more accessible loading area.

Discussion of the condition of the recovered hardware, including the decelerator, is covered in later appropriate paragraphs. It is noted that the base cover and interior of the recovered vehicle contained fairly heavy deposits of white material, probably cornstarch. It is also noted that the recovery crew reported finding wet vehicle interior surfaces with ice formations on the rocket motor support structure surfaces.

TABLE IV-1

## AV-3 VEHICLE FLIGHT SEQUENCE OF EVENTS

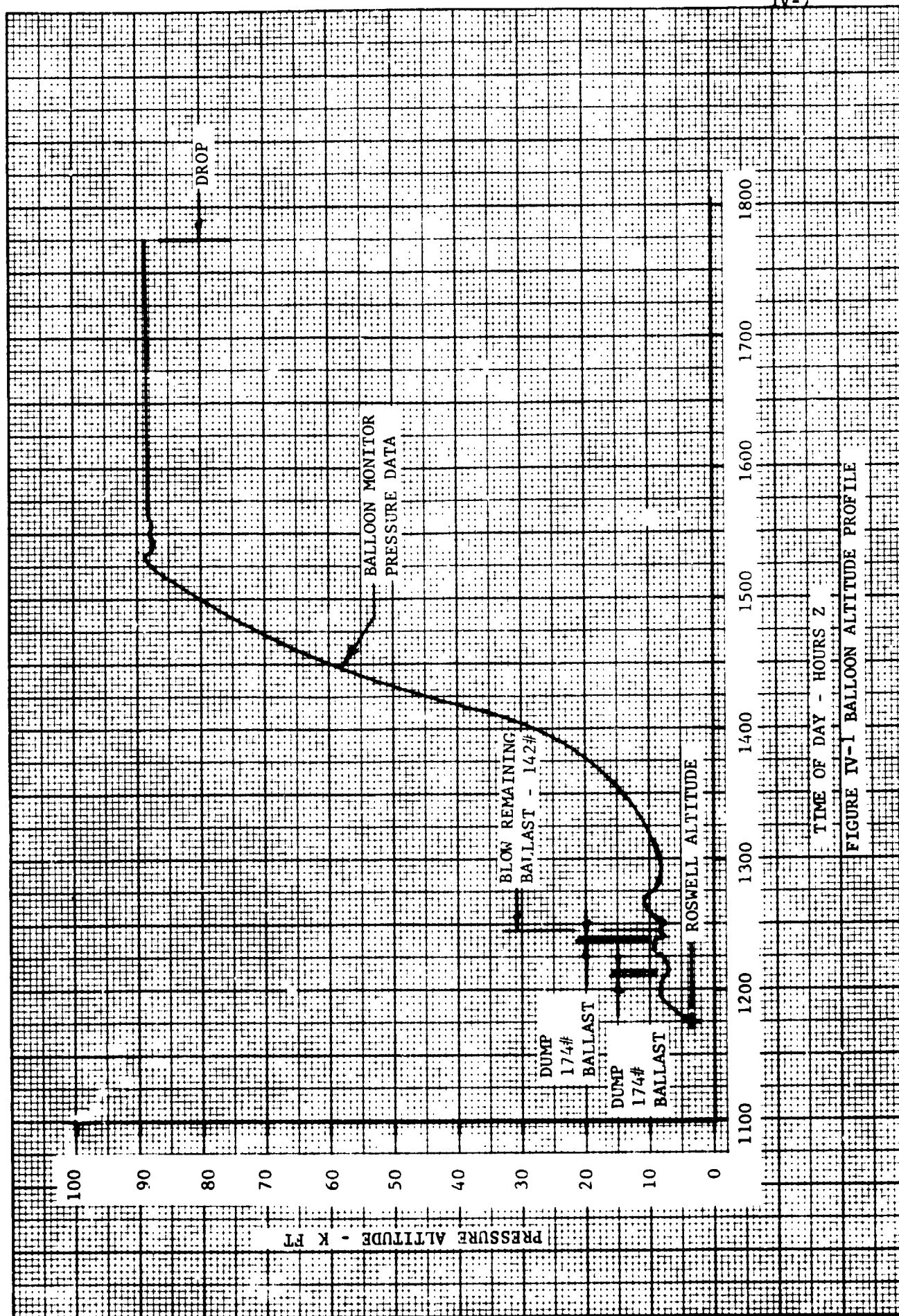
	<u>PROGRAMMED TIME (SECONDS)</u>	<u>ACTUAL TIME (SECONDS)</u>	<u>SOURCE</u>
1. Drop from Load Bar/ Initiate A/B Programmer	0	0	Ground Command
2. Start Aft Milliken Camera/ Enable Mortar Fire Conditions	+12.0	+12.09	A/B Programmer
3. Initiate Mortar Fire Conditions/ Start Aft Photosonics Camera Start Forward Milliken Camera	+16.4	+16.47	Ground Command
4. Initiate Mortar Fire B/U, Start Aft Photosonics Camera B/U, Start Aft Milliken and Forward Milliken B/U	+18.0	+18.17	A/B Programmer
5. Separate Aeroshell	+30.0	+30.23	A/B Programmer

TABLE IV-2  
SUMMARY OF FLIGHT PARAMETERS

	<u>PREDICTED</u>	<u>ACTUAL</u>
A. Drop Time, GMT	--	17:45:00.60
B. Drop Conditions		
1. Longitude (DEG)	--	106.244
2. Latitude (DEG)	--	34.0136
3. Altitude, Geometric (FT)	93,350	91.148
C. Mortar Fire Conditions		
1. Mach Number	.468	.471
2. Dynamic Pressure (PSF)	6.15	6.90
3. Velocity (FPS)	460	464
4. Axial Acceleration (g's)	-0.36	-0.38
5. Altitude (FEET)	89,325	87,027
6. Angle of Attack (DEG)	-4.5	3.5
7. Sideslip Angle (DEG)	0.0	-4.5
D. Aeroshell Separation Conditions		
1. Velocity (FPS)	194	190
2. Mach Number	.198	.192
3. Dynamic Pressure (PSF)	1.32	1.38
4. Time for 1 Foot (SEC)	0.17	.215
5. Time for 50 Foot (SEC)	3.0	2.05
6. Distance at 3 seconds (FEET)	50.0	97

46 1327  
GAG 18 S.F.A.

K-E 10 X 10 TO 1/2 INCH  
7 X 10 IN. - ALUMINUM  
NEUFFEL & ESSER CO.



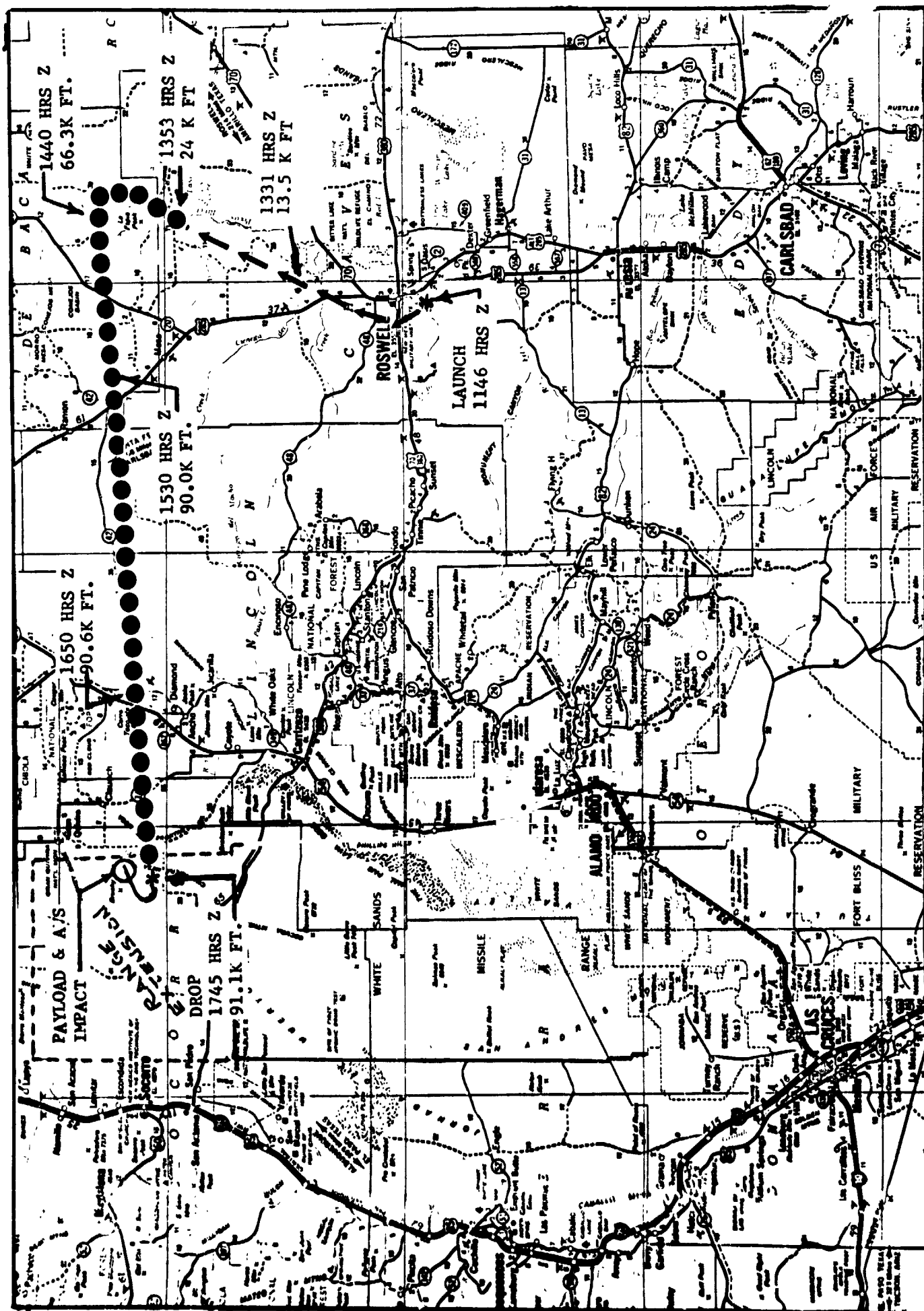


**FIG IV-2**  
**MISSION GROUND TRACK AV3**



## V. DECELERATOR SYSTEM PERFORMANCE

### A. System Description

The objective of this test of the Viking decelerator is to deploy it at a dynamic pressure and velocity condition in which the velocity is lower than the lowest velocity expected on Mars as shown in Figure VI-1. Low speed inflation and canopy stability behind a blunt forebody are therefore of primary concern.

The Viking decelerator is a 53-foot nominal diameter Disk-Gap-Band parachute with dimensions and general arrangement shown in Figure V-1. The parachute is fabricated entirely of Dacron type 52 except for the three-legged bridle which uses a special Goodyear proprietary fiber. The band cloth material is a 1.53 oz/sq. yd. rip-stop material having a minimum specified strength of 50 lb/in. The disk cloth is a 2.25 oz/sq. yd. rip-stop material having a minimum specified strength of 104 lbs/in. The minimum specified strength of the radial tapes, circumferential tapes and suspension lines are 900 pounds, 1800 pounds and 880 pounds respectively. The above parachute strength numbers correctly reflect a change made during development to improve the structural integrity of the canopy. The BLDT AV-2 and AV-4 flight test reports erroneously reported the former development strength values.

The parachute is packed in a deployment bag to a density of 43 lbs/ft<sup>3</sup> and stored in a mortar can aboard the BLDT vehicle in much the same manner as the Viking system. The BLDT vehicle itself is practically identical in shape and size to the Viking Lander Capsule. At mortar fire, the deployment bag is ejected straight back by a mortar whose

reaction force is nominally oriented through the vehicle c.g. A breakdown of the ejected weight is seen in Figure V-2 to total 97 lbs. The relative velocity imparted to the deployment bag is expected from ground mortar test experience to be  $112 \pm 3$  FPS.

Additional geometric data on the parachute are tabulated in Table V-1.

#### B. Mortar Fire Conditions

This flight test, unlike the other three BLDT powered flight tests, involved simply a 16.5 second free fall drop from a balloon load bar. The vehicle dynamics motions at mortar fire were therefore less than on the other flights. The vehicle was undergoing a  $\pm 5$  degree oscillation with a small roll rate of 0.5 degree/second at mortar fire. STEP trajectory reconstructed values of angle of attack and sideslip at mortar fire are 3.5 and -4.5 degrees respectively with pitch and yaw rates being 2.1 and -5.8 degrees/second. The aerodynamic trim angles of attack and sideslip for this BLDT vehicle at M.N. = .47 are -4.3 and zero. This means that the vehicle was approximately 9 degrees away from trim at mortar fire. Airborne camera data was obscured by ice on the camera lens and was therefore of little help in corroborating the mortar fire conditions.

The important conditions at mortar fire are compared to nominal values in the summary below:

<u>Mortar Fire Conditions</u>	<u>Nominal</u>	<u>Flight</u>
Mach Number	.469	.471
Dynamic Pressure, psf	6.22	6.9
Velocity, fps	461	464
Axial acceleration	-.36	-.34

<u>Mortar Fire Conditions</u>	<u>Nominal</u>	<u>Flight</u>
Altitude, ft.	88800	87027
Angle of Attack, degrees	-4.5	2.5
Angle of Sideslip, degrees	0	-4.5
Total Angle of Attack, degrees	4.5	5.7
Spin Rate, deg/sec	0	-.5
Pitch Rate, deg/sec	0	2.1
Yaw Rate, deg/sec	0	-5.8
Parachute Temperature, °F	< 80	26

The mortar fire conditions for the flight produced dynamic pressure and velocity conditions at peak load which fell within the desired envelope of test conditions shown in Figure II-1, Section II.

#### C. Mortar Performance

The mortar performance has been evaluated on the BLDT flights by observing the bag stripping process from the on-board cameras. On the flight of AV-3, however, ice on the camera lens made visual identification of events difficult. The time at which the canopy first starts emerging from the deployment bag is identified from the film data as 1.02 seconds from mortar fire. Since the camera data was questionable, the telemetered bridle load traces were used to confirm the above line stretch time. The actual distance the deployment bag must travel for the suspension lines to be pulled from the bag is defined by the length of the lines themselves. By simulating the mortar firing process with complete aerodynamic forces on the forebody and the deployment bag, the mortar velocity can be established. The AV-3 flight conditions of Mach number, dynamic pressure and flight path angle at mortar fire are used.

The following assumptions were used where detailed data are not precisely known:

1. Deployment bag  $C_D S = 1.6$
2. Dynamic pressure gradient behind blunt forebody (Reference 3).
3. Forebody aerodynamic coefficients (Reference 4).
4. Line and canopy stripping forces of 2 and 6 lbs. respectively (Reference 5).
5. Line bowing due to aerodynamic forces on the lines is negligible.

The line stripping simulation for AV-3 shows a mortar velocity of 106 FPS. This value does not fall within the expected range of  $112 \pm 3$  FPS, but is above the minimum requirement of 104 FPS established by Reference 2. The stripping process sequence derived by simulation is shown below.

<u>Time-Seconds</u>		<u>Relative Velocity - FPS</u>
Mortar Fire	0	106
Line Stretch	1.02	91.8
Bag Strip	1.32	84.3

The relative velocity at bag strip is seen to be more than adequate to assure positive bag strip. The bag strip time shown above is purely analytical since this event cannot be clearly seen in the film data.

#### D. Decelerator Inflation Sequence

The on-board Milliken and Photosonics camera films were examined in detail to establish event times and to document the character of the

parachute inflation. In the sequence shown below, certain events such as peak load and aeroshell separation were obtained from telemetry data:

<u>Sequence of Events</u>	<u>Time - Seconds</u>
Mortar Fire	0
Line Stretch	1.02
Bag Strip	1.31
Peak Load	1.77
First Full Open	1.83
Aeroshell Separation	13.76

The peak load on this flight of AV-3 occurred prior to maximum projected area of the canopy (referred to above as first full open). This characteristic was observed on the flight of AV-2 which was also a low dynamic pressure test.

The growth of the canopy from line stretch was obtained by tracing the projected area images from the Milliken camera and integrating these images with a planimeter. A canopy growth parameter curve of normalized area versus time is then constructed in Figure V-3. The projected area at any time is divided by the projected area observed in the final seconds of airborne film coverage. The time scale is normalized by the total filling time. The canopy growth curve is seen to be very similar in shape to the curve for AV-2 (the low dynamic pressure, transonic case).

A plot of the projected area ratio,  $S_p/S_{p_{final}}$ , versus time from line stretch is presented in Figure V-4. The initial canopy area oscillations are significantly smaller than observed on the other BLDT flights. Stable canopy inflation is also achieved sooner than the higher speed BLDT flights.

Parachute inflation was smooth and very symmetrical. The time from line stretch to first full inflation is seen in Figure V-4 to be .81 seconds. This value is plotted in Figure V-5 along with similar data from PEPP and UADT flight tests. The filling time for AV-3 falls near the lower edge of the expected uncertainty in this parameter.

#### E. Opening Load

Figure V-6 shows the time history of the total longitudinal parachute load recorded by the bridle attach point tensiometers for time periods of 0-10 and 10-20 seconds after mortar fire. The peak load is seen to be 12906 lbs. occurring 1.77 seconds after mortar fire. This load compares favorably with a load of 12558 lbs. obtained by simulating AV-3 deployment conditions in a dynamic loads analysis program.

The individual tensiometer readings at each bridle leg are recorded in Figures V-7, V-8 and V-9. The tensiometer trace for bridle leg number 1 is noisy with this noise being reflected in other data which uses the tensiometer readings as input data. By proper combination of the three tensiometer readings, the equivalent parachute load pull angles in pitch and yaw are obtained and plotted in Figures V-10 and V-11. These angles are projections in the pitch and yaw planes of the total angle between the parachute load and the forebody vehicle centerline. The total pull angle is shown in Figure V-12. The structurally significant pull angle occurring at peak load is approximately 3.5 degrees.

Accelerometer readings in the X, Y and Z axis directions are shown in Figures V-13, V-14 and V-15. The peak longitudinal acceleration of 7.86 g's occurs at 1.76 seconds after mortar fire and reflects a parachute

opening load of 13400 lbs. This is based on subtracting out the aeroshell drag component using  $C_D$  of 1.06, a dynamic pressure of 7.18 psf, and a payload mass of 56.08 slugs. The load thus obtained is 494 lbs. larger than the load indicated by the tensiometers. Aeroshell separation occurring 13.76 seconds after mortar fire is clearly visible on the accelerometer traces.

#### F. Vehicle Stability

The AV-3 test vehicle has a 1.35 inch center-of-gravity offset along the yaw axis which produces an aerodynamic trim condition at low subsonic speed of -4.5 degrees angle of attack at zero sideslip angle. During the 16.5 second free fall from the balloon load bar, the vehicle can be seen to oscillate in pitch and yaw about the natural trim condition in Figure VI-12, Section VI. At mortar fire, the vehicle had a negligible roll rate (-.5 degree/second) but had pitch and yaw rates of 2.1 and -5.8 degrees/second respectively. The angles of attack and sideslip were 3.5 and -4.5 degrees respectively. This means that in spite of very passive drop conditions, the vehicle was 9 degrees away from aerodynamic trim at mortar fire and oscillating at about 6 deg/sec. Mars conditions are less severe, being limited to oscillations of  $\pm 3$  degrees and rates of 1 deg/sec by virtue of an attitude control system.

The actual vehicle attitude rate time-histories are shown in Figures V-16, V-17 and V-18. The peak attitude rate of 118 degrees/second occurs shortly after peak load. Pitch and yaw rates fall below 30 degrees/second in 14 seconds and remain below 17 degrees/second after 30 seconds from mortar fire. Figure V-18 shows that a roll rate of 6 degrees/second is induced by parachute deployment but for the most part hovers near zero throughout the flight.

### G. Parachute Drag Performance

The evaluation of the drag of the parachute was conducted in two overlapping phases. The first used the onboard instrumentation to evaluate the parachute forces and the second was based on the radar tracking data. The best estimate of meteorological data was used in both phases. The velocity and altitude for generating the dynamic pressure in the first phase was obtained by integrating the onboard accelerometer data twice, starting at mortar fire. The tensiometer and accelerometer data are converted to incremental parachute force coefficients ( $C_{F_T}$ ,  $C_{F_A}$  respectively) using the equations:

$$C_{F_A} = A_x \times W_t / Q S_p - C_D S_V / S_p$$

$$C_{F_T} = (F_t - A_x \times W_p) / Q S_p$$

where:  $A_x$  = Vehicle axial acceleration, g's  
 $Q$  = Dynamic Pressure, psf  
 $W_t$  = Vehicle weight, 1901 lb.  
 (1541 lb after Aeroshell Separation)  
 $W_p$  = Parachute weight, 97 lb.  
 $S_p$  = Parachute reference area, 2206 ft<sup>2</sup>  
 $C_D S_V$  = Vehicle drag area, 108 ft<sup>2</sup>  
 $F_t$  = Summation of tensiometer data, lb.

This phase continued for 37 seconds after mortar fire.

The second phase was begun just after aeroshell separation and evaluated the drag coefficient necessary to obtain the radar altitude at various subsequent times.

Parachute force coefficients derived from accelerometer and tensiometer data are plotted versus Mach number in Figures V-19 and V-20. The two plots are seen to be very similar in character and reflect almost identical average



drag coefficient magnitude. Both plots contain the oscillatory character of the opening load and the natural frequency of the two body, spring mass system. Dropping the 352 lb. aeroshell results in no noticeable parachute projected area change and only a minor perturbation in the force coefficient of Figure V-19. Aeroshell separation analysis in paragraph V-H confirms that parachute drag area remains near nominal after the separation event.

When near steady state descent conditions are achieved, the tensiometer and accelerometer data become poor sources of parachute drag performance. The vehicle is so near equilibrium that noise on the traces becomes larger than variation in the parameter of interest. The quasi-steady state drag performance is then determined by iterating on drag coefficient until the altitude change over a time increment matches the tracking radar. Drag coefficients determined in this manner are included on the plots in Figure V-19 and V-20.

The expected dispersion limits of parachute drag from wind tunnel results in Reference 7 are superimposed over the flight results of AV-3 in Figures V-19 and V-20. Both the transient response and the quasi-steady state drag coefficient data fall very near the middle of the expected drag performance range.

Plots of parachute force coefficient versus time in Figures V-21 and V-22 are included for convenience in correlating this data with time. The trajectory parameters of dynamic pressure and Mach number used in post-mortar fire trajectory reconstruction are presented in Figures V-23 and V-24.

#### H. Aeroshell Separation

The aeroshell separation system on all BLDT vehicles is similar in design and construction to the system to be used on the Viking lander. The aeroshell is separated 7 seconds after mortar fire in the current Viking sequence. On BLDT, aeroshell separation is timed to occur when specific Mach number and dynamic pressure conditions occur in the Earth atmosphere.

Basically, separation is achieved by virtue of a favorable relative acceleration between bodies as indicated below:

$$\text{Relative Acceleration} = q \times \left( \frac{1}{B_{\text{chute}}} - \frac{1}{B_{A/S}} \right)$$

where  $B = \frac{M}{C_D A}$  for each body.

A guide rail system is used to provide positive clearance during separation. This system involves three guide rails symmetrically oriented on the aeroshell which mate with roller guides mounted on the lander body. Moment constraint is provided by two sets of roller guides separated by 6 inches for each rail. The effective length of the rail is 12 inches, the first 6 inches of which provide moment constraint and shear constraint, whereas the last 6 inches provide only shear constraint. A compression spring inside each rail provides 200 lbs. force when compressed three inches at the start of separation. Three dummy electrical disconnects were included on BLDT to simulate the Viking hardware. These disconnects are of the type which require a positive force of 50 to 150 lbs/connector to engage them. The connector force, which assists the separation, decays to near zero in one-fourth inch of travel.

The objectives of the separation demonstration are:

- (1) To determine that there are no unpredictable aerodynamic disturbances at separation that would compromise the Viking mission,

- (2) To exercise the separation hardware and concept to insure that analytical evaluation of separation dynamics are valid, and
- (3) To determine that parachute drag is adequate to produce a minimum of 50 feet of separation between aeroshell and lander in 3 seconds.

It was intended on this flight to achieve aeroshell separation conditions of 1.32 psf dynamic pressure at a Mach number of .198. Actual conditions at aeroshell separation were 1.38 psf dynamic pressure and Mach number of .193. These conditions approximate the lowest dynamic pressure expected at aeroshell separation on Mars and therefore should produce as slow a separation as will be seen on Mars.

The vehicle was pitching near 30 degrees per second during the separation interval. This is equal to the 30 degree/second criteria used in the design of the guide rail system.

Evaluation of the forward looking Milliken camera film shows a well behaved aeroshell separation. Separation distance versus time is obtained from this film by knowing the diameter of the aeroshell to be 11.5 feet, the horizontal field of view of the camera to be 54.9 degrees and the frame rate to be 32 frames per second. This separation distance versus time plot in Figure V-25 shows 97 feet of separation in 3 seconds. Simulation of this separation using actual AV-3 flight conditions shows fair agreement with the flight results. The difference is attributed in part to ice accumulation on the vehicle from a rainstorm that occurred during balloon ascent. Ice was observed on the airborne camera lenses.

The first foot of aeroshell separation is recorded by three airborne extensimeters and plotted in Figure V-26. Again we observe a slight mismatch between actual and simulated traces that is attributed to ice accumulation mentioned above. The fact that all three extensimeter traces

fall very close to one another is an indication of little angular rotation between bodies as they separate. In order to compute the extent of angular rotation, the guide rail and extensiometer locations must be defined as in Figure V-27. The relative angle between bodies may then be computed and is plotted in Figure V-28. This plot confirms that little relative angular rotation occurred on this separation. The constraining influence of the rails may be seen to limit the angular rotation to about 0.8 degrees. This value agrees well with the expected looseness of fit of .5 to 1.0 degree between mating parts of the system. Comparison of this data with the other three BLDT aeroshell separations and a ground test in which a 1.53 degree relative angle was recorded when the rails were subjected to a bending moment of 560 ft-lbs, indicates that the rail loads on this flight were probably very low. The rail separation system functioned satisfactorily with no evidence of any damage to the system.

#### I. Parachute Recovery Assessment

A post-test inspection of the parachute was conducted by MMC and GAC. A report of this inspection by the parachute contractor is presented in Appendix C. A graphic description of canopy anomalies is included as Figure C-1 therein. In general, the parachute suffered no significant damage and this test is therefore considered a successful qualification of the decelerator.

Pre-flight and post-flight parachute dimensions are recorded in Appendix D. Between pre-flight and post-flight measurement, however, the packed parachute is exposed to a heat compatibility test. Experience has shown that suspension line lengths shrink approximately 2 percent during the heat cycle. If we also assume that the lines do not shrink as a result of flight

loads, the line length prior to load must be no longer than the shortest post-flight line length of 87 feet, 11 inches. The maximum suspension line length increase is therefore 10 inches. This is an indication of rather light parachute loading. The bridle leg length increases were  $11/16$ ,  $5/8$  and  $11/16$  inch respectively. Other dimensional changes were minor.

TABLE V-1

## PARACHUTE GEOMETRIC PROPERTIES

<u>Item</u>	<u>Relative Value</u>	<u>Value</u>
Nominal diameter	$D_o$	53 feet
Geometric porosity*	$0.125 S_o$	$276 \text{ ft}^2$
Total area ( $S_o$ )**	$(\pi/4) D_o^2$	$2206.2 \text{ ft}^2$
Disk area+	$0.53 S_o$	$1169.3 \text{ ft}^2$
Disk diameter	$0.726 D_o$	38.5 ft
Disk circumference	$2.285 D_o$	121 ft
GAP area	$0.12 S_o$	$264.7 \text{ ft}^2$
GAP width	$0.042 D_o$	2.2 ft.
Band area	$0.35 S_o$	$772.2 \text{ ft}^2$
Band width	$0.121 D_o$	6.4 ft
Vent area	$0.005 S_o$	$11.0 \text{ ft}^2$
Vent diameter	$0.07 D_o$	3.7 ft
Number of suspension lines	--	48
Length of suspension lines	$1.7 D_o$	90 ft

\* Vent plus gap provide 12.5 percent geometric porosity

\*\* Disk + gap + band

+ Includes vent

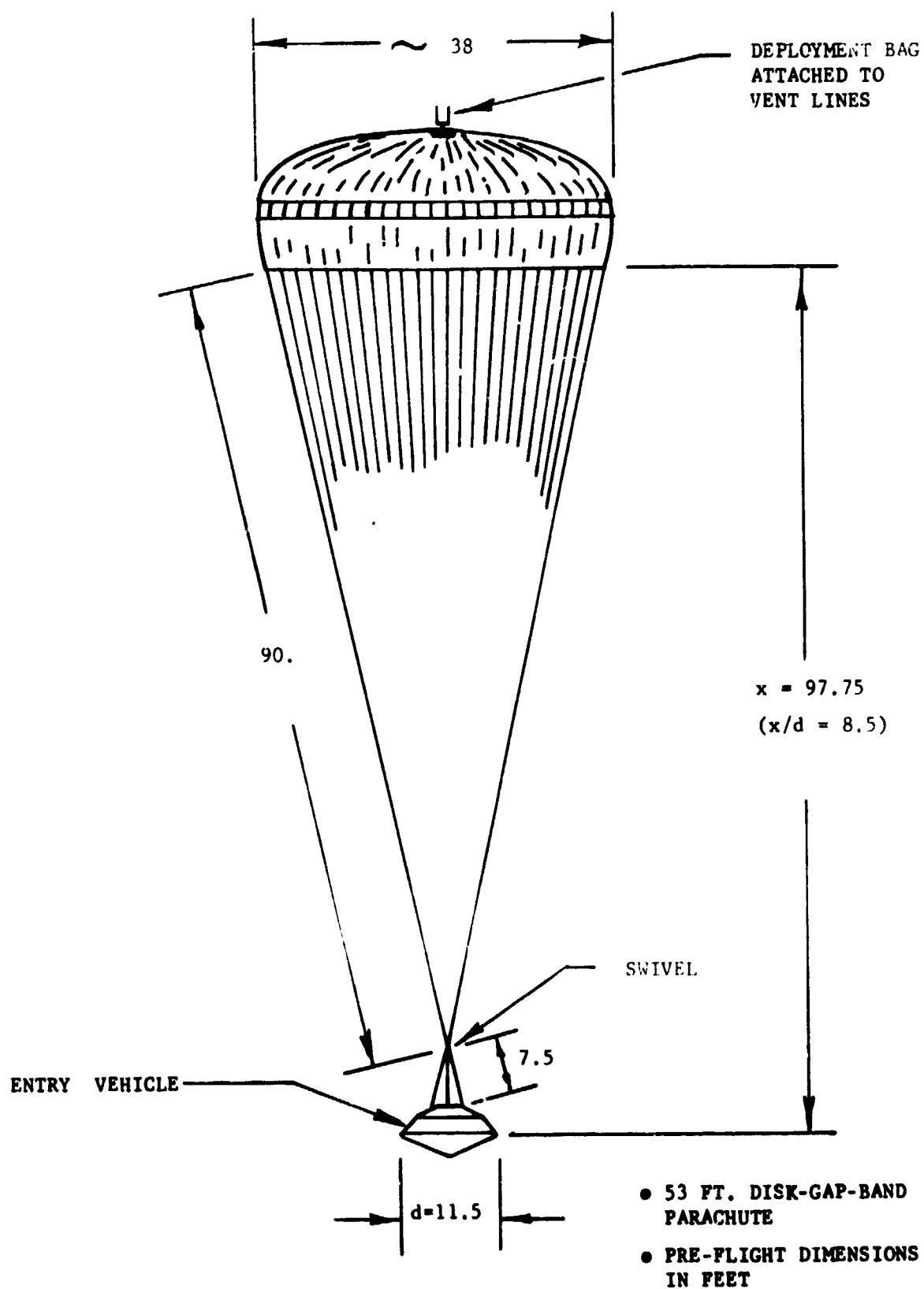
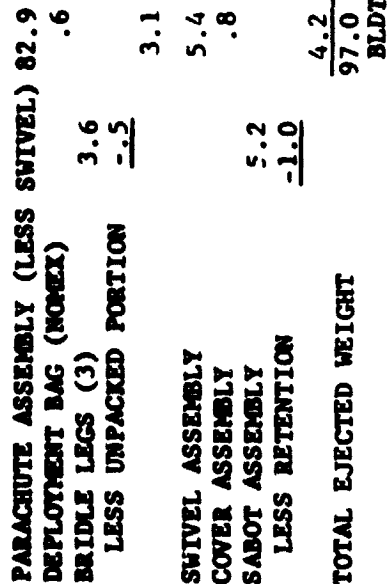


FIGURE V-1 VIKING DECELERATOR SYSTEM



**FIGURE V-2**



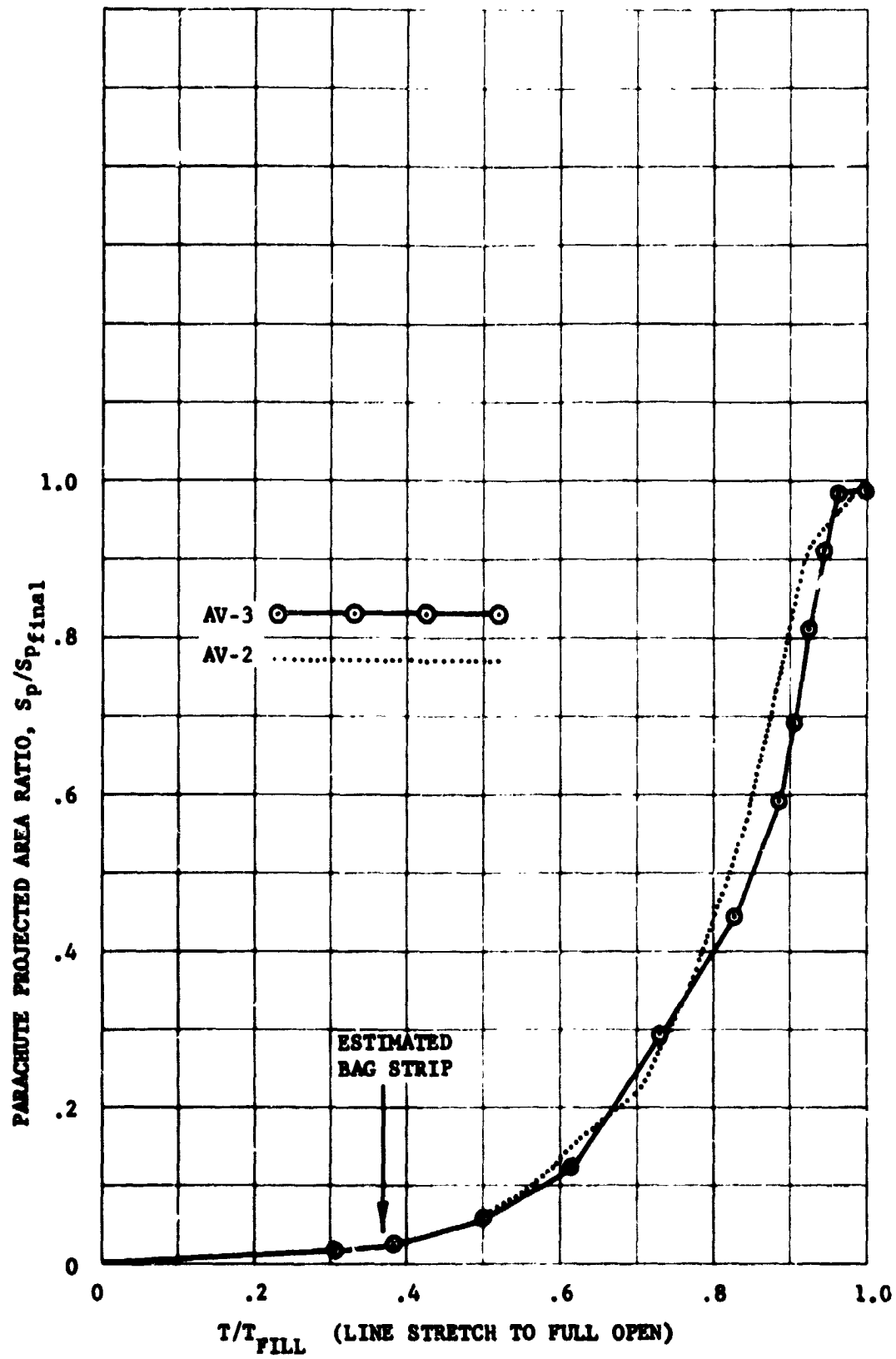


FIGURE V-3 CANOPY GROWTH PARAMETER

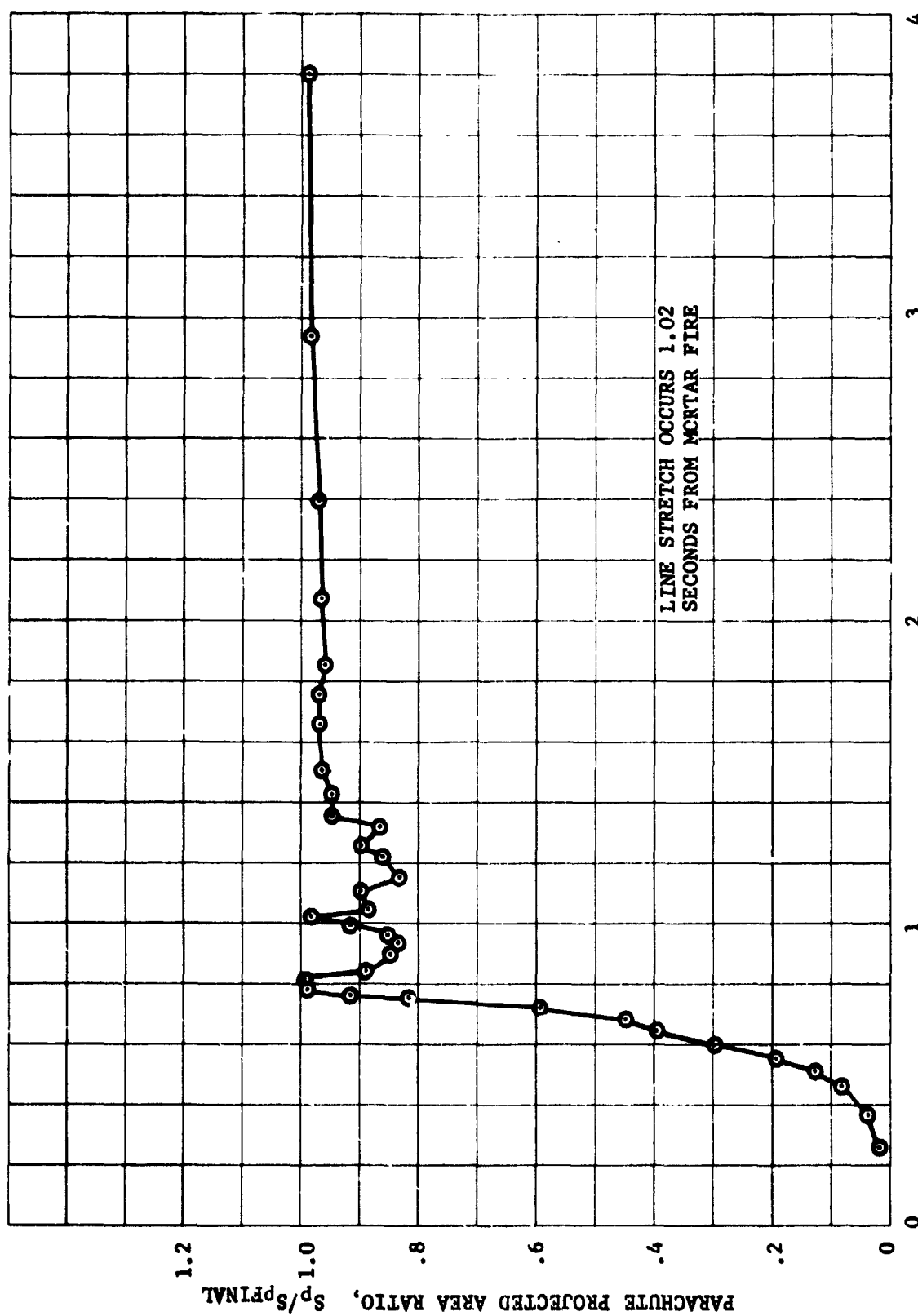


FIGURE V-4 CANOPY AREA OSCILLATIONS

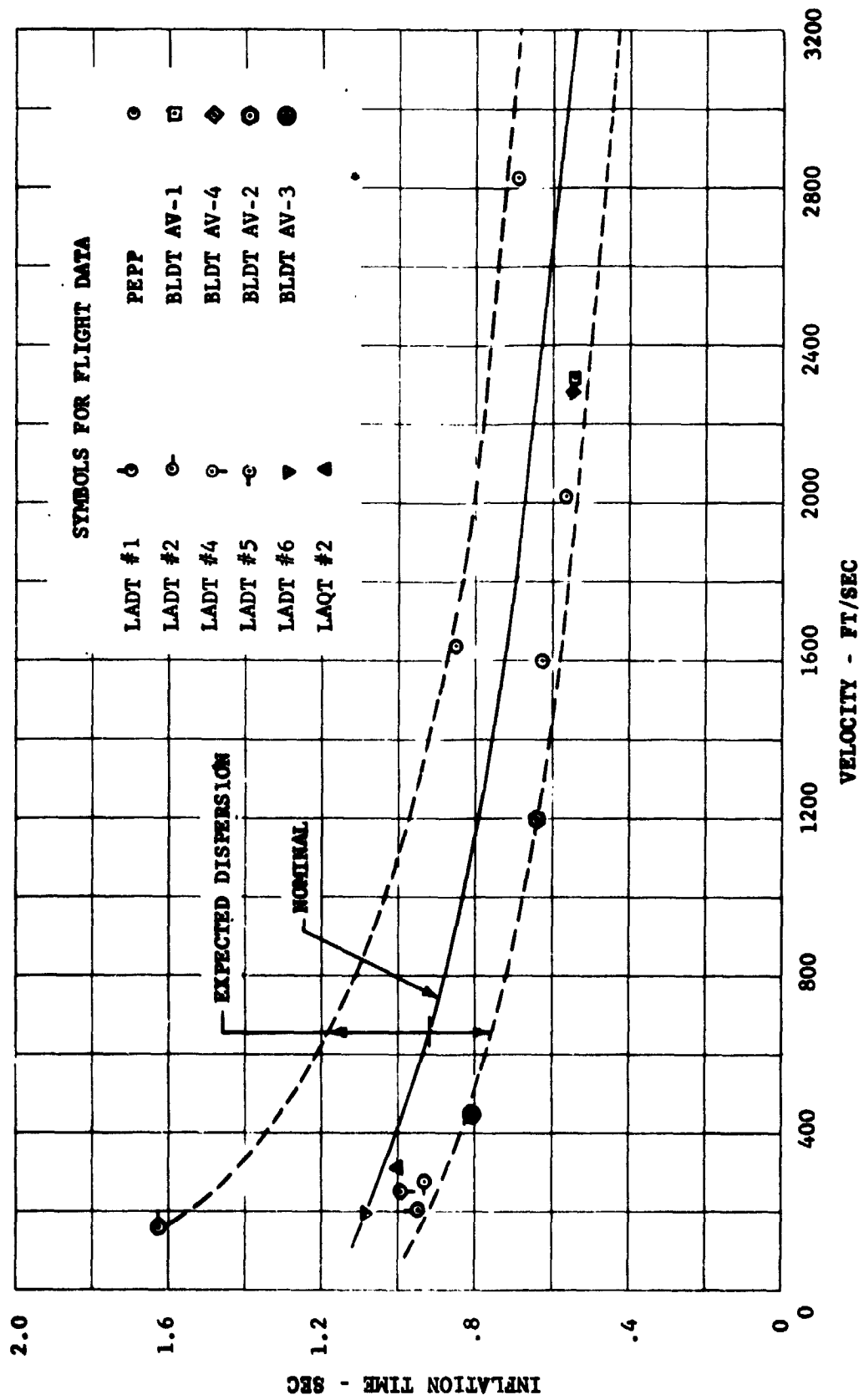
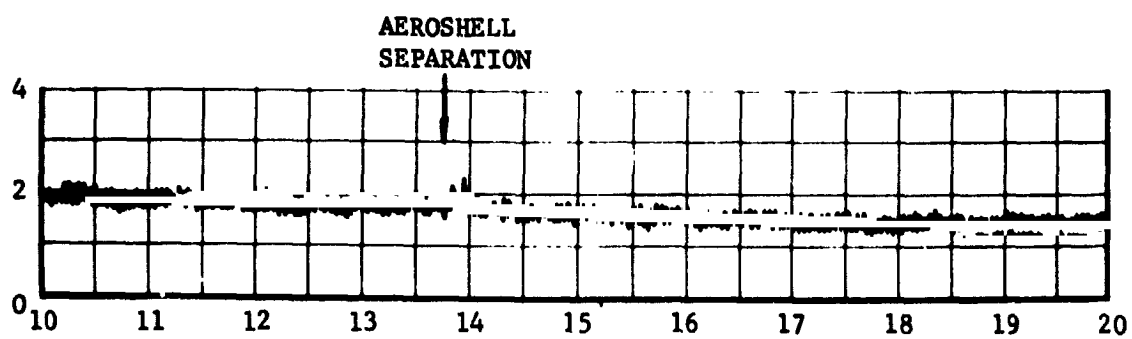
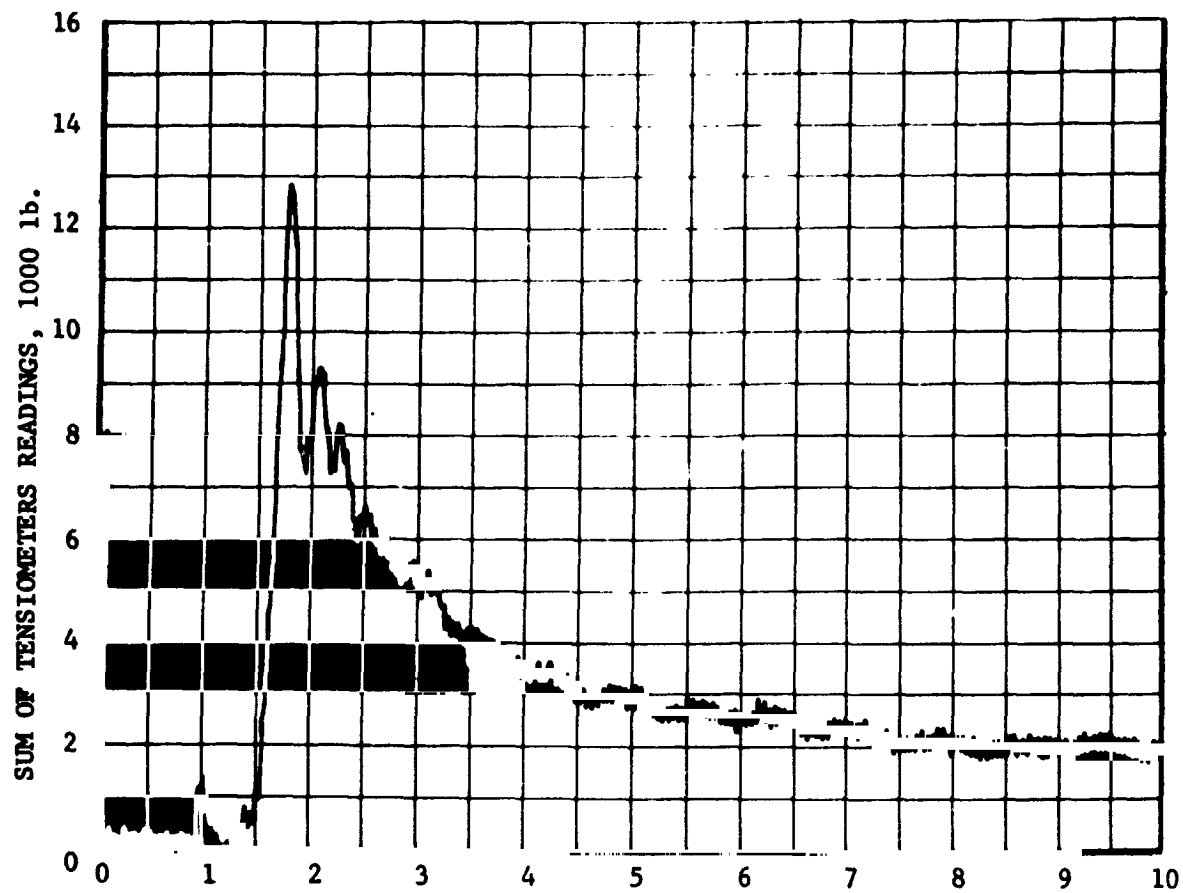


FIGURE V-5 PARACHUTE FILLING TIME FROM LINE STRETCH



TIME FROM MORTAR FIRE, SECONDS

FIGURE V-5 PARACHUTE OPENING LOAD

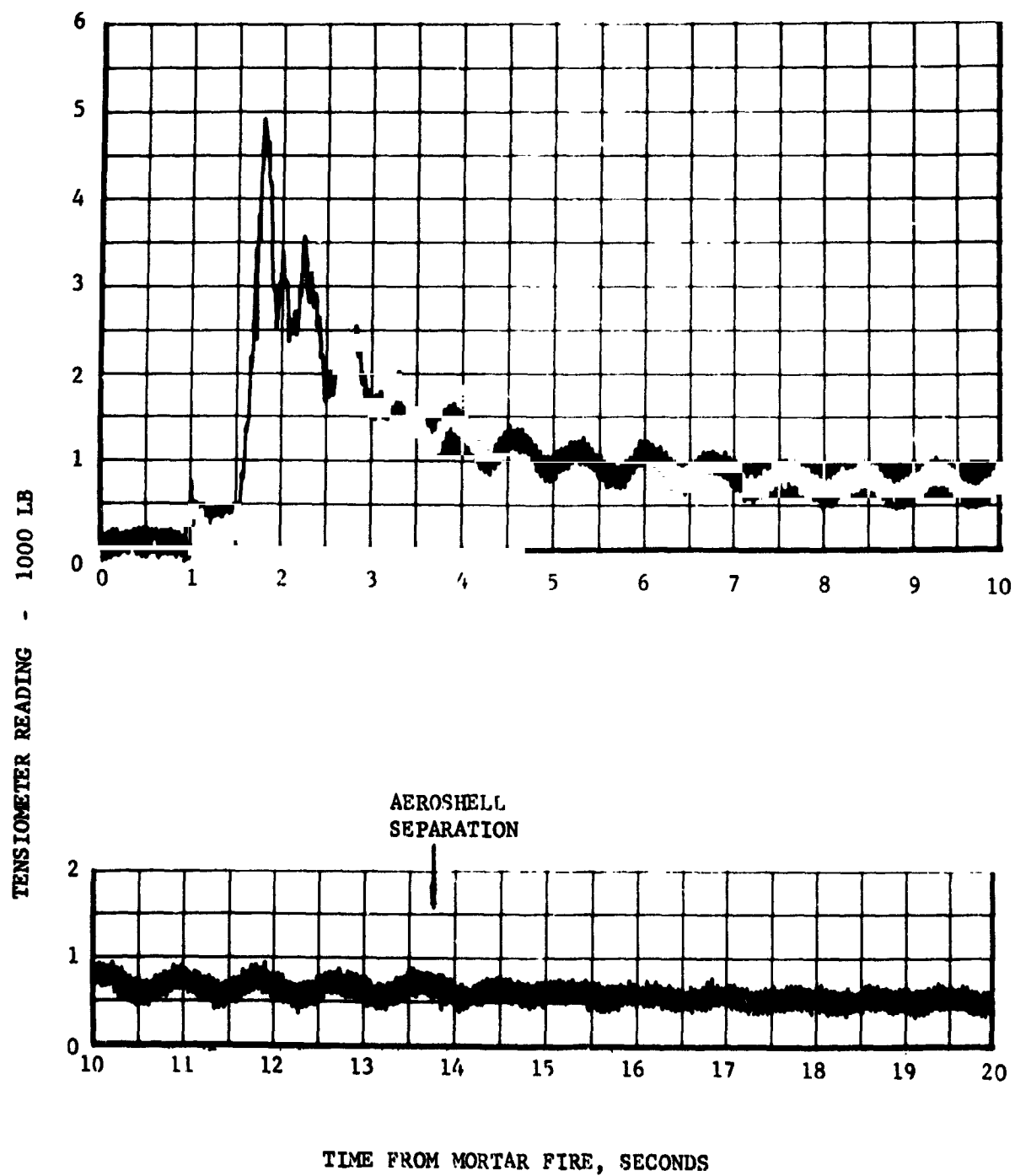
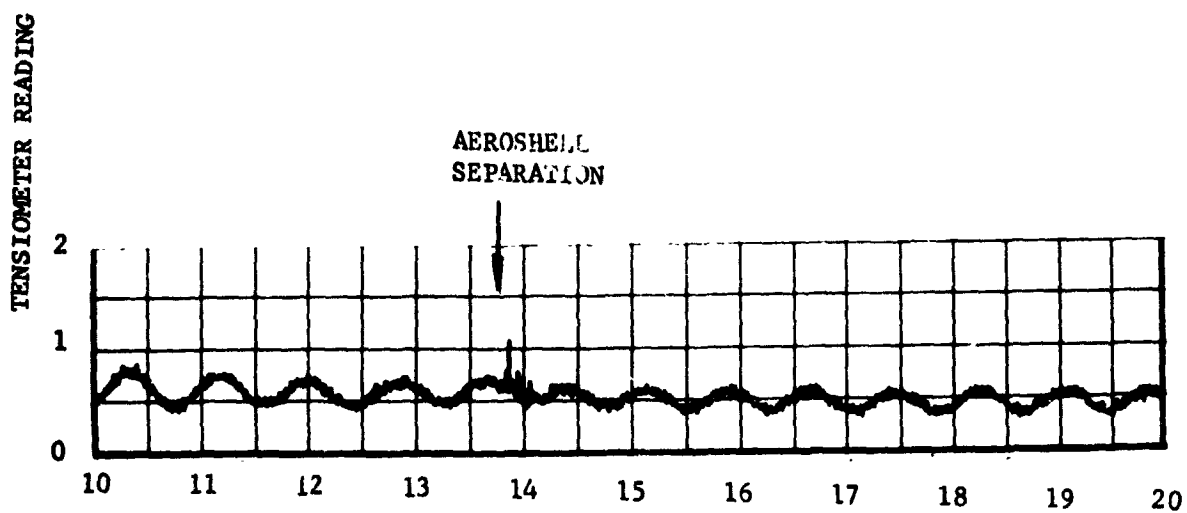
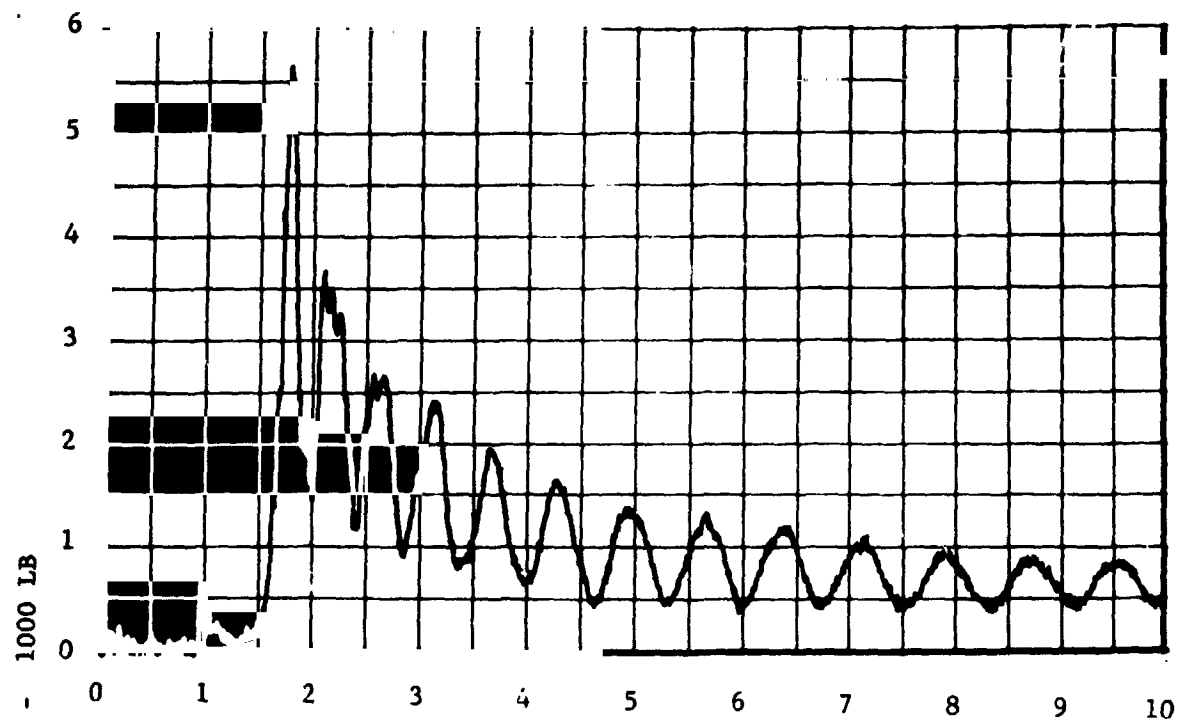


FIGURE V-7 TENSIO METER READING, BRIDLE  
LEG NO. 1



TIME FROM MORTAR FIRE, SECONDS

FIGURE V-8 TENSIO METER READING, BRIDLE LEG NO. 2

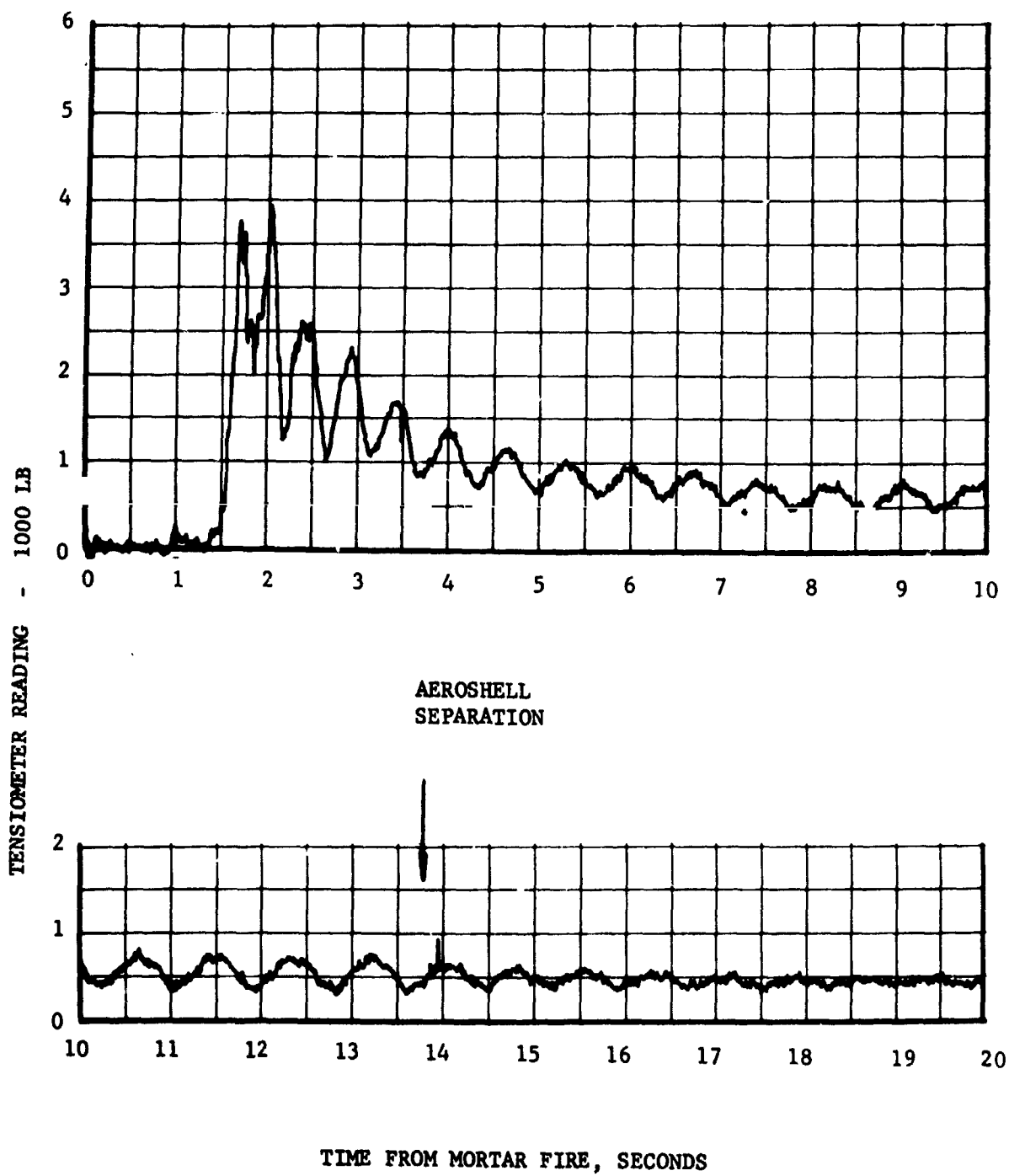


FIGURE V-9 TENSIO METER READING, BRIDLE LEG 3

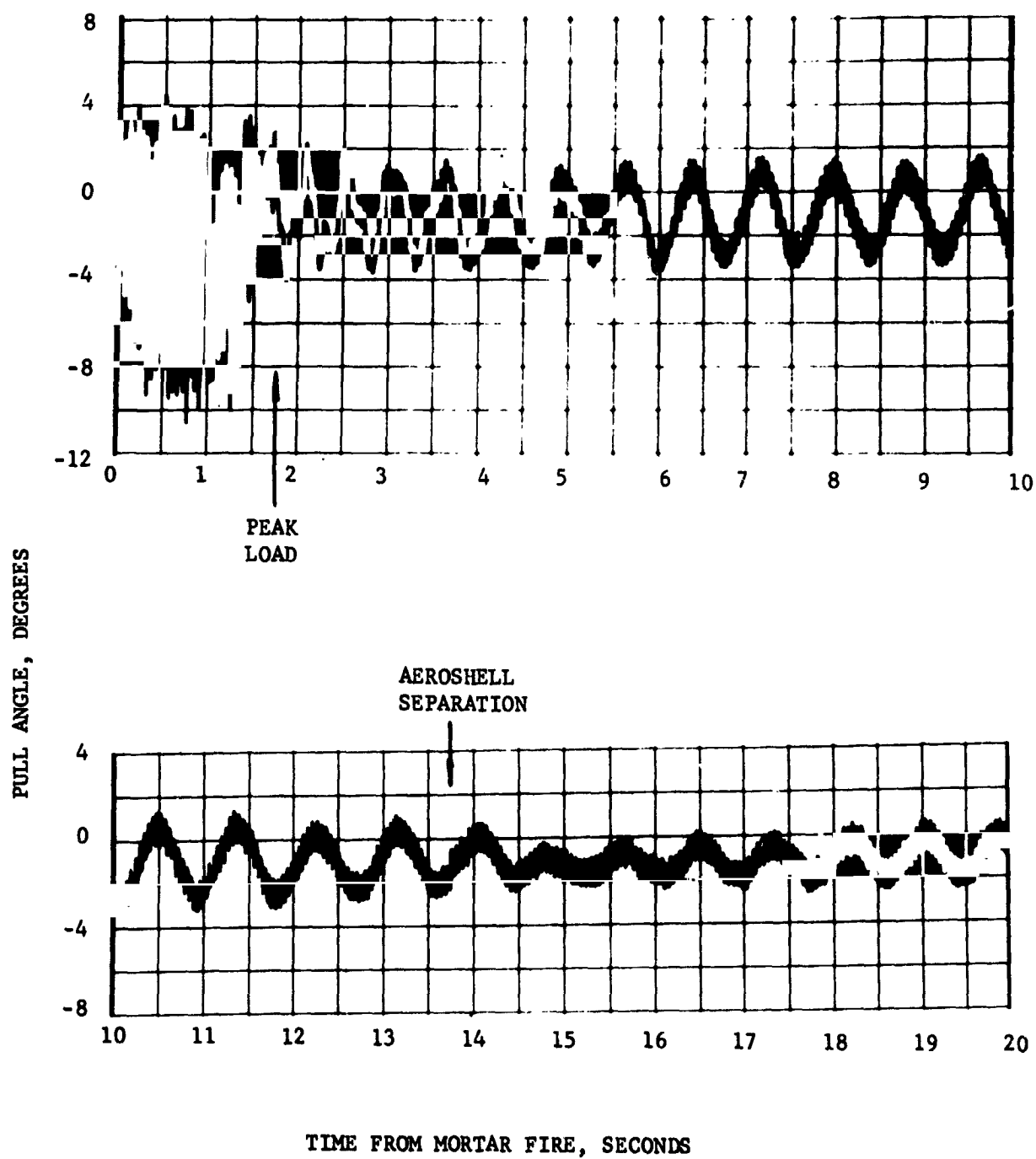


FIGURE V-10 PARACHUTE PULL ANGLE, PITCH PLANE



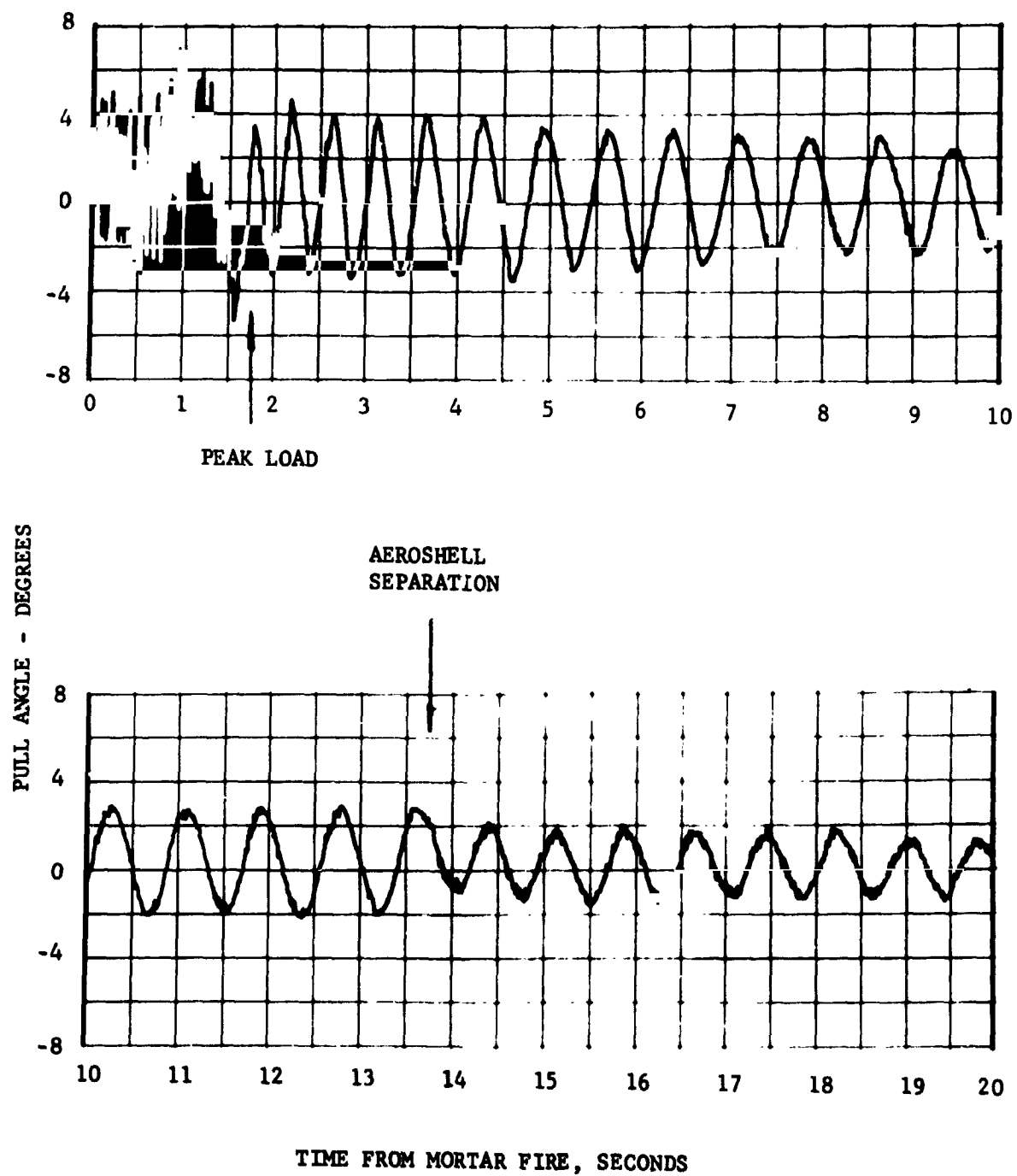


FIGURE V-11 PARACHUTE PULL ANGLE, YAW PLANE

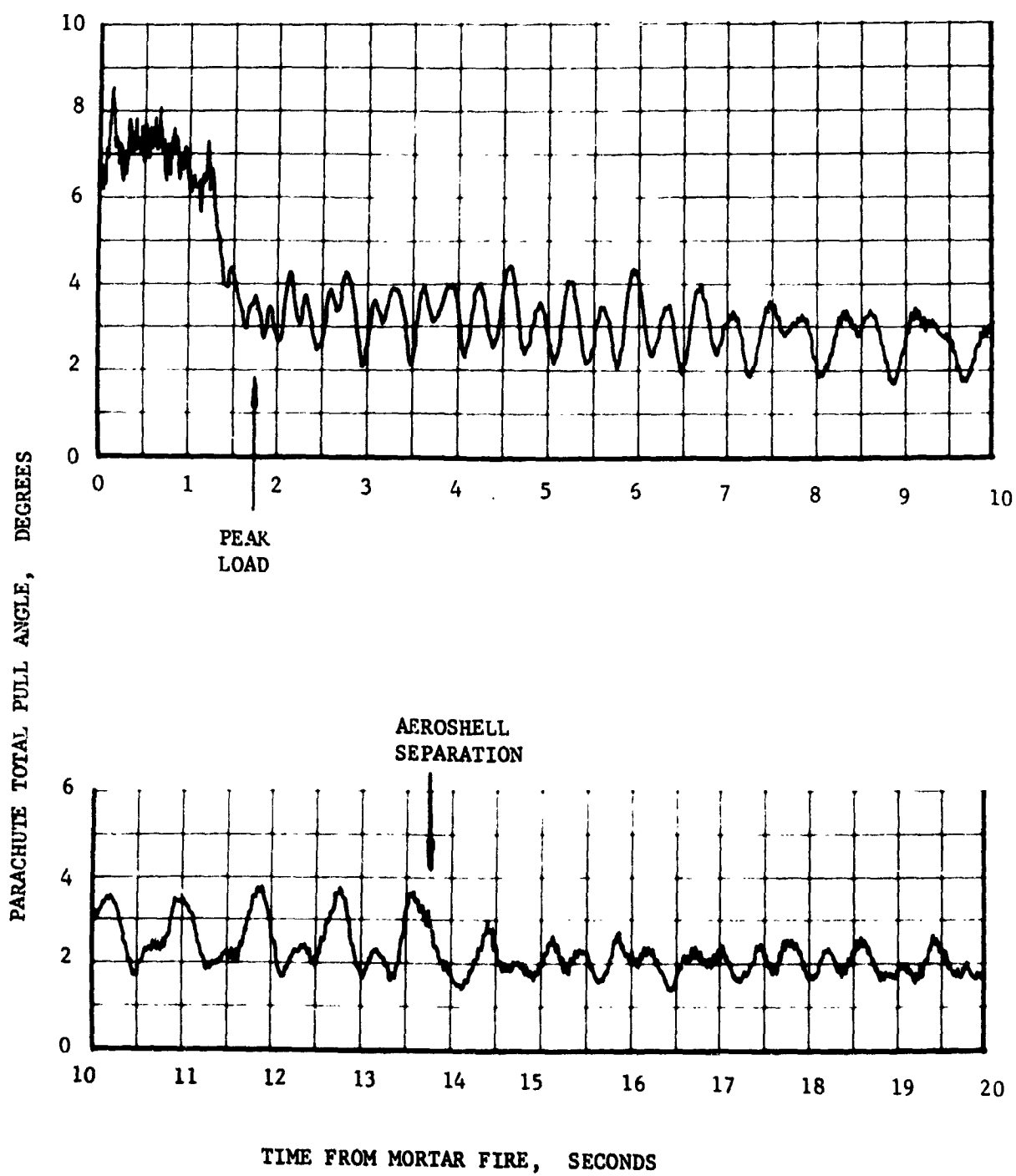


FIGURE V-12 PARACHUTE TOTAL PULL ANGLE

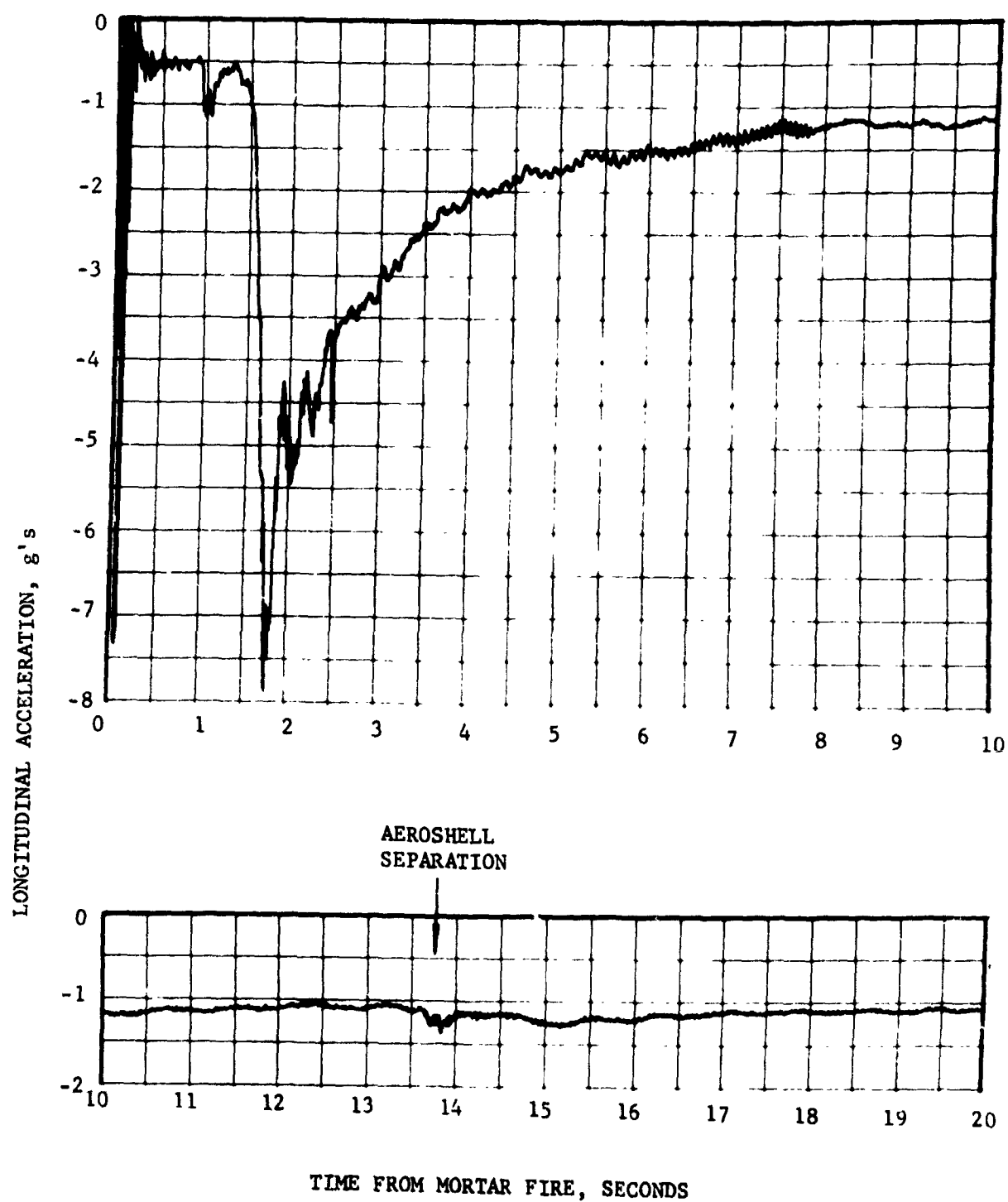


FIGURE V-13 LONGITUDINAL ACCELERATION

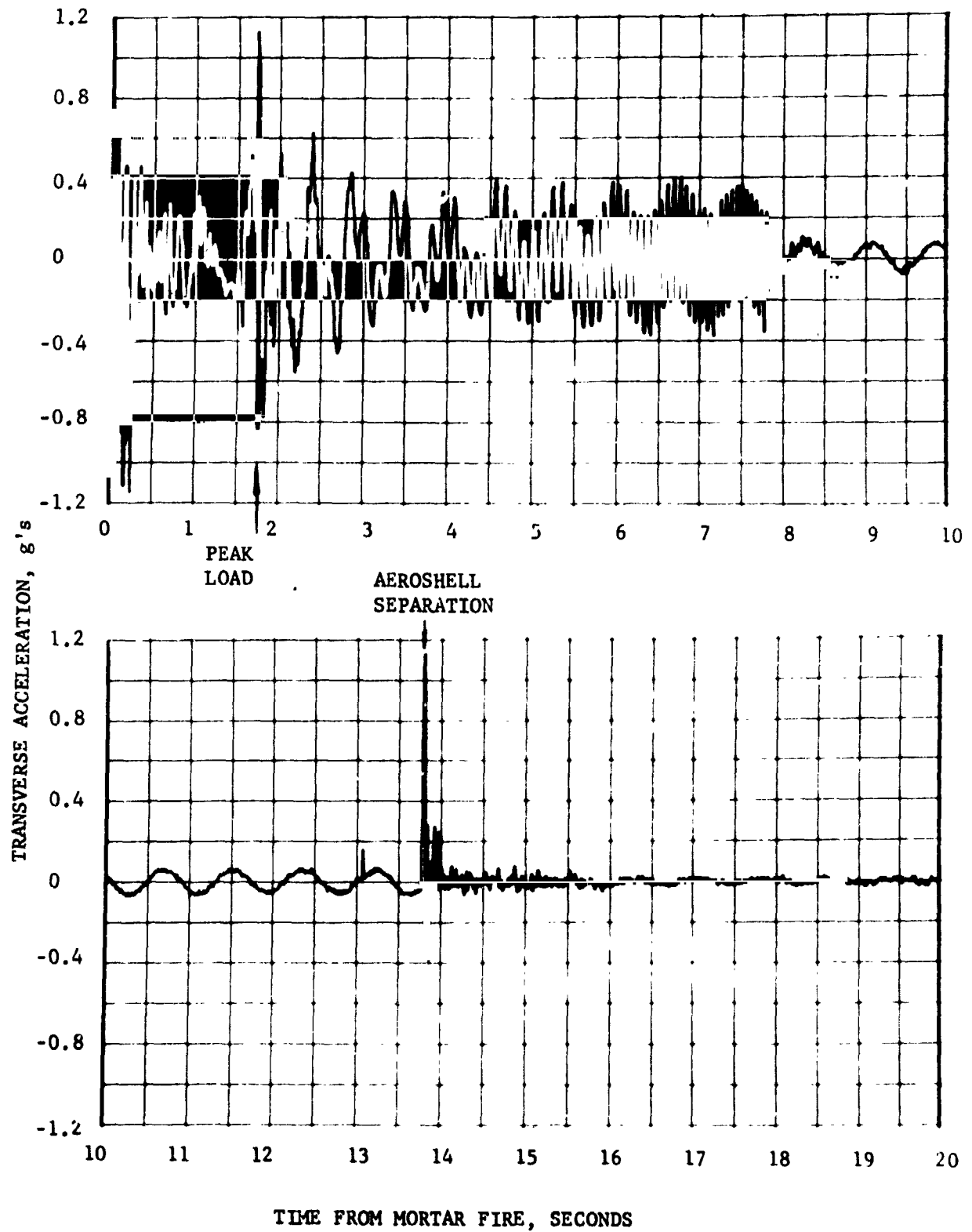


FIGURE V-14 TRANSVERSE ACCELERATION

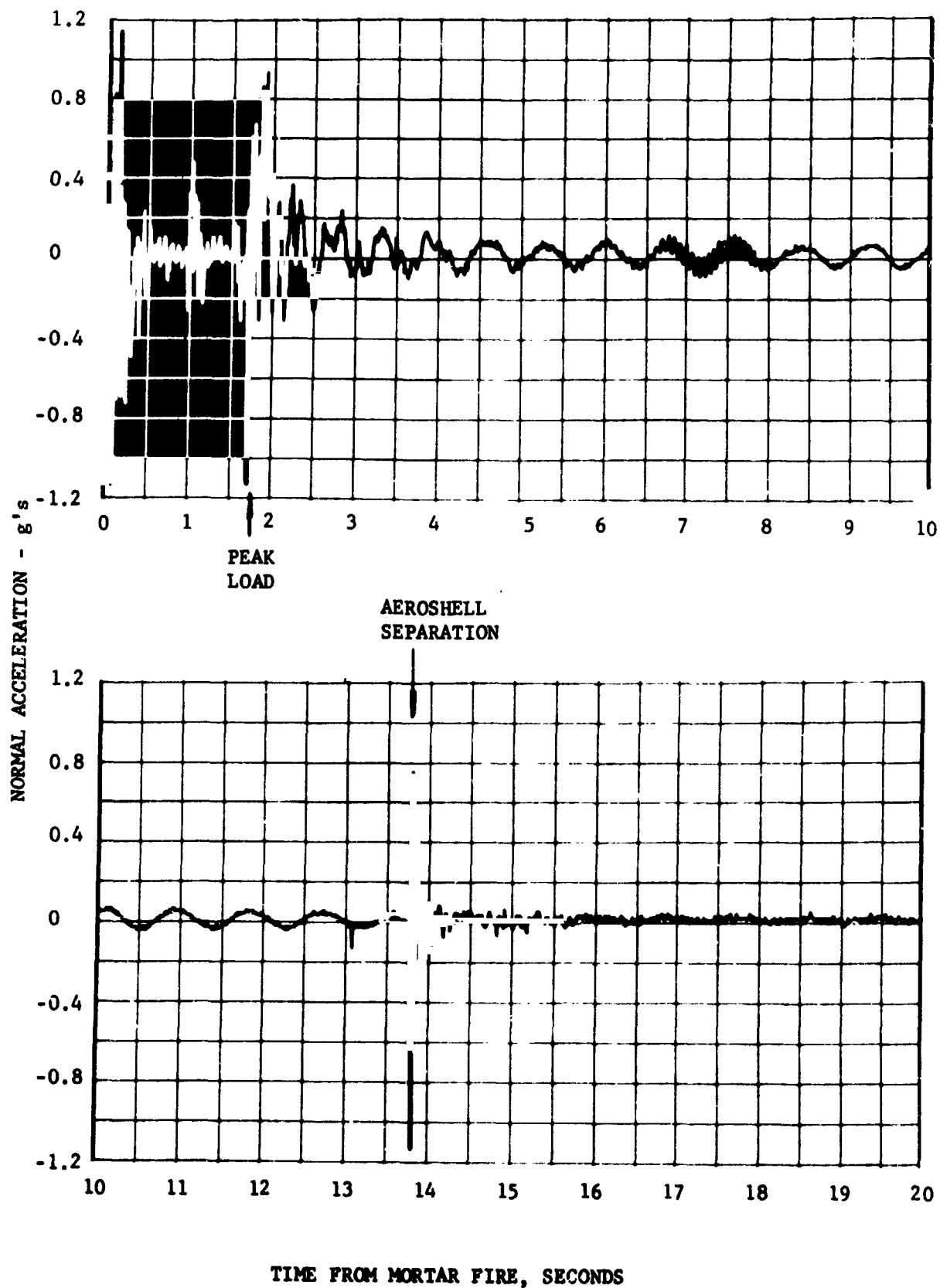


FIGURE V-15 NORMAL ACCELERATION

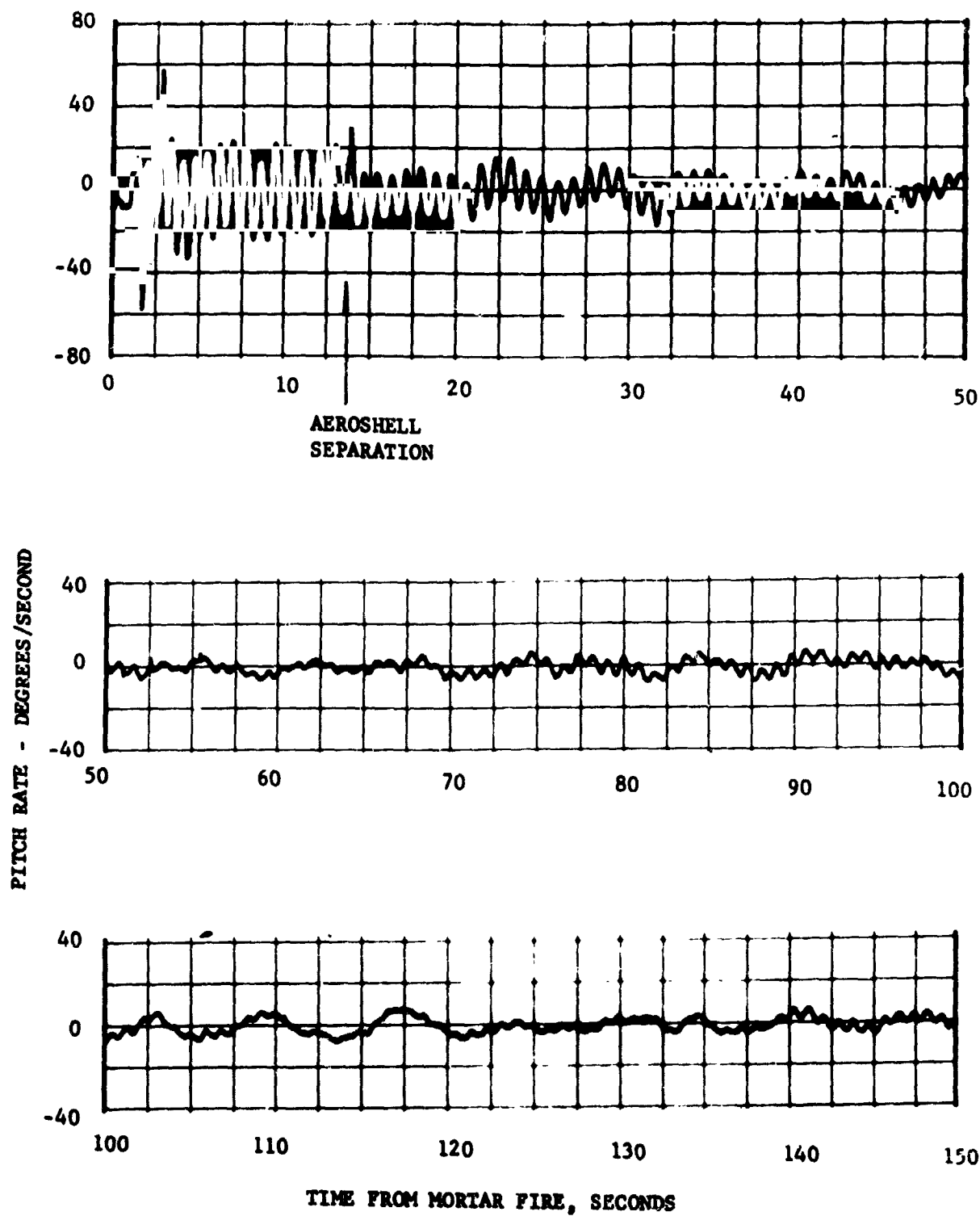


FIGURE V-16 VEHICLE PITCH RATE

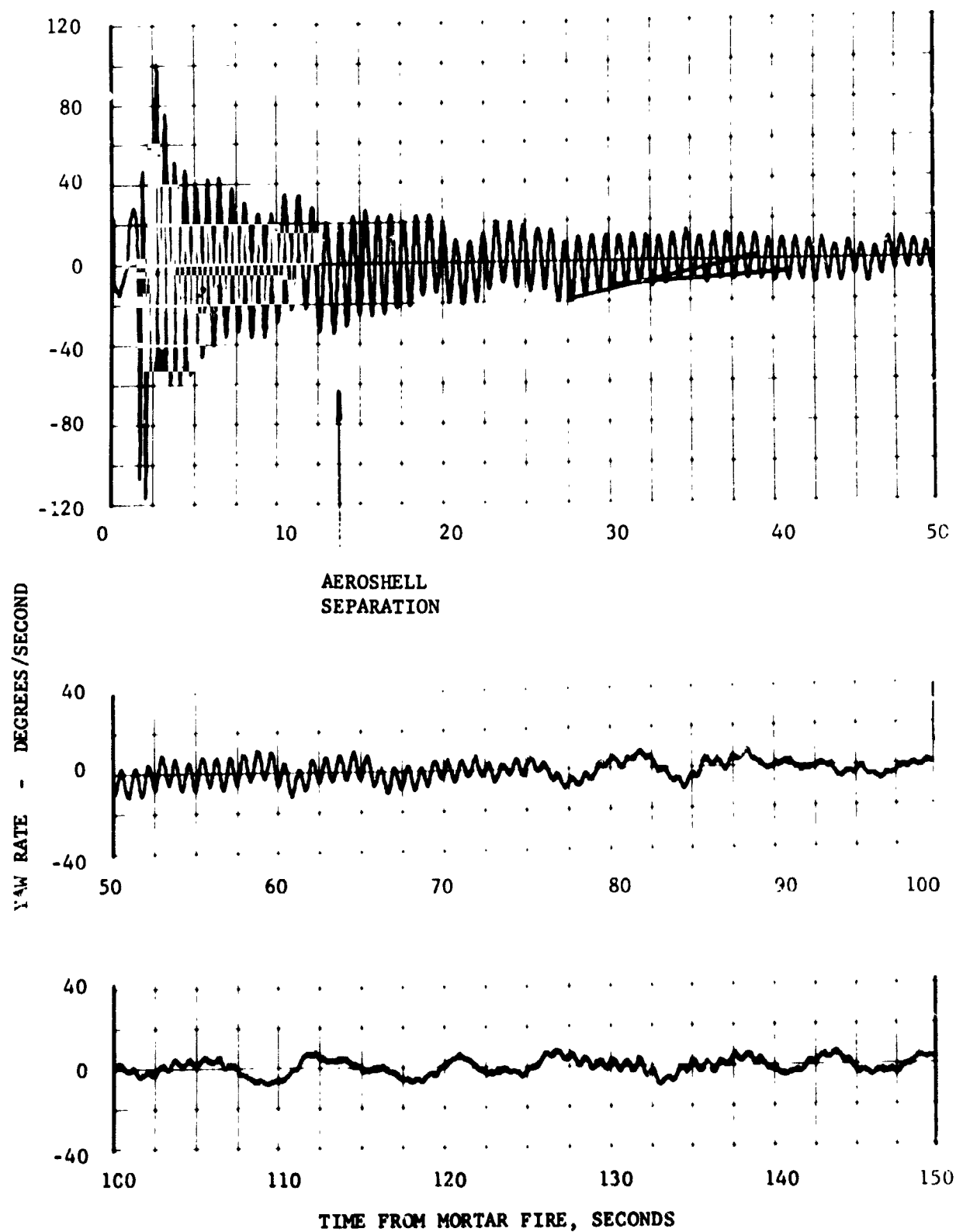


FIGURE V-17 VEHICLE YAW RATE

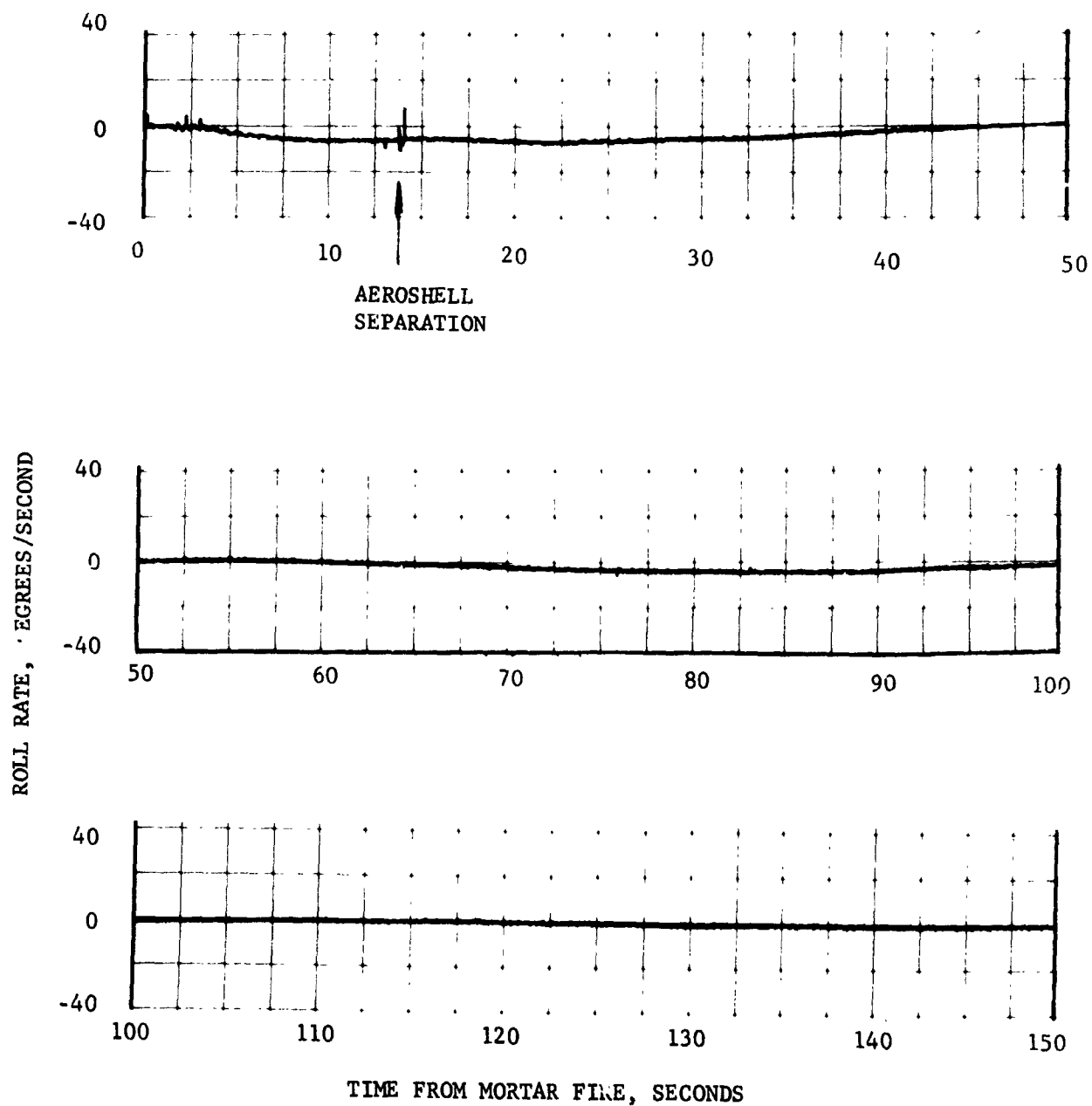


FIGURE V-18 VEHICLE ROLL RATE



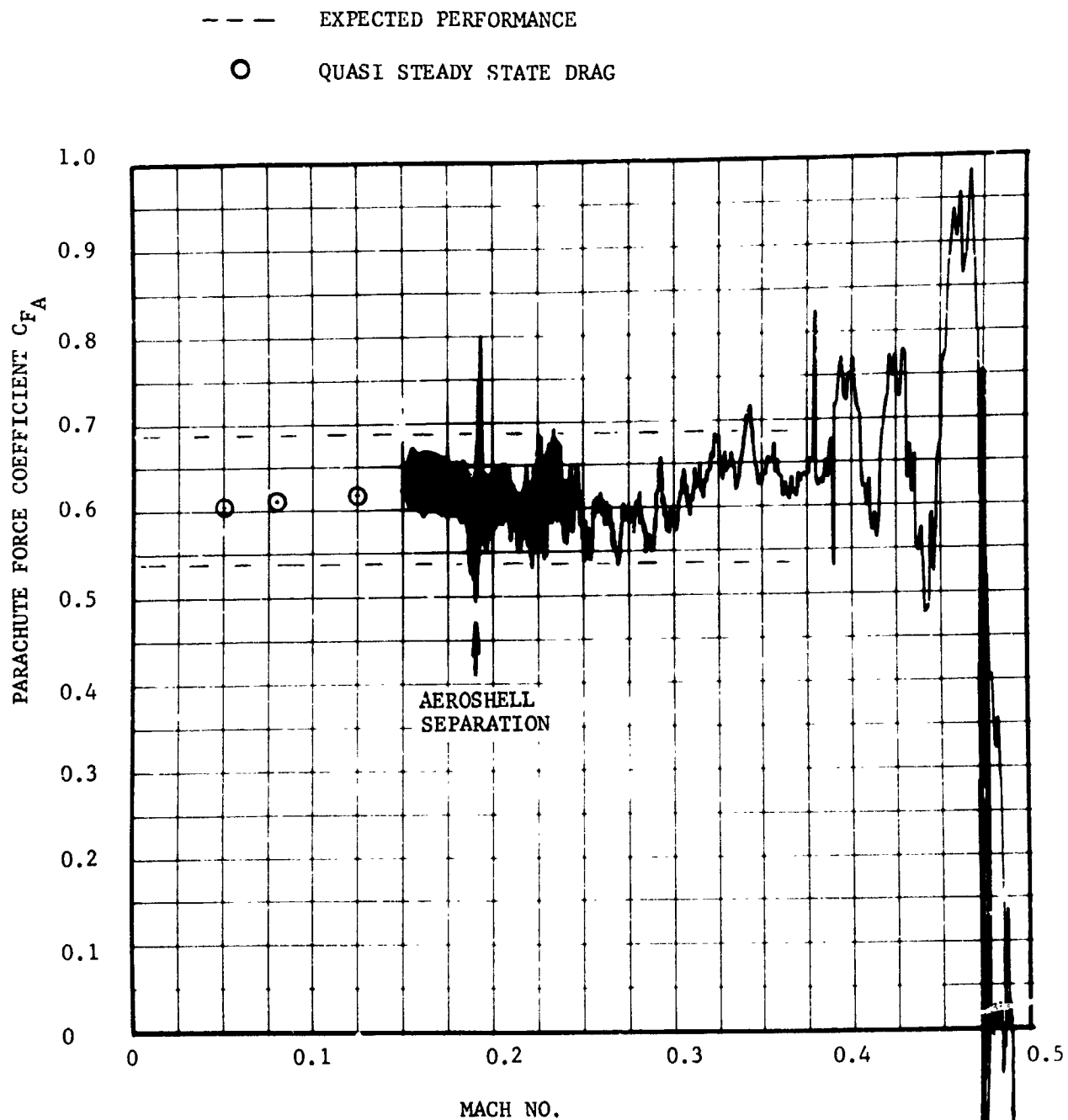


FIGURE V-19 PARACHUTE FORCE COEFFICIENT  
(ACCELEROMETER DATA)

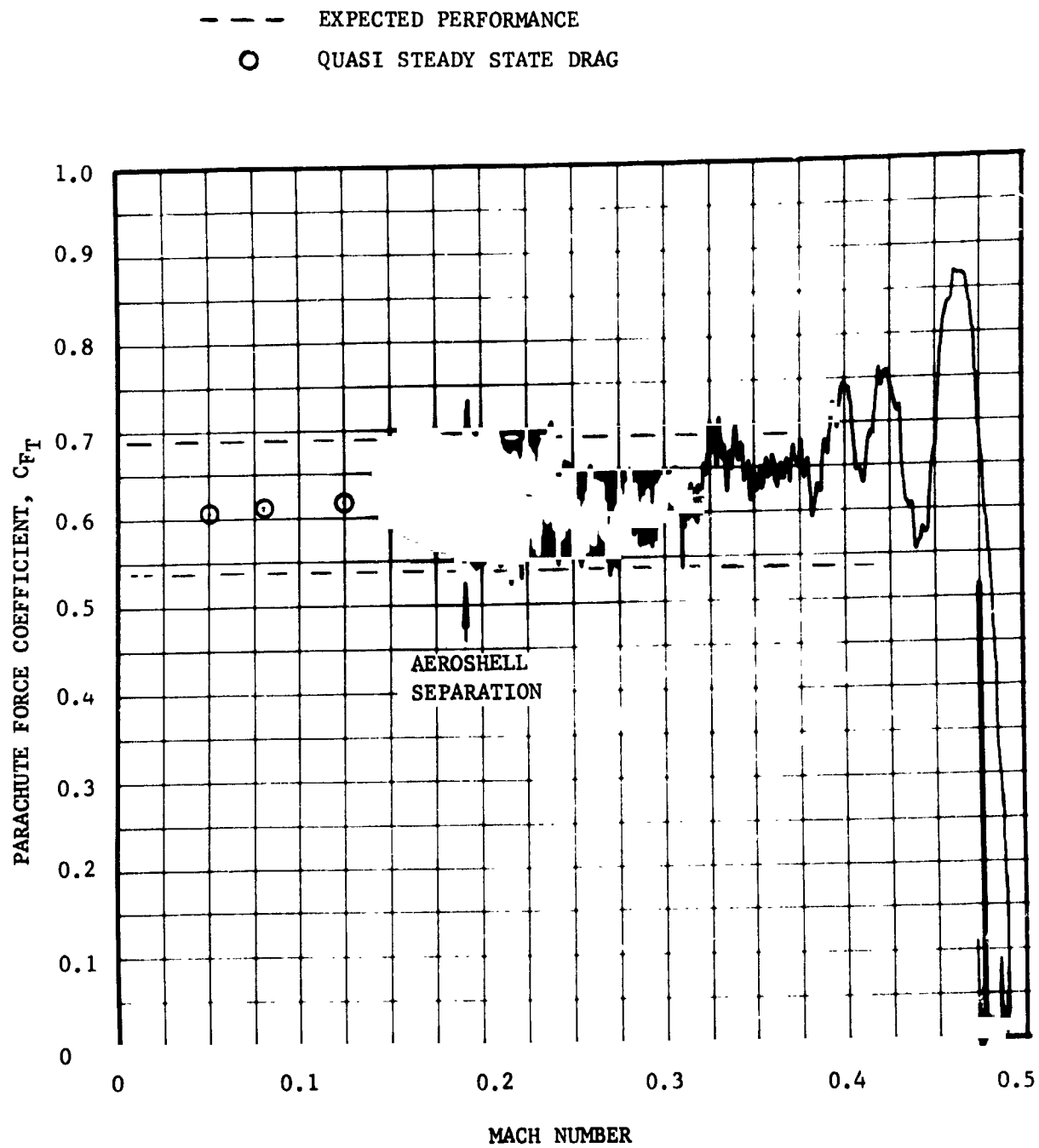


FIGURE V-20 PARACHUTE FORCE COEFFICIENT  
(TENSIMETER DATA)

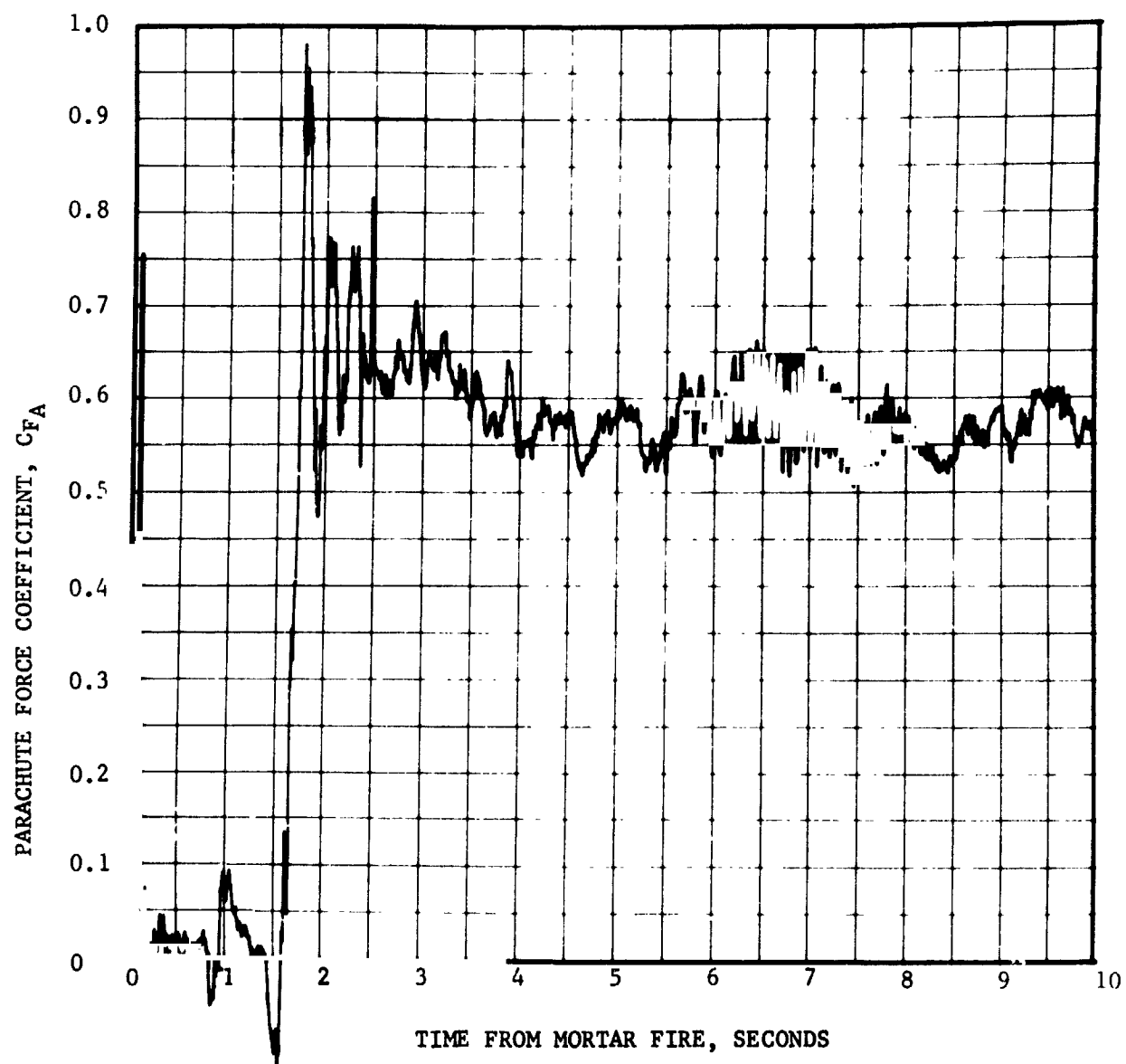


FIGURE V-21 PARACHUTE FORCE COEFFICIENT TIME HISTORY  
(ACCELERATION DATA)

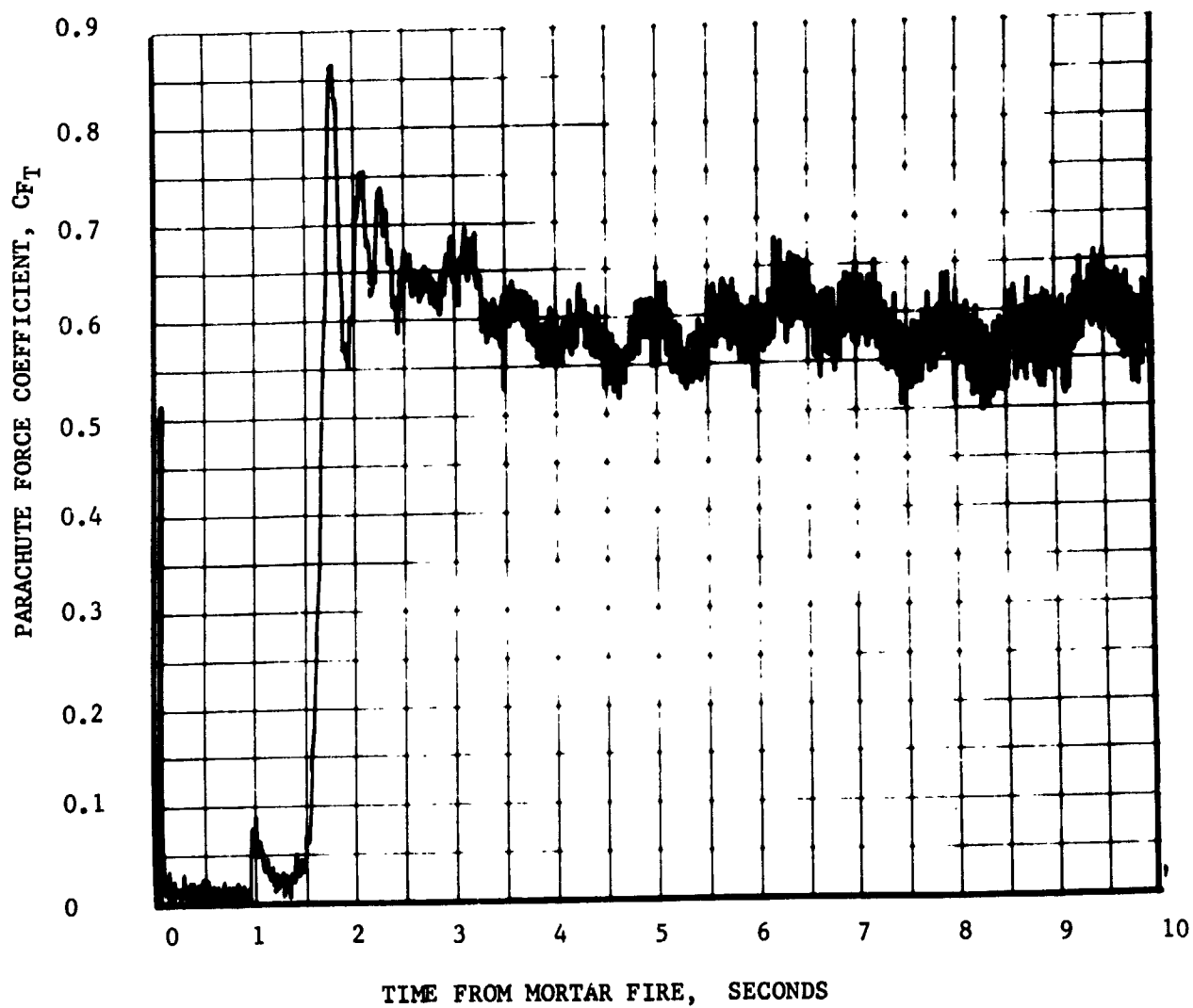


FIGURE V-22 PARACHUTE FORCE COEFFICIENT TIME HISTORY  
(TENSIMETER DATA)

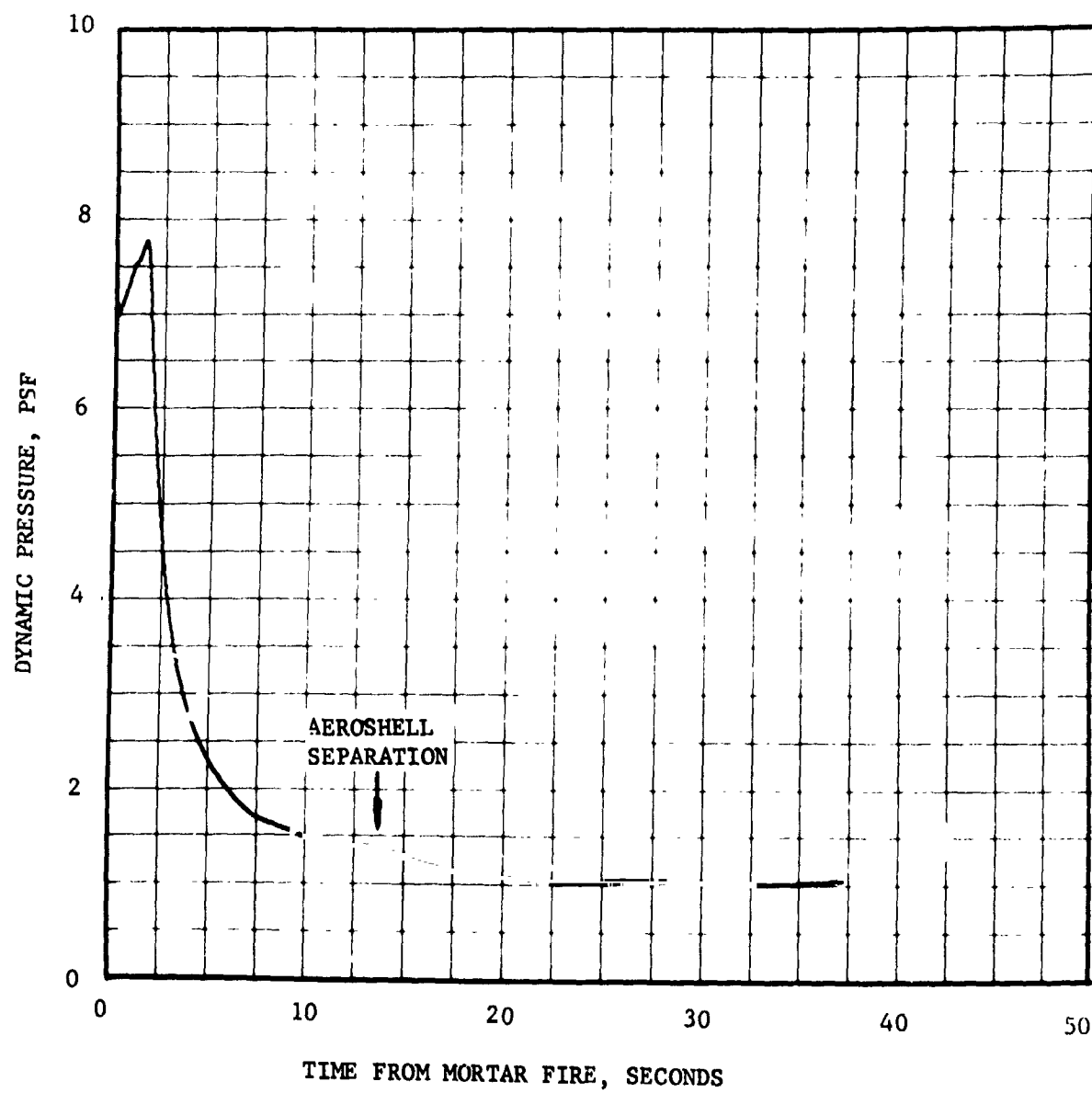


FIGURE V-23 DYNAMIC PRESSURE TIME HISTORY

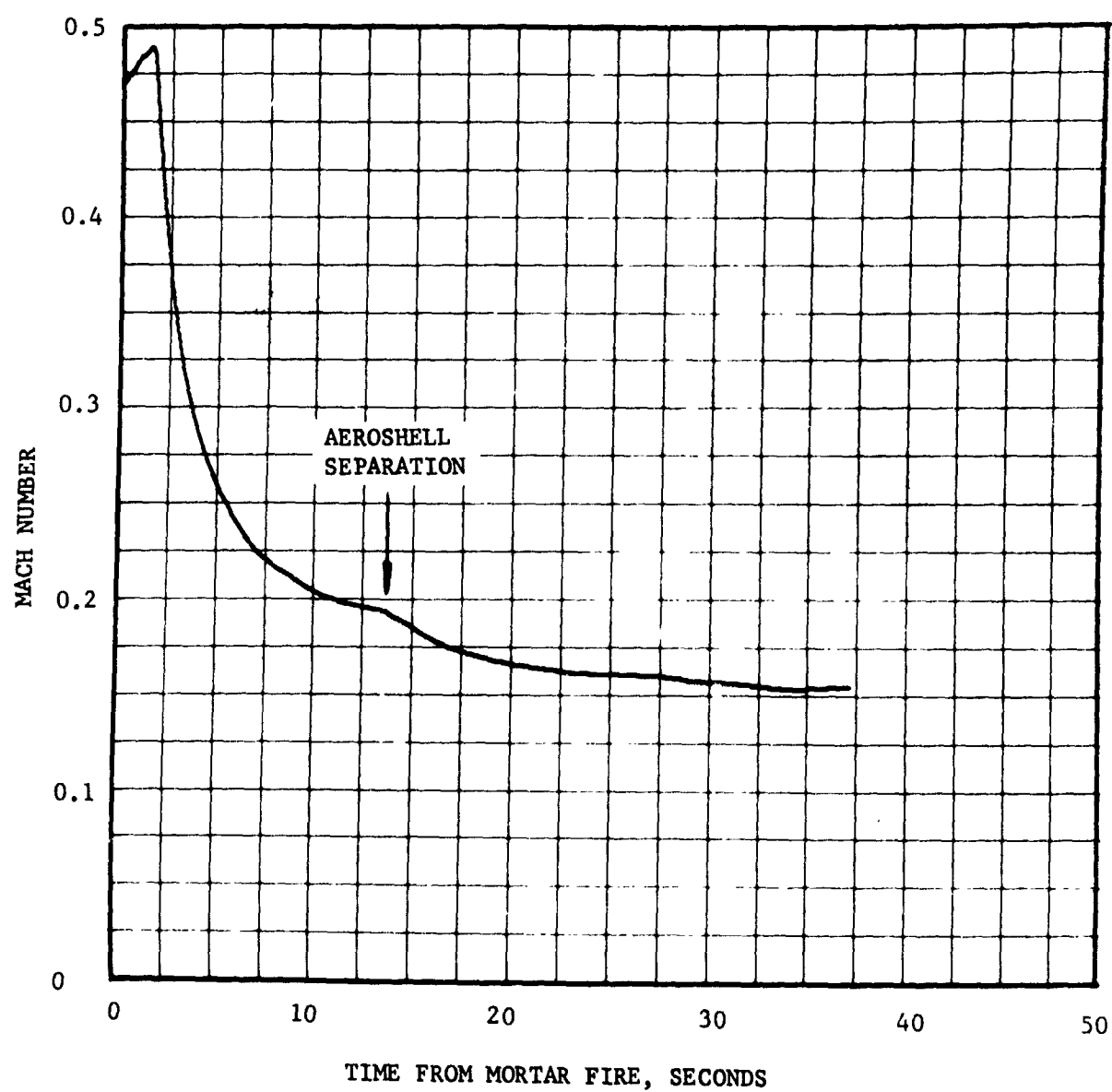


FIGURE V-24 MACH NUMBER TIME HISTORY

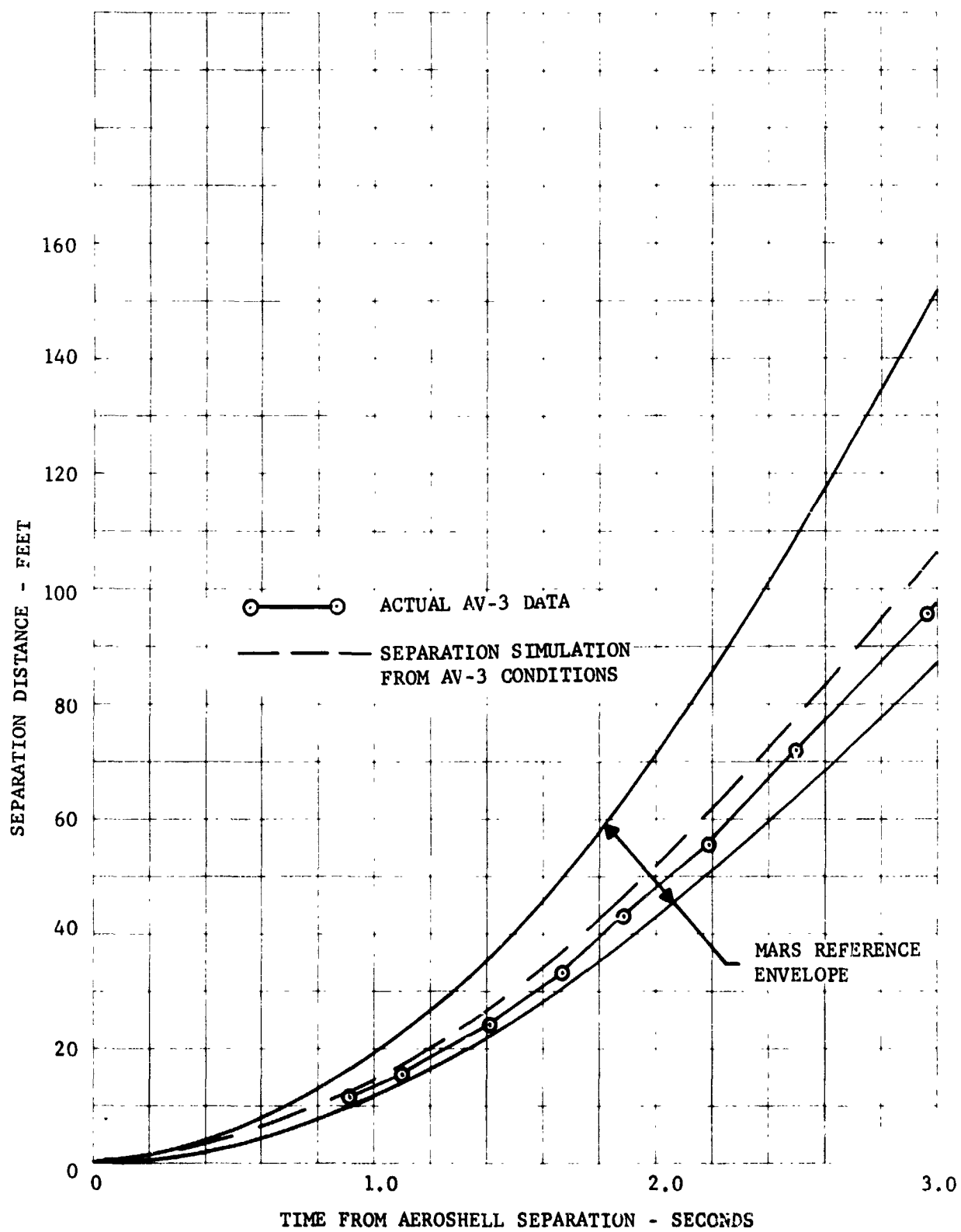


FIGURE V-25 AEROSHELL SEPARATION DISTANCE - 0-3 SECONDS

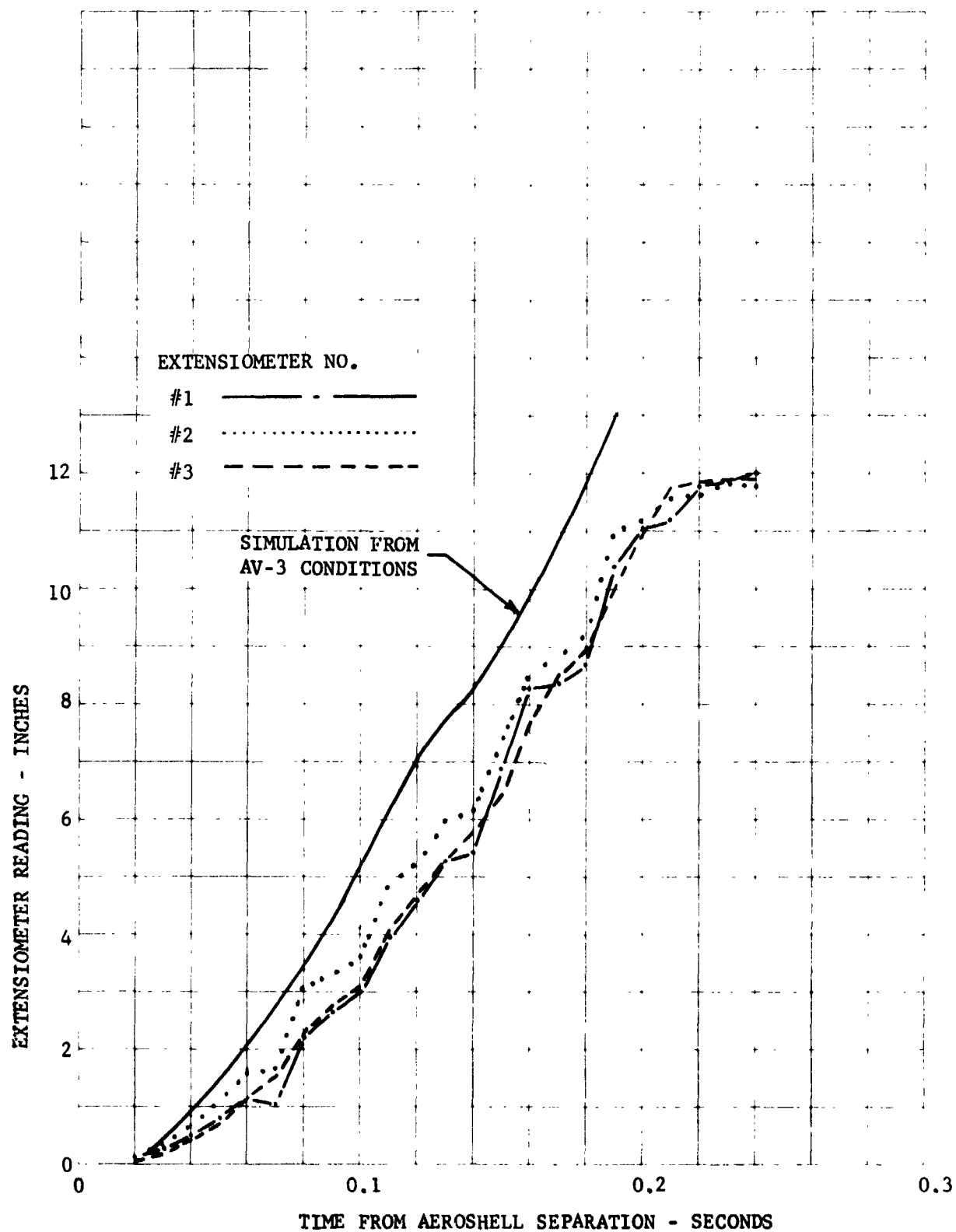


FIGURE V-26 EXTENSOMETER SEPARATION DISTANCE



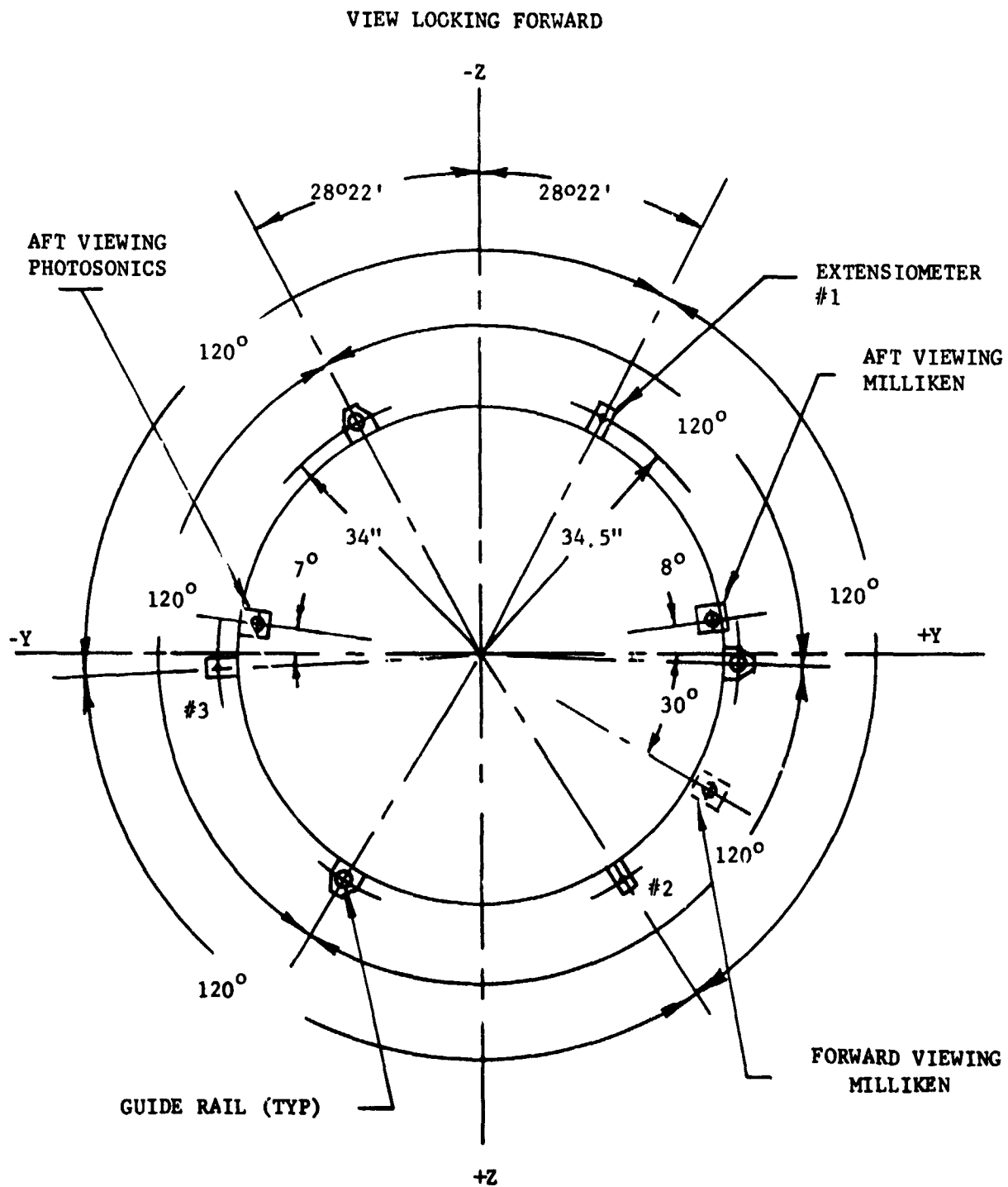


FIGURE V-27 EXTENSIOMETER AND GUIDE RAIL LOCATION

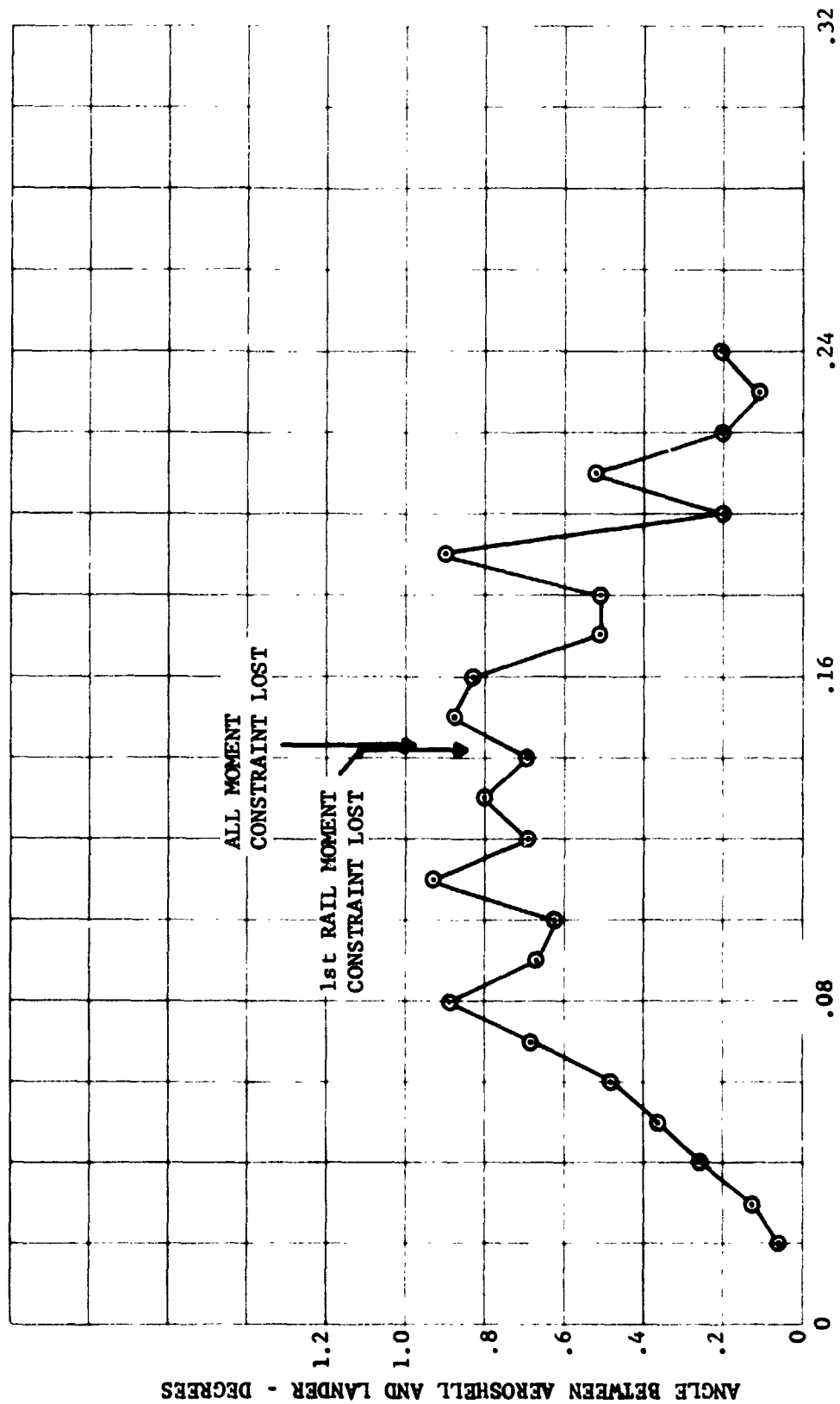


FIGURE V-28 RELATIVE ANGULAR MOTION BETWEEN AEROSHELL AND LANDER

## VI. VEHICLE PERFORMANCE ANALYSIS

The following is a summary assessment of the BLDT AV-3 free fall and deployment. The summary is presented by subsystem/discipline.

### A. Flight Dynamics

The objective of this portion of the report is to establish the actual free fall flight performance of the AV-3 vehicle from the command for vehicle release from the load bar through the command for decelerator mortar fire. The flight test of vehicle AV-3 was required to qualify the parachute in a subsonic, minimum velocity, domain to assure that the parachute would indeed inflate at low velocities without detrimental deployment effects such as squibbing.

The vehicle flight requirements for the subsonic test are established based on Mars anticipated environments and minimum entry velocities. The flight requirements stipulate that the velocity and dynamic pressure at peak load must be within the test envelope shown in Figure VI-1. Also shown are the target mortar fire and predicted conditions for both the onboard programmer and the ground computer generated command. These target conditions are:

	MACH NO.	DYNAMIC PRESSURE
Ground Command		
Mortar Fire	.469	6.224
Peak Load	.462	6.290
Onboard Programmer		
Mortar Fire	.498	7.270
Peak Load	.491	7.336

The above conditions were established such that the dynamic pressure is between 5.6 and 7.9 lbs/ft<sup>2</sup> and the velocity is less than 490 ft/sec.

1. Data Sources

The intent of this section is to evaluate the flight profile and parachute test conditions of BLDT AV-3 by reconstructing its trajectory using flight test data. The reconstruction is primarily based on three sources of data:

- o Meteorological data (density, velocity of sound, and winds);
- o Telemetry data (accelerometers and gyros); and
- o Radar data (slant range, azimuth and elevation).

a. Meteorological Data - Meteorological data were obtained by standard WSMR radiosonde observation (RAOB) probes. The RAOB probe produced pressure, wind direction and velocity and temperature at 5000 foot intervals from surface to approximately 110,000 feet. Four atmospheric profiles were obtained for the AV-3 flight as follows:

T-24 hr. data:

RAOB #544                      launched 18 August 1972 (White Sands)

T-6 hr. data:

RAOB #228                      launched 19 August 1972 (Jallen)

T-1 hr. data:

RAOB #0139                    launched 19 August 1972 (SMR)

T+1 hr. data:

RAOB #0495                    launched 19 August 1972 (Holloman)

A comparison of the density of the above data shows that the T+1 hr. data were closest to the T-24 hr. data and representative of the

average of all the data. Therefore, the T+1 hr. data as shown in Table VI-1 were used for all flight analyses.

b. Telemetry Data - The flight vehicle telemetry (TM) data was transmitted via an S-band link to the WSMR receiving stations J-10 and J-67 where it was recorded and retransmitted via microwave links to the flight operations control station at building 300. These receiving stations are geographically located to provide continuous coverage of the real time mission. Their locations are shown in Figure VI-2. At Building 300, the TM data were recorded for post-flight usage and also transmitted to various displays for observation and control of the mission.

The drop time reference used for the radar data reduction at WSMR was 63900.00 Z. The TM data were referenced to a 63900.540 Z drop time resulting in a .540 second time shift between the two data sources. The actual drop time may be determined within limits from the received and recorded TM tones. Tones A-reset and B-reset start the onboard programmer and tones 1, 3 and 7 initiate parachute mortar fire. The tone commands are interigated at .033 second intervals (commutator channels) preventing an exact determination of the time of command receipt. The recorded times for the TM tones are:

TONE	TIME (Z)
7	63900.6007
1B	63900.6249
A-Reset	63900.6249
B-Reset	63900.6250
3	63900.6286

Drop must have occurred between 63900.5953 and 63900.6007 Z and the actual drop time was defined as 63900.600. The time shift in the

TM reference drop time (.06 sec) was assumed negligible, but the time shift in the radar data (.6 sec) was significant and corrected prior to the use of these data.

The conditioned and smoothed TM rate gyro and accelerometer data, which were used for flight analysis, are shown in Figures VI-3 through VI-6. Figures VI-3 and VI-4 are gyro and accelerometer data respectively for the time period prior to the vehicle release from the load bar.

Figures VI-5 and VI-6 are the same data during vehicle powered flight. It is noted that all of the accelerometer and gyro data were smoothed and conditioned except the accelerometer data prior to drop which was only conditioned. These data were filtered with a seventy (70) point standard least squares quadratic leading edge filter. The conditioning was based on a two sigma ( $2\sigma$ ) dispersion limit of the filtered data with wild points replaced by the quadratic prediction.

The initial estimates of instrumentation bias were obtained from these plots by integrating the gyro data during the float period (Figure VI-3) and adjusting the accelerometer data for zero setting during the free fall portion of flight immediately after release from the load bar (Figure VI-4). The TM instrumentation system is designed to provide a 5% end to end error tolerance limit but with the above biases it is judged that the instrumentation accuracies can be assumed to be 2%. This provides the following accuracies:

<u>FUNCTION</u>	<u>TOLERANCE</u>
Gyros	6 deg/sec
Lateral Accelerometers	0.02 g's
Longitudinal Accelerometer	0.10 g's

c. Radar Data - The BLDT vehicle was tracked by (3) WSMR FPS-16 radar sets, two (2) were beacon track and one was skin track. The beacon track radars (R122 and R113) were used for continuous track of the vehicle until loss of beacon ( $T + 400$  sec) at which time they switched to skin track. The skin track radar was utilized to track other system components such as balloons, load bar and aeroshell. The stated accuracy of the FPS-16 radars is 0.1 to 0.3 mils in angles and 15 to 45 feet in range, which is approximately 50 feet of space position.

The radars provided slant range (R), azimuth (a) and elevation (e) data with respect to the radar site. Only the beacon track radars were considered for performance analysis. These radar locations are shown in Figure VI-2. An analysis of the radar data consisted of transforming the (R), (A) and (E) from a given site to an (R), (A) and (E) of a second site where the derived (R), (A) and (E) were compared with the actual measured data for the second site. This analysis was completed for radar sites R122 vs. R113. This analysis indicates that there was a systematic bias between the two radars. This bias is 85 ft. in slant range, 50 ft. in azimuth and 125 ft. in elevation. The time plots of (R), (A), and (E) differences between the two radars are presented in Figure VI-7. R122 was selected as the prime radar due to the fact that it was much closer to the drop location than R113.

The radar data were post-flight corrected by WSMR for systematic errors which were determined by pre-flight calibrations. Raw data of range, azimuth and elevation were smoothed by standard WSMR filter techniques to produce velocity, altitude, flight path angle and azimuth. These velocity and altitude data are presented in Figure VI-8 and VI-9 for radar site R122. These data are earth reference measurements and are not ambient aerodynamic conditions.

## 2. STEP Trajectory Reconstruction

The Statistical Trajectory Estimation Program (STEP) (Reference 9) was used to determine the reconstructed trajectory. This program solves for the initial conditions (position, velocity, and attitude of the vehicle) so that by integration of the gyros and accelerometers the trajectory matches the radar data (range, azimuth and elevation). Besides solving for initial condition it has the capability of determining the systematic errors (biases and scale factors) on the gyros and accelerometers. The program gives a minimum variance solution on the radar measurements (range, azimuth and elevation). The trajectory is considered to be the optimum when the radar data are randomly dispersed about the reconstructed trajectory and the variance of the range, azimuth and elevation is within the expected tracking accuracies of the radar.

STEP requires an estimate of the biases and scale factors on the gyros and the accelerometers. In order to obtain these biases on the gyros, the telemetry data were examined from T-45 seconds to T+0 (vehicle drop). These data are shown in Figure VI-3. At this time the vehicle had approximately 0.5 deg/sec rotational motion on the load bar.

The combination of this motion with the telemetry data was used to determine the biases on the gyros. These biases are:

Roll gyro (P)	-8.0 degrees/second
Pitch gyro (Q)	-3.99 degrees/second
Yaw gyro (R)	-7.61 degrees/second

To determine the biases on the accelerometers, the data between T+0 and T+1 second were analyzed. These are shown in Figure VI-4. At this time the vehicle is in a near zero force field which permits establishing a zero setting. The average values of the accelerometer readings at this time were:



X-accelerometer	-0.05 g's
Y-accelerometer	+0.0 g's
Z-accelerometer	+0.0 g's

The scale factors on the gyros and accelerometers were initialized at unity.

The initial estimates of position and velocity at drop were obtained from smoothed radar data:

Latitude	34.0136 deg.
Longitude	-106.2438 deg.
Altitude	91,148 ft.
Velocity	55 ft/sec
Flight Path Angle (Gamma)	0 deg.
Azimuth	95.0 deg.

The initial estimates of the body Euler angles are required for body heading (PSI), pitch (THETA) and roll angle (PHI). The initial Euler angle estimates are:

PSI	16°
THETA	-94°
PHI	0°

The initial estimate for PSI was taken from the load bar camera at drop while THETA was estimated at -94° based on nominal value. Given these initial conditions and previously established biases and scale factors STEP provides a very good fit to the radar (R122) data between T+0 and T+20 seconds. The radar tracking data deviated from the reconstructed trajectory by the following standard deviation.

$\sigma_{\text{slant range}}$	= 4.9 ft.	
$\sigma_{\text{azimuth}}$	= $7.5 \times 10^{-3}$ deg.	55 ft. (position error)
$\sigma_{\text{elevation}}$	= $5.7 \times 10^{-3}$ deg.	43 ft. (position error)

STEP reconstructed trajectory provides a very accurate measurement of altitude and velocity. Combining these values with the meteorology data, velocity relative to the wind, Mach number and dynamic pressure were computed. Time history of altitude, velocity, Mach Number and dynamic pressure are shown in Figures VI-10 and VI-11. The conditions established by STEP at mortar fire and peak load, provided in Table VI-2, show that the flight performance did meet the requirements for dynamic pressure as required in Figure VI-1. The angle of attack, sideslip and total angle of attack are shown in Figures VI-12 and VI-13.

In conclusion, the actual velocity dynamic pressure test conditions were well within the success criteria deployment box (Figure VI-1) for the subsonic flight test. However, the dynamic pressure and altitude at deployment were not within their computed  $2\sigma$  dispersion limits. This anomaly in predicted test conditions was because of a low drop altitude. The drop altitude was consistently low for all the BLDT flights.

The predicted flight conditions with respective statistical dispersion estimates are compared below with the actual flight conditions.

	<u>Predicted Value</u>	<u><math>2\sigma</math> Dispersion</u>	<u>Actual Value</u>
Dynamic Pressure	6.22	5.84 - 6.60	6.90
Velocity	461	456 - 466	464.3
Mach Number	.469	.463 - .475	.471
Altitude	88,800	87,336 - 90,264	87,027
Total Angle of Attack	4.2	2.8 - 5.7	5.7

It is noted that if the drop altitude had not been 1,700 ft. low, all flight conditions would have been within estimated  $2\sigma$  dispersions at deployment.

## B. Capsule Aerodynamic Characteristics

The aerodynamic forces and moments on the vehicle were evaluated during the free fall trajectory based on the gyros and accelerometer data. The axial force coefficient is shown in Figure VI-14, and appears to be slightly lower than predicted. The transverse and normal accelerations were essentially zero, as expected, as was the roll acceleration. The pitch/yaw gyro rate data was differentiated to obtain the rotational acceleration and applied moments using the equation:

$$\begin{aligned} PM &= \dot{Q} \times IYY \\ YM &= \dot{R} \times IZZ \end{aligned}$$

where:

$$\begin{aligned} PM &= \text{Pitch moment, ft-lb} \\ YM &= \text{Yaw moment, ft-lb} \\ IYY &= \text{Pitch moment of inertia, } 339 \text{ slug-ft}^2 \\ IZZ &= \text{Yaw moment of inertia, } 296 \text{ slug-ft}^2 \\ \dot{Q} &= \text{Pitch acceleration, rad/sec}^2 \\ \dot{R} &= \text{Yaw acceleration, rad/sec}^2 \end{aligned}$$

The angles of attack and sideslip at which the predicted aerodynamics would generate these moments are compared to the STEP reconstructed angles in Figure VI-14. There is good agreement near parachute deployment between these two methods for obtaining vehicle attitude, however, near drop, the deviations need discussion. The STEP results are based on inertial rates and motions which are then corrected for the relative wind using meteorological data. When the velocity is low, large relative angles are produced by small wind inaccuracies. Conversely, the differentiation of the gyro data is inherently noisy, however, the applied moments are dependent on the slope of the rate data which makes this method insensitive to biases in the instrumentation. The period and phasing of both pitch and yaw oscillations are more indicative of an initial vehicle attitude error as opposed to a tip-off rate at drop.

The pitch/yaw motions are judged to be the result of a wind shear during the initial descent.

### C. Thermal Control Subsystem

The design requirements for the BLDT Thermal Control subsystem were based on maintaining previously qualified hardware within the maximum and minimum specified qualification temperatures. Except for several isolated electrical heaters, a passive thermal control system was utilized on the BLDT vehicle for ascent and float control. The passive system was based on vehicle attitude and vehicle ascent rate to float altitude with convection, solar radiation, reflected solar radiation and infrared radiation being the major heat transfer parameters being considered.

The design ascent profiles are shown in Figure VI-15 with a fast ascent rate, when integrated with the above mentioned parameters, producing the hot case and the slow ascent rate producing the cold case. Figures VI-16, VI-17, VI-18 and VI-19 show select hot and cold case predicted temperature profiles for the base cover, rocket motor support structure, aeroshell and S-band transmitter respectively. Also shown in these figures are discrete point actual temperatures, extracted from the TM data which were recorded at approximately half hour intervals.

It can be seen in Figure VI-15 that the ascent rate was the equivalent of a fast ascent when the system broke out of the low altitude float mode. The actual heat transfer condition deviated from the prediction as follows:

1. Prior to actual ascent, the system was probably enclosed in clouds.

2. The vehicle was wetted by atmospheric moisture with ice formation affecting the actual temperatures.
3. The vehicle base cover exterior was somewhat coated with cornstarch.

With the above conditions, it is probable that a hot case condition would result due to rapid ascent and freezing moisture as shown on the plots for the base cover, RMSS and aeroshell, the temperature histories do approach a hot case, once the system starts the actual ascent.

Since the S-Band transmitter is subject to heating due to electrical power consumption, the temperature profile for the transmitter is probably more effected by the unpredicted moisture and ice formation. This contributes to a cold case transmitter profile as shown in Figure VI-19.

Presented below is a table showing the temperatures measured by the "on-board" thermistors at the time of vehicle release from the load bar and at aeroshell separation compared with the specified requirement at vehicle drop.

	SPECIFICATION REQUIREMENT (°F)		ACTUAL TEMPERATURE (°F)	
	MAX	MIN	DROP	A/S SEPARATION
Rate Gyro	125	0	47	47
Equipment Ballast	165	0	55	57
S-Band Transmitter #1	165	0	60	61
Instrument Beams #1	125	0	29	29
Bridle #1	210	-90	0	0
Aeroshell #1	175	-115	9	6
Mortar Cannister #1	80	No Min	25	61
Mortar Breech	75	25	45	91
Instrument Beam #2	125	0	27	27
Bridle #2	210	-90	18	16
Aeroshell #2	173	-115	19	19
Rocket Motor Support Structure	(No Prediction)		22	21
Mortar Cannister #2	80	No Min	26	67
Mortar Breech Flange	75	25	27	46
Bridle #3	210	-90	13	11
*Main Battery	80	50	15	13

\* The thermistor titled "main battery temperature" is misnamed, it really measures rocket motor support structure temperature.

#### D. Structural Subsystem

The structural system provided support and dynamic operation during all phases of the AV-3 mission. There was no evidence of any structural failure in the load carrying structure and the aeroshell separation system functioned as required. The sponge seal installed between the mortar cannister and the BLDT vehicle did prohibit the flow of mortar gases into the BLDT vehicle.

Inspection of the recovered hardware revealed the following conditions:

1. Aeroshell - Nose cap poked out, separated outer panels and bent outer ring. All damage was due to ground impact or ground handling.
2. Rocket Motor Support Structure - The RMSS and instrument beam appeared undamaged except that the ballast was sheared from the main structure. Several components on the instrument beam were damaged with one command receiver/decoder being sheared from the beam. All damage was due to ground impact or ground handling.
3. Base Cover - The base cover appeared structurally sound with minor scratches and dents due to ground handling. One hole appears in the base cover of unknown origin. The hole was punched from external to internal and, as reported by the recovery crew, was probably not from ground impact or ground handling. It was hoped that the slant load bar camera would give clues concerning this hole, but the camera film detail was not adequate due to contaminated lens elements.
4. Parachute Truss - No visible damage.
5. Load Bar Support Structure - TBD.

It is noted that the recovered vehicle displayed considerable white deposits, probable cornstarch, on the external surfaces of the base cover and inside of the rocket motor support structure. Also, the recovery crew indicated that the general condition of the vehicle was wet internal and external with small patches of ice internally.

#### E. Propulsion, Azimuth Pointing and Ordnance Subsystems

The subsonic vehicle required no propulsion or azimuth pointing elements and all pyrotechnic devices performed as planned. Visual inspection of the recovered hardware revealed that all pyrotechnic initiators operated as planned.

The release of the vehicle from the load bar was by means of three pyrotechnic operated release nuts. The instrumentation did not indicate any gross late release function. The slant load bar camera, which would have provided a view of the vehicle drop away, had ice and water deposits on the lens elements which precluded seeing the drop away in sufficient detail to establish ordnance firing simultaneity.

#### F. Electrical Subsystem

The electrical power and sequencing systems operated satisfactorily during the complete flight operation. All battery voltage and timed events occurred within predicted/required limits.

Flight batteries were activated on August 14, using previously established activation procedures. No battery activation problems occurred. Battery voltages were above minimum at launch as shown in Table VI-3 during the mission.

Camera batteries functioned satisfactorily as evidenced by "on-board" camera operation during the vehicle flight sequence.

The actual airborne programmed sequence times are provided in Table IV-1. The vehicle command system operated as required, receiving and executing the following commands subsequent to balloon launch.

<u>TIME</u>	<u>COMMAND</u>
15:10 hrs Z	Safe/Safe/B/u (Command System Check)
17:33 hrs Z	Arm Vehicle
17:33:30 hrs Z	Clockwise command (Power A/B Programmers)
17:45:00.54 hrs Z	Vehicle Drop
17:45:17.07 hrs Z	Mortar Fire

#### G. Instrumentation Subsystem

All instrumentation hardware operated properly during the various phases of flight with the exception of the cameras which were recording various test functions. The following data is available concerning post-flight films:

1. Aft Viewing Milliken - The aft viewing Milliken camera film provides sufficient detail to view the parachute deployment process despite the presence of ice in the lens elements and sun reflection.

2. Aft Viewing Photosonics - The aft viewing photosonics films are of poor quality due to heavy ice deposits on the lens elements.

3. Forward Viewing Milliken - The forward viewing Milliken films are of good quality.

Although not a part of the BLDT vehicle instrumentation, the post-flight film for the load bar cameras reveals:

1. Slant Camera - The quality of the slant camera film is poor due to ice/water deposits. The separation sequence is visible but no details can be seen.

2. Load Vertical Camera - The post-flight film from this camera reveals that the load bar was not stable enough to view the decelerator deployment. Due to the narrow field of view, the BLDT vehicle is out of the camera view most of the time.



#### H. R. F. Subsystem

The airborne S-Band telemetry, C-Band tracking and command control RF subsystems performed without malfunction throughout the flight. Signal acquisition for TM and tracking frequencies occurred after attaining an altitude of approximately 24,000 feet. The command system capture was firm at about 15:10 hrs Z when the vehicle was at an altitude of 85<sup>0</sup>F K feet.

Command system ground station checkouts were performed at launch -2 hours. All command transmitters were monitored at the J-67 site for center frequency, single tone deviation and triple tone execution of commands. Command system checkouts were satisfactory, however the north Oscura Peak transmitter "B" was inoperative due to a component malfunction. Consequently, the Test Conductor requested that transmitter "A" at NOP be utilized as the primary transmitter for the mission.

Telemetry data was monitored at J-67 and appeared satisfactory in all respects.

#### I. TSE/OSE

The Test Support Equipment and Operational Support Equipment performed within the design requirements for this equipment.

#### J. Mass Properties

The BLDT vehicle mass property requirements, at decelerator mortar fire, were established, based on the Viking Lander Capsule, to be as follows:

Vehicle Weight

Y Axis cg Location - 0 Offset  $\pm 0.30''$   
Z axis cg Location -  $-1.41 \pm 0.30''$   
X Axis cg Location -  $31.7''$  to  $33.7''^*$

For vehicles AV-1, 2 and 4, the tolerance on the Y and Z axis cg location was  $\pm 0.030$ . This required spin balancing of the vehicles. For vehicle AV-3, the tolerance was established at  $\pm 0.300$ . This broad tolerance permitted balancing with predicted values rather than actually spin balancing.

The vehicle AV-3 vehicle mass properties are summarized in Table VI-4.

---

\* Referenced to Aerochell Theoretical Apex.

TABLE VI-1  
BLDT AV-3 ATMOSPHERIC PROPERTIES

<u>ALTITUDE</u> <u>(5000 FT)</u>	<u>EAST-WEST</u> <u>WIND</u> <u>(FT/SEC)</u>	<u>NORTH-SOUTH</u> <u>WIND</u> <u>(FT/SEC)</u>	<u>SPEED</u> <u>OF SOUND</u> <u>(FT/SEC)</u>	<u>DENSITY</u> <u>(SLUGS/FT<sup>3</sup>)</u>
1	11.	1.	1132.	.19468-2
2	1.	1.	1108.	.16961-2
3	5.	3.	1089.	.14586-2
4	9.	13.	1070.	.12455-2
5	14.	33.	1052.	.10565-2
6	37.	27.	1024.	.90500-3
7	61.	11.	1002.	.75849-3
8	55.	1.	978.	.63431-3
9	20.	27.	952.	.52565-3
10	10.	31.	937.	.421839-3
11	-7.	18.	941	.32463-3
12	-18.	9.	949.	.24798-3
13	-29.	8.	959.	.19016-3
14	-27	2.	965.	.14728-3
15	-48.	4.	973.	.11429-3
16	-47	9.	975.	.90034-4
17	-46	5.	983.	.70242-4
18	-56	-5.	990	.54913-4
19	-71	-3.	998	.43270-4
20	-54	19.	1003.	.34151-4

TABLE VI-2

## STATE VECTOR DATA - BLDT AV-3

	<u>DROP</u>	<u>MORTAR FIRE</u>	<u>FULL OPEN</u>
Time (t) - Sec	0	16.5	18.27
Altitude (h) - ft	91130	87027	86192
Velocity (V) ft/sec	--	464.3	455.6
Gamma ( $\gamma$ ) - deg.	--	-89.5	-88.9
PSI ( $\psi$ ) - deg.	-16.1	55.2	-90.97*
Theta ( $\theta$ ) - deg.	-94.	-84.7	-84.22*
PHI ( $\phi$ ) - deg.	0	-50.0	94.60*
Mach No. (MN)	--	.471	.462
Dynamic Pressure (q) - lb/ft <sup>2</sup>	--	6.90	6.91
Angle of Attack ( $\alpha$ ) - deg.	--	3.5	+1.3
Sideslip Angle ( $\beta$ ) - deg.	--	-4.5	+3.0
Total Angle of Attack ( $\eta$ ) - deg.	--	5.7	3.5
Spin (p) - deg/sec	-.5	-.5	-.5

\*These values are at t = 18.3

TABLE VI-3

## BATTERY PERFORMANCE DATA

	<u>Main Battery</u>	<u>Transient Battery</u>	<u>Pyro A Battery</u>	<u>Pyro B Battery</u>	<u>Camera Battery Positive</u>	<u>Camera Battery Negative</u>
1. Activation Voltage						
a. Open Circuit	33.28	32.94	36.75	36.82	16.56	-16.56
b. 5 Second Load*	28.0	26.2	28.9	28.9	13.05	-13.05
2. Prelaunch Voltage						
No Load	34.13	32.96	34.67	35.12	16.28	-16.21
3. Float Voltage						
Drop - 2 hours	29.1	27.8	35.1	35.7	No TM	No TM
Drop - 1 hour	29.0	27.9	35.1	35.7	Data	Data
Drop - 1 minute	29.1	27.4	31.1	31.1		
4. Flight Voltage						
T + 1 minute	29.2	27.9	30.5	30.5		
T + 6 minutes	29.2	27.8	30.5	30.5		
5. Main Battery Amps.	3-11 amps					

\* 5 Second Load Levels

- a) 30 amps for main battery
- b) 10 amps for all others.

TABLE VI-4  
FINAL BLDT MASS PROPERTIES STATUS - AV-3

Condition	Weight (lb)	Center of Gravity (Vehicle Sta.)			Moment & Product of Inertia (Slug Ft <sup>2</sup> )			
		X	Y	Z	I <sub>xx</sub>	I <sub>yy</sub>	I <sub>zz</sub>	P <sub>xy</sub> P <sub>xz</sub> P <sub>yz</sub>
On Load Bar	1973*							
At Drop	1901	36.52	+0.06	-1.35	409	339	296	-.05 .98 1.07
At Mortar Fire	1901	36.52	+0.06	-1.35	409	339	296	-.05 0 1.07
With Decelerator Deployed	1806	35.34	+0.06	-1.35	408	327	264	0 .98 1.07
With Decelerator Deployed and Aeroshell Dropped	1454	38.75	+0.05	-1.69	201	219	175	-.09 2.87 1.10
Aeroshell	352	21.26	0	0	176	90	90	

\*Pointing System Excluded

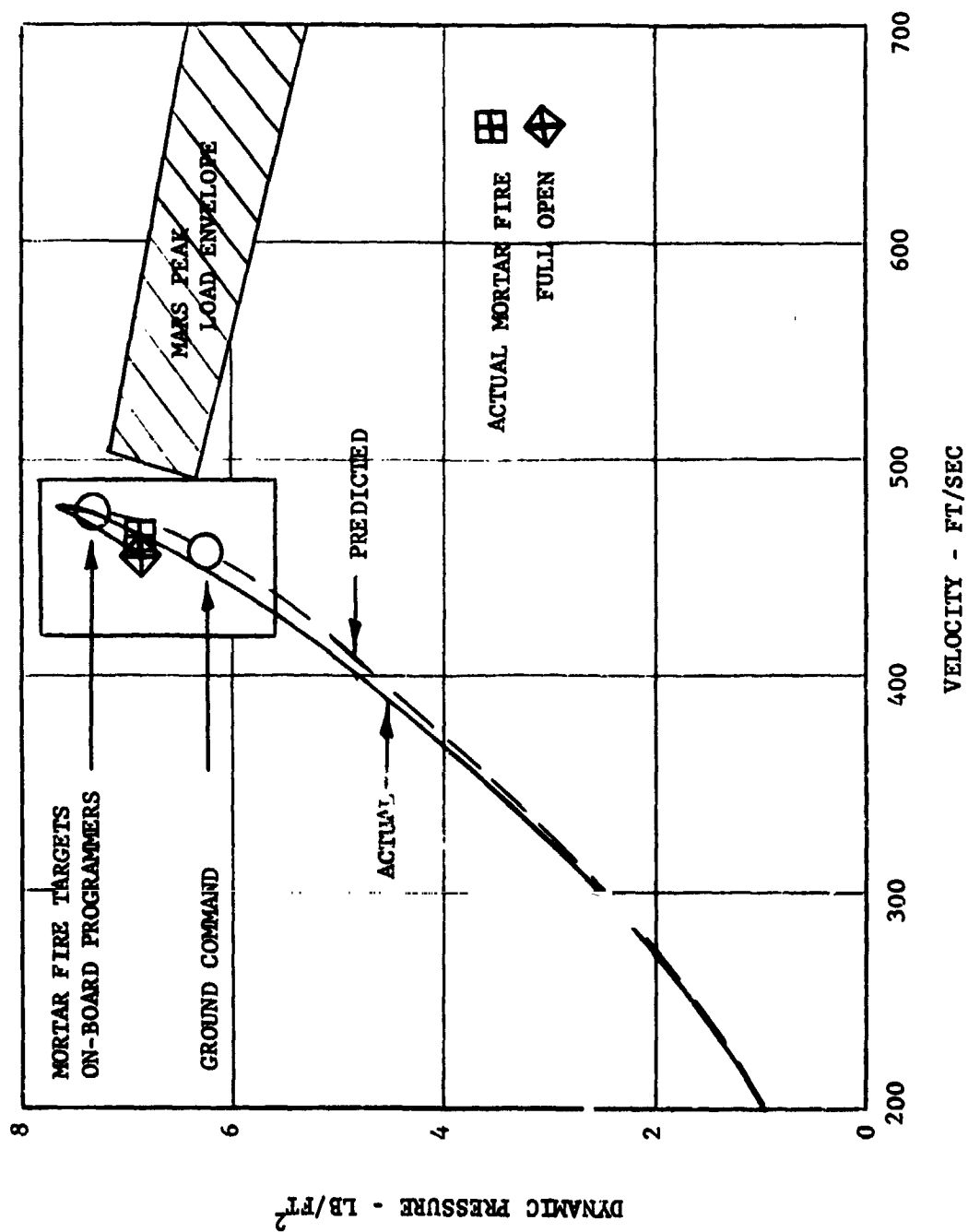
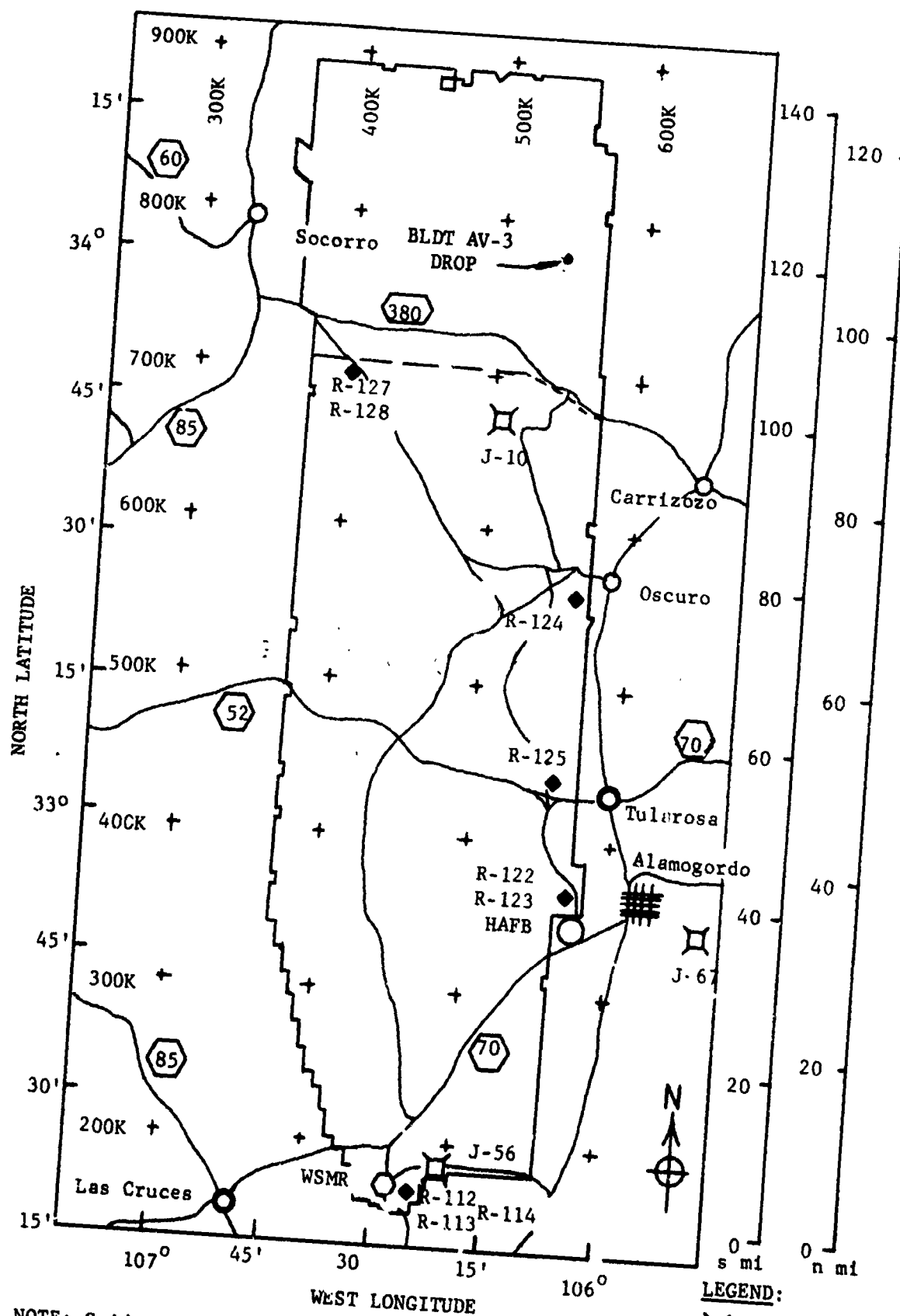


FIGURE VI-1 BLDT AV-3 TEST CONDITIONS



NOTE: Grids are WSTM COORDINATES

FIGURE VI-2 WSMR MAP SHOWING TELEMETRY AND RADAR SITES

LEGEND:  
 S-Band TLM  
 C-Band Radar  
 Highway



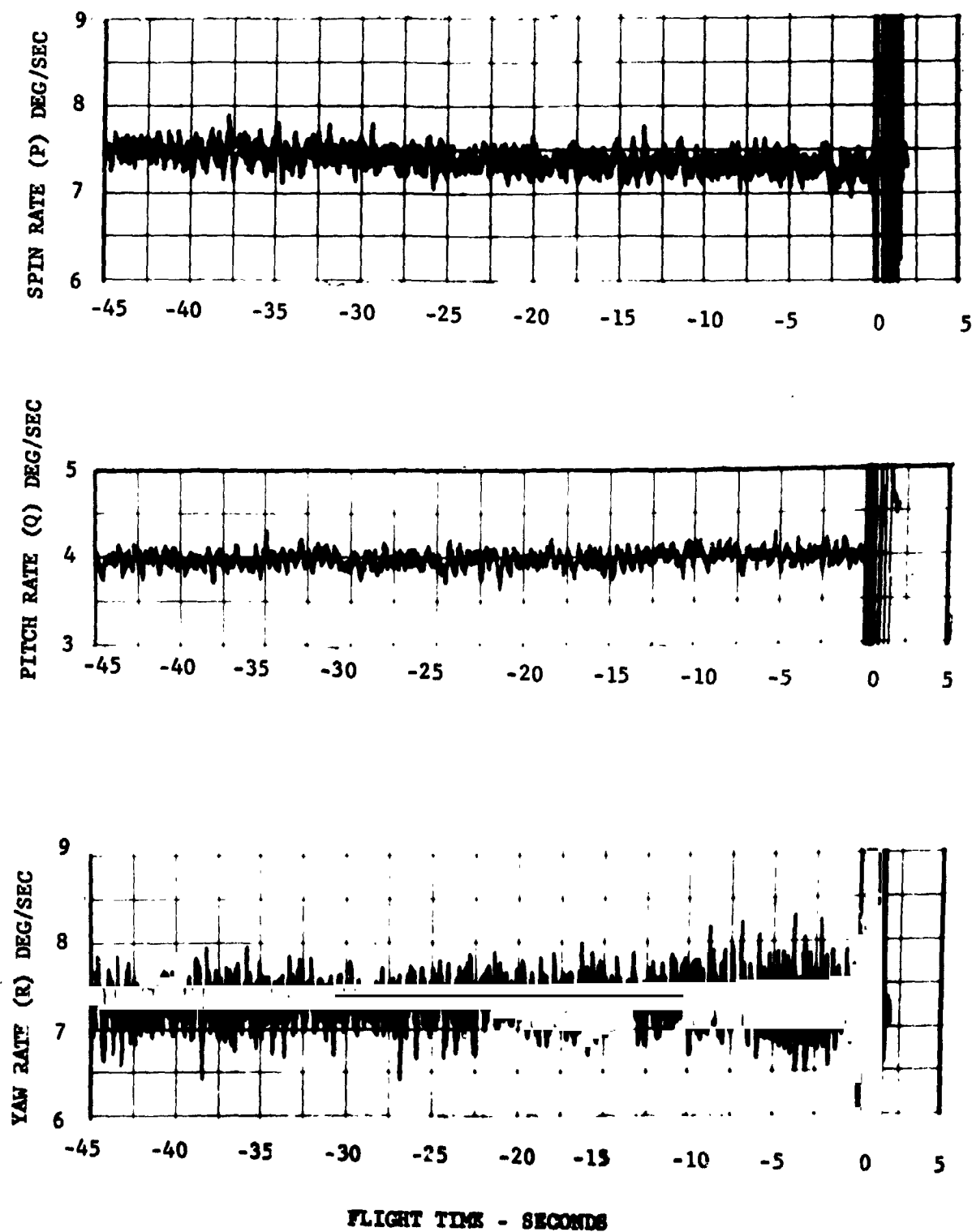
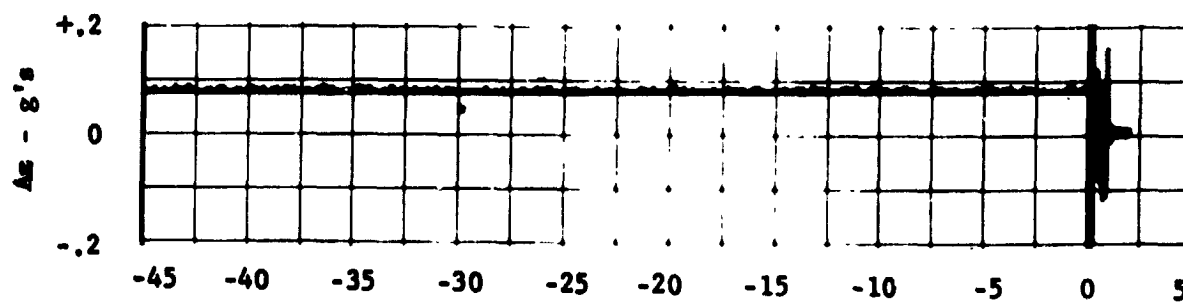
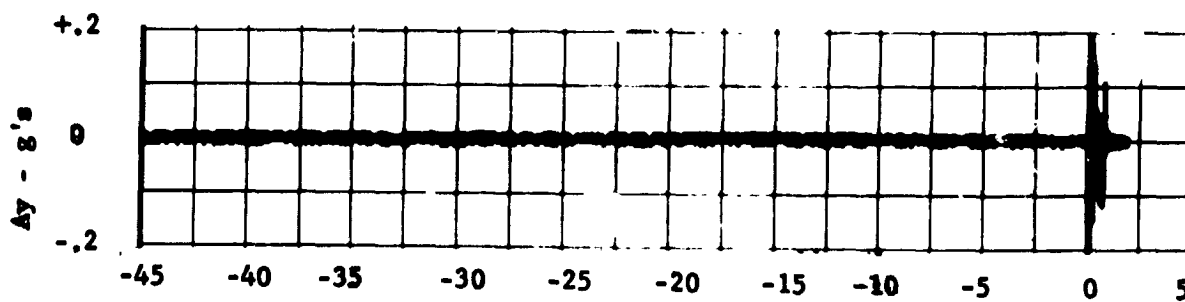
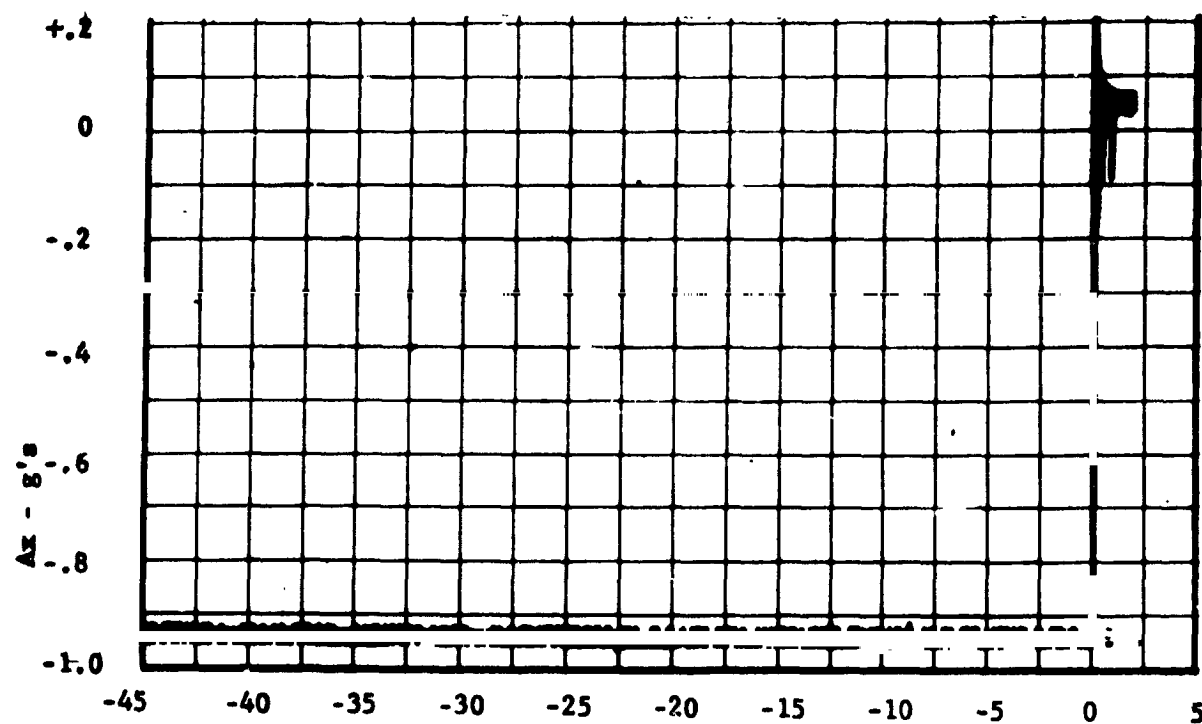


FIGURE VI-3 GYRO DATA PRIOR TO DROP



FLIGHT TIME - SECONDS

FIGURE VI-4 ACCELEROMETER DATA PRIOR  
TO DROP

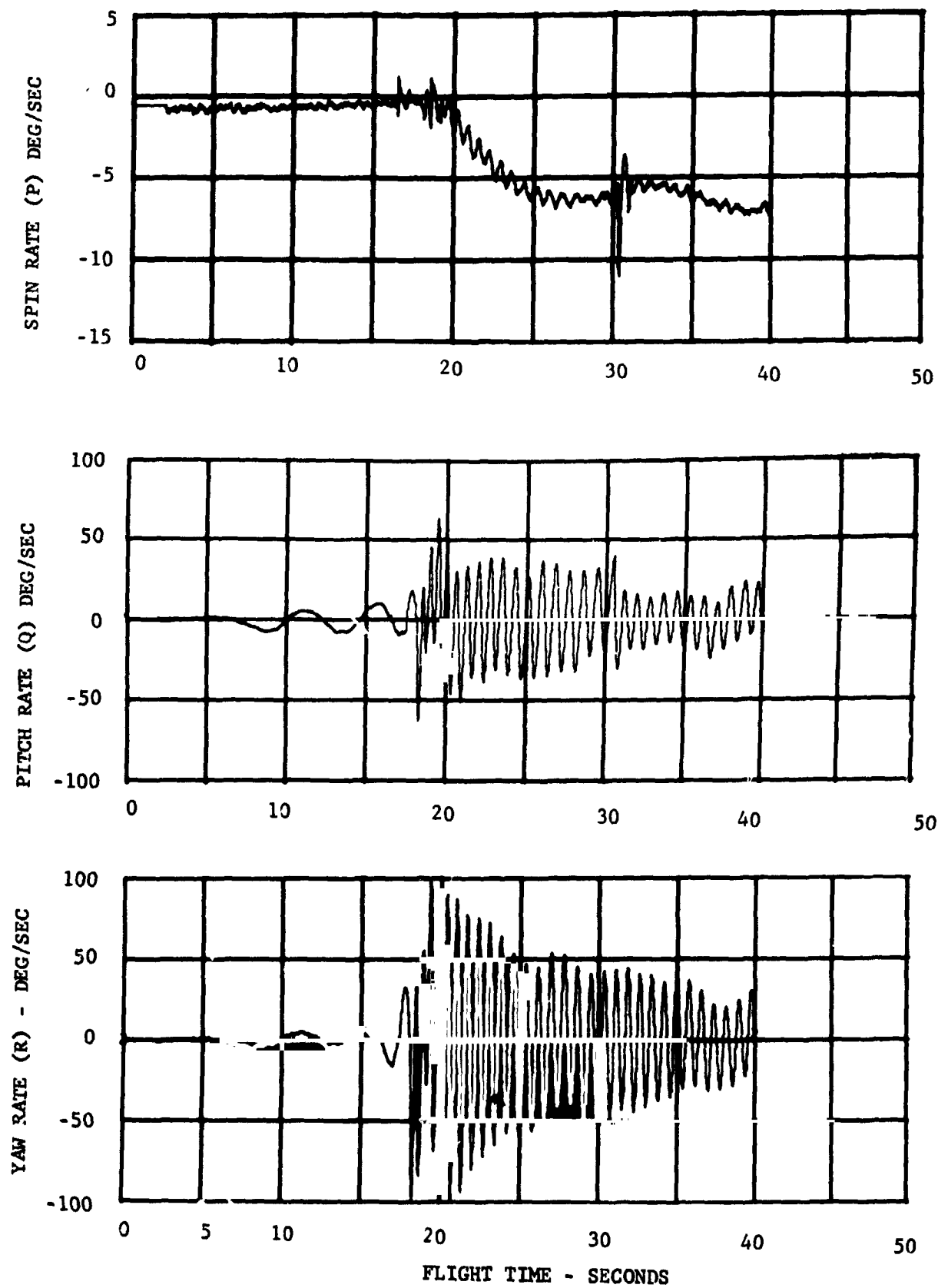


FIGURE VI-5 GYRO DATA DURING POWERED FLIGHT

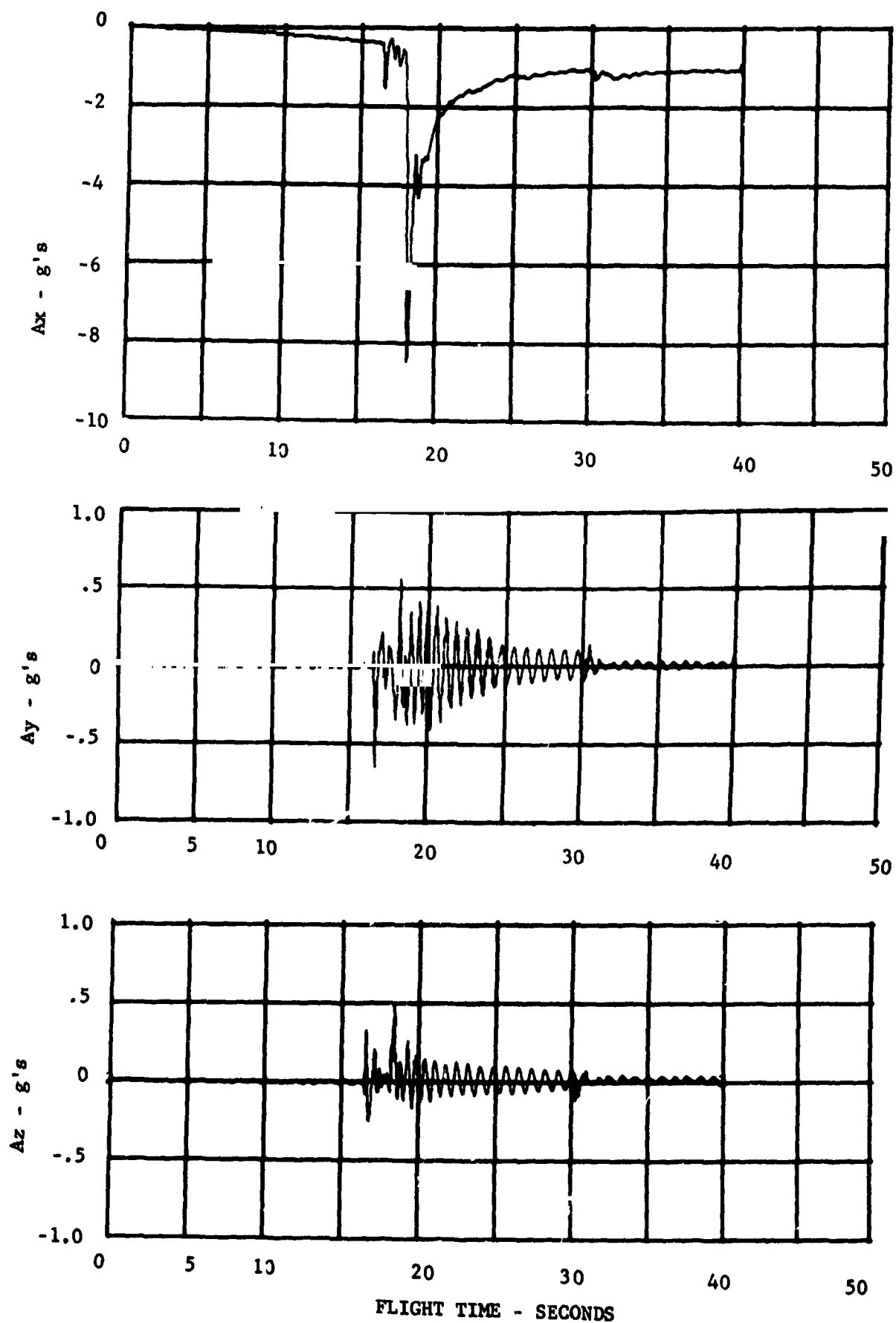


FIGURE VI-6 ACCELEROMETER DATA DURING  
POWERED FLIGHT

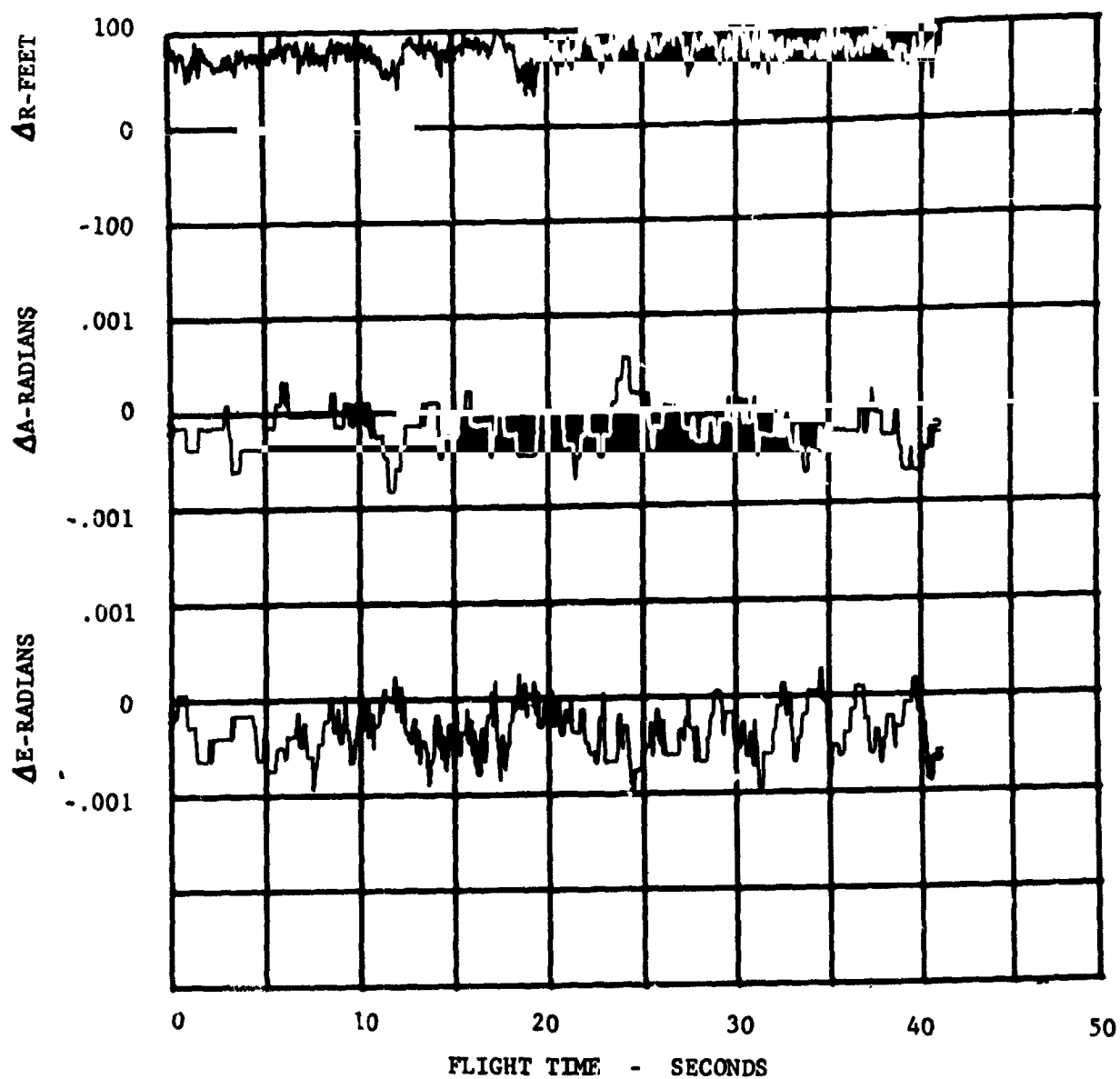


FIGURE VI-7 COMPARISON BETWEEN RADAR DATA  
(R122 TRANSFORMED TO R113)

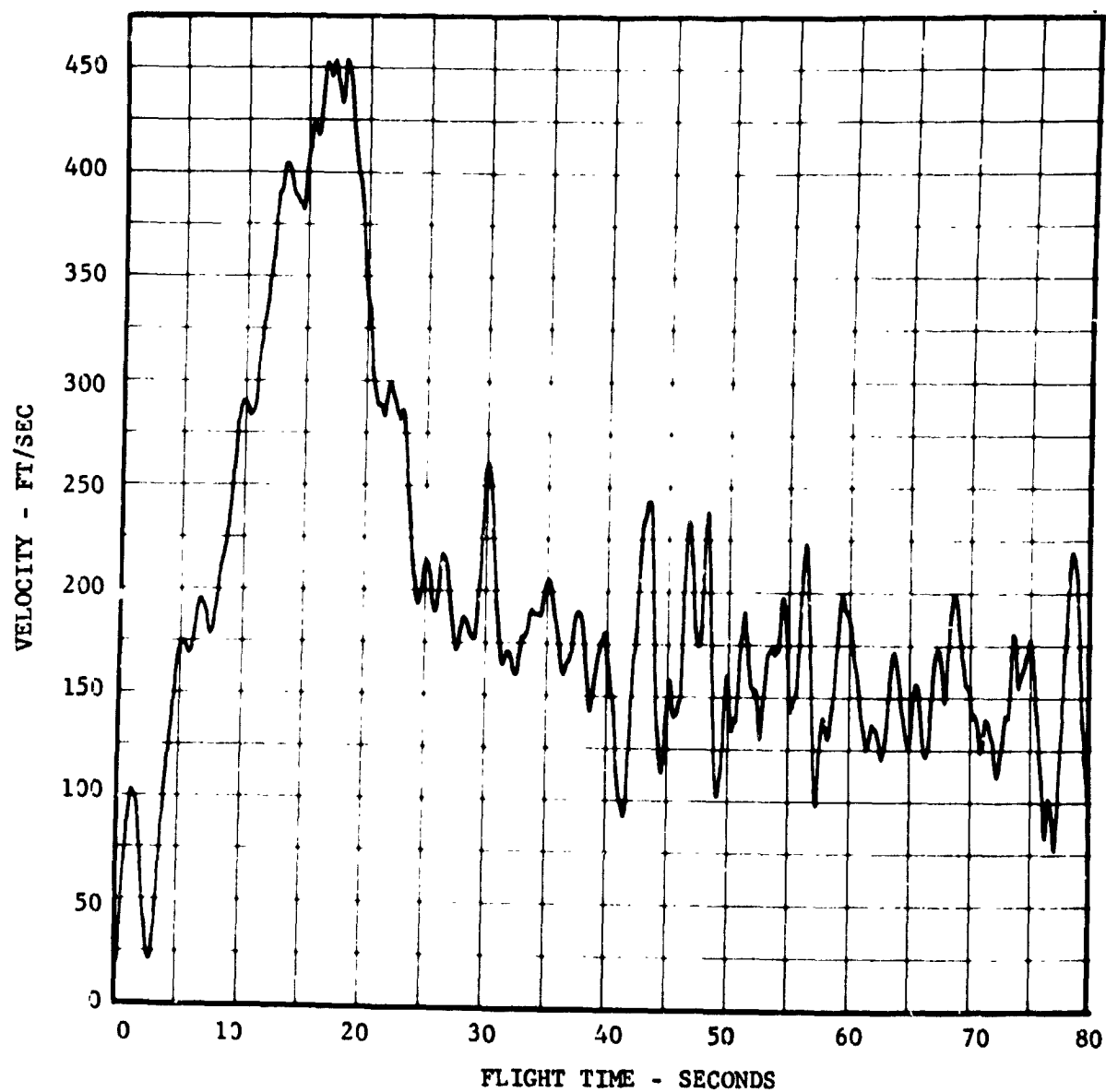


FIGURE VI-8 RADAR (R122) VELOCITY VS. FLIGHT TIME

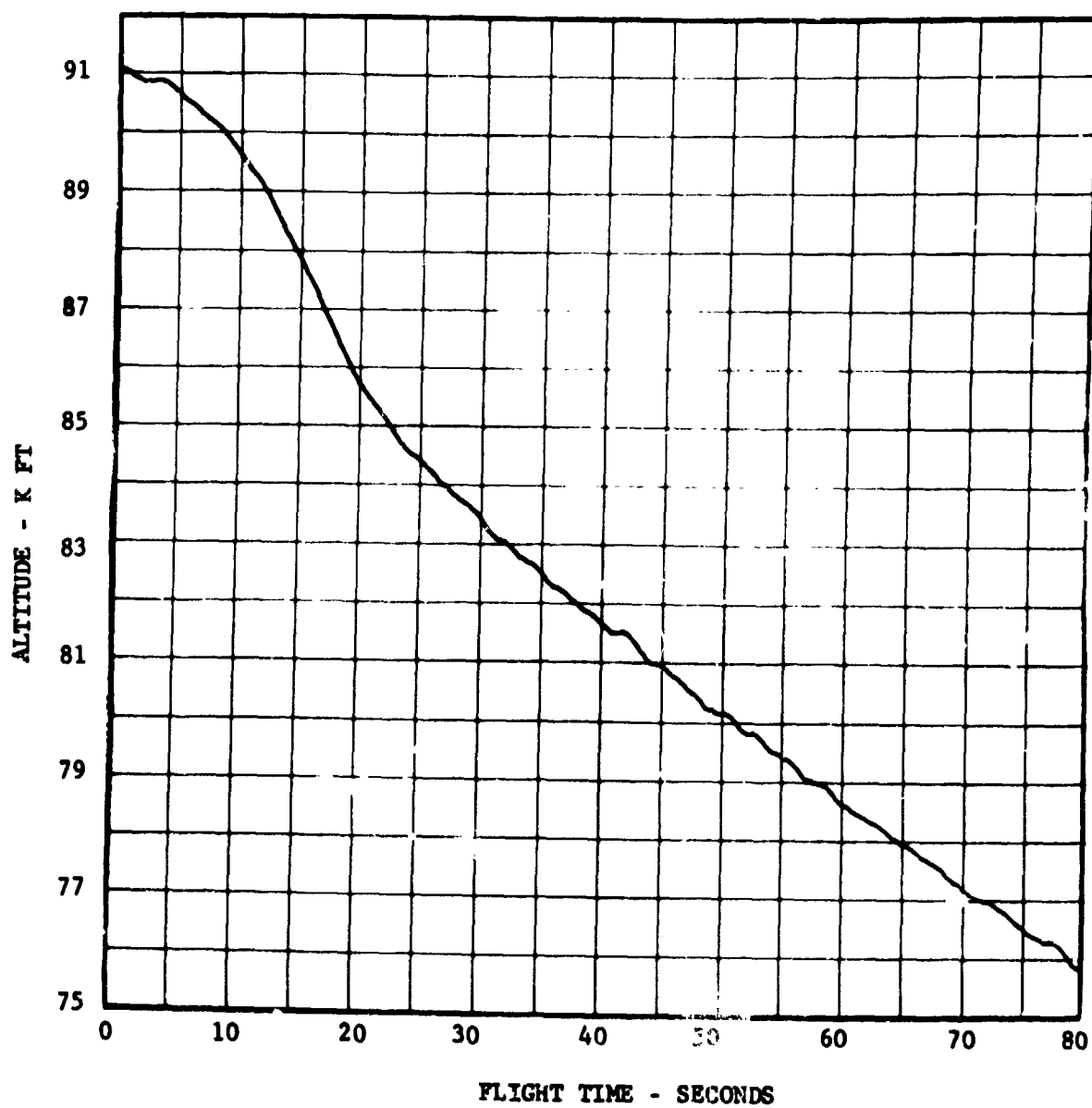


FIGURE VI-9 RADAR (R122) ALTITUDE (MSL) VS. FLIGHT TIME

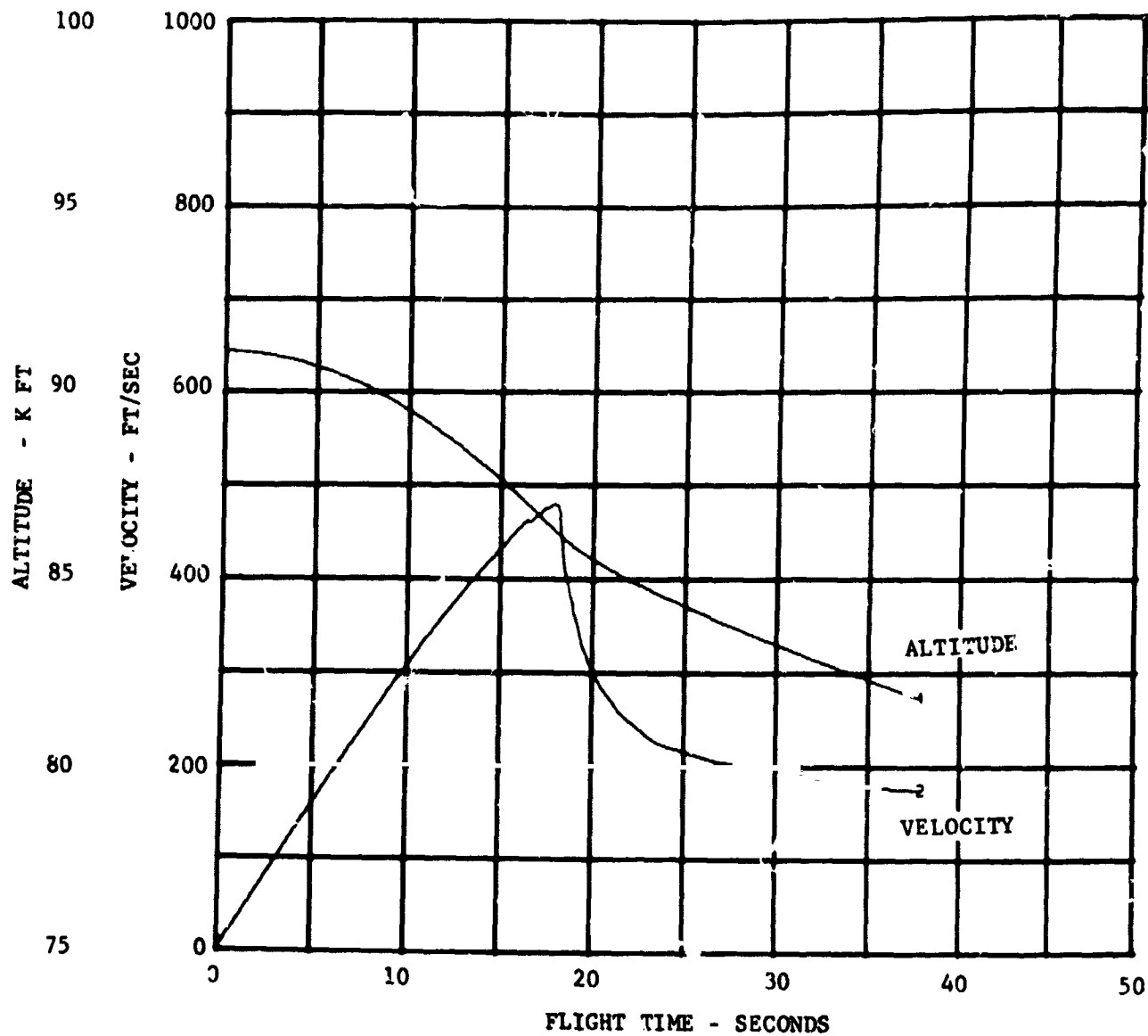


FIGURE VI-10 STEP TRAJECTORY RECONSTRUCTION OF ALTITUDE AND VELOCITY



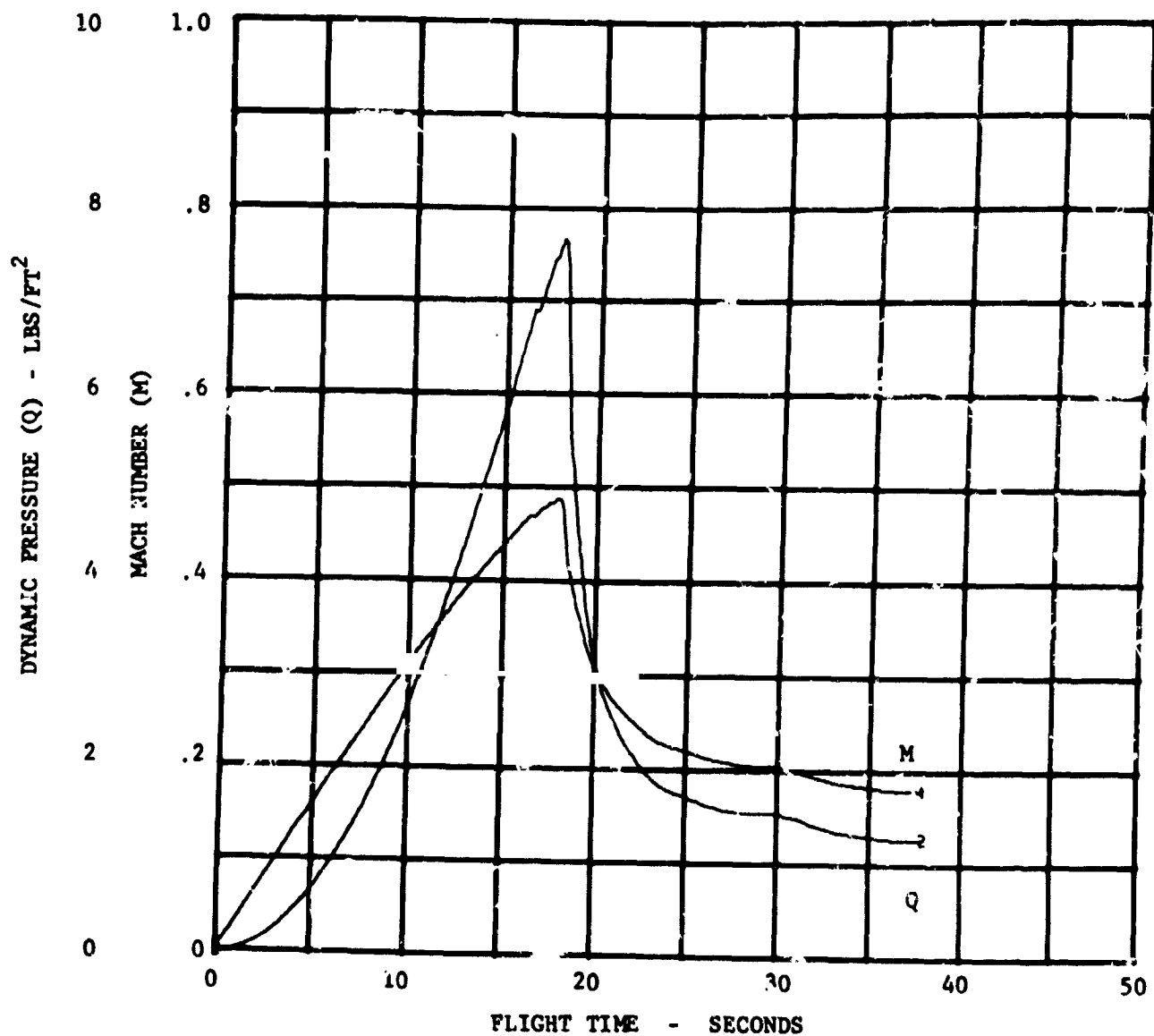


FIGURE VI-11 STEP TRAJECTORY RECONSTRUCTION OF  
MACH NUMBER

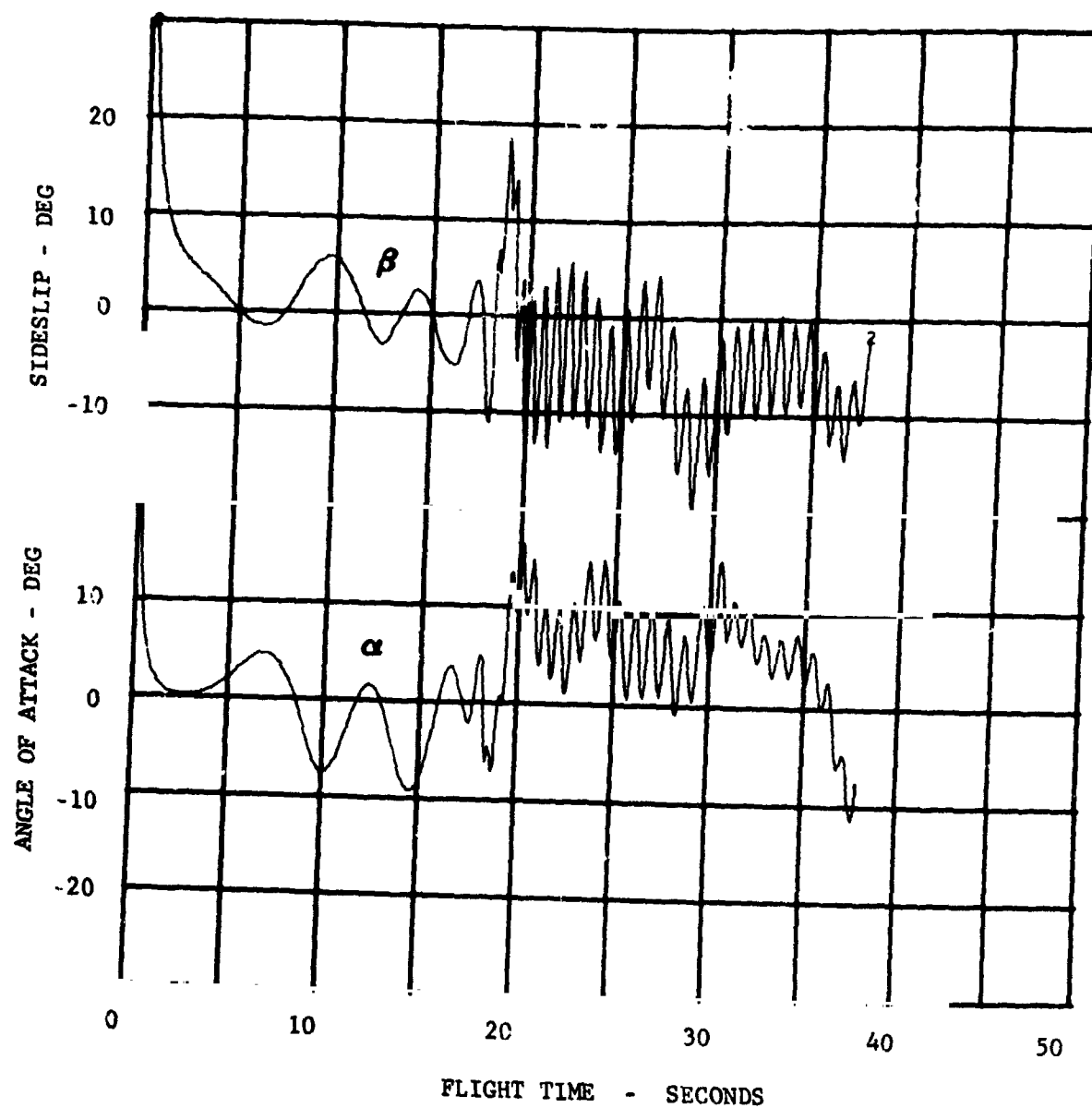


FIGURE VI-12 STEP TRAJECTORY RECONSTRUCTION OF ANGLE OF  
ATTACK AND SIDESLIP

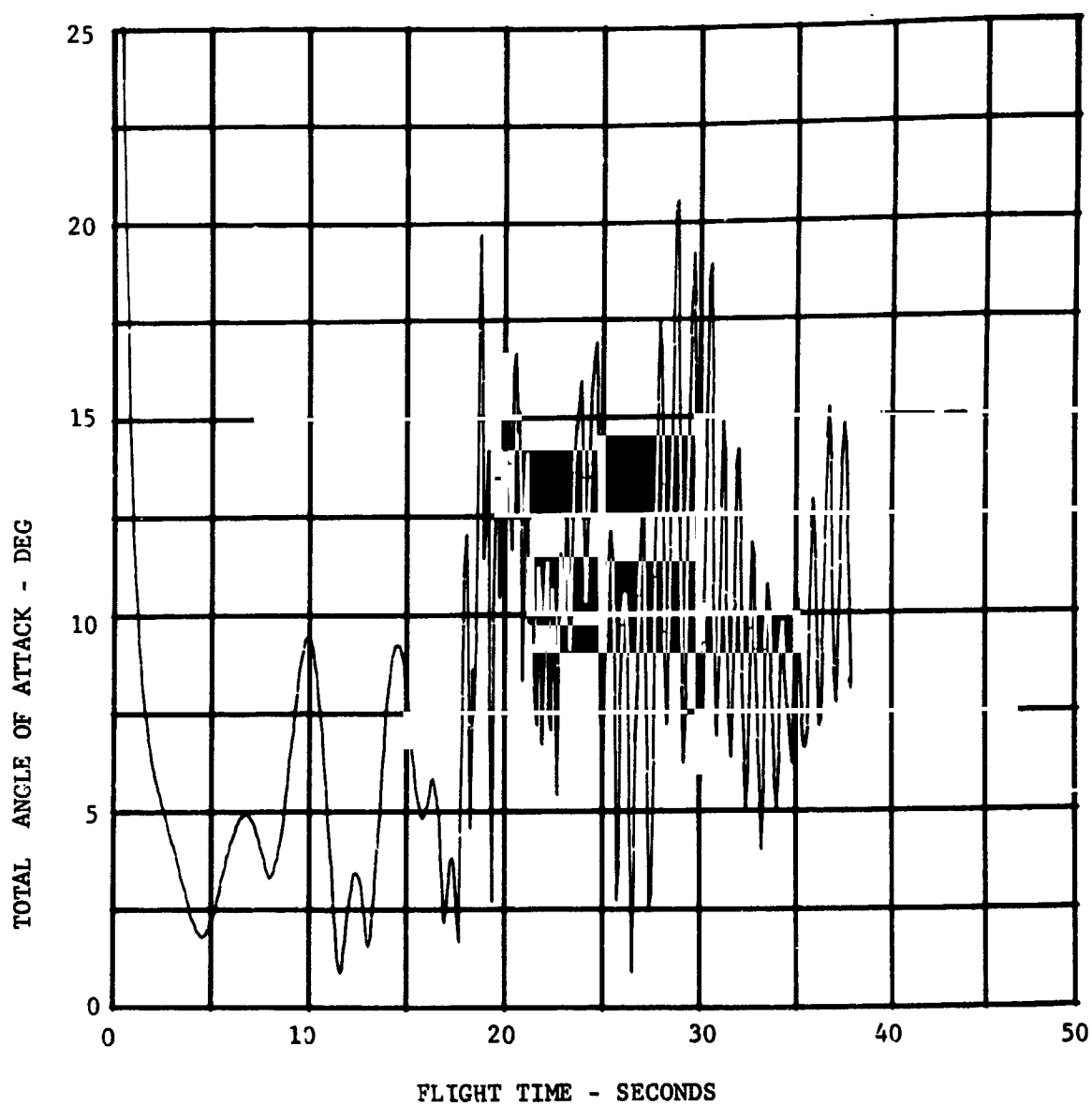


FIGURE VI-13 STEP TRAJECTORY RECONSTRUCTION OF  
TOTAL ANGLE OF ATTACK

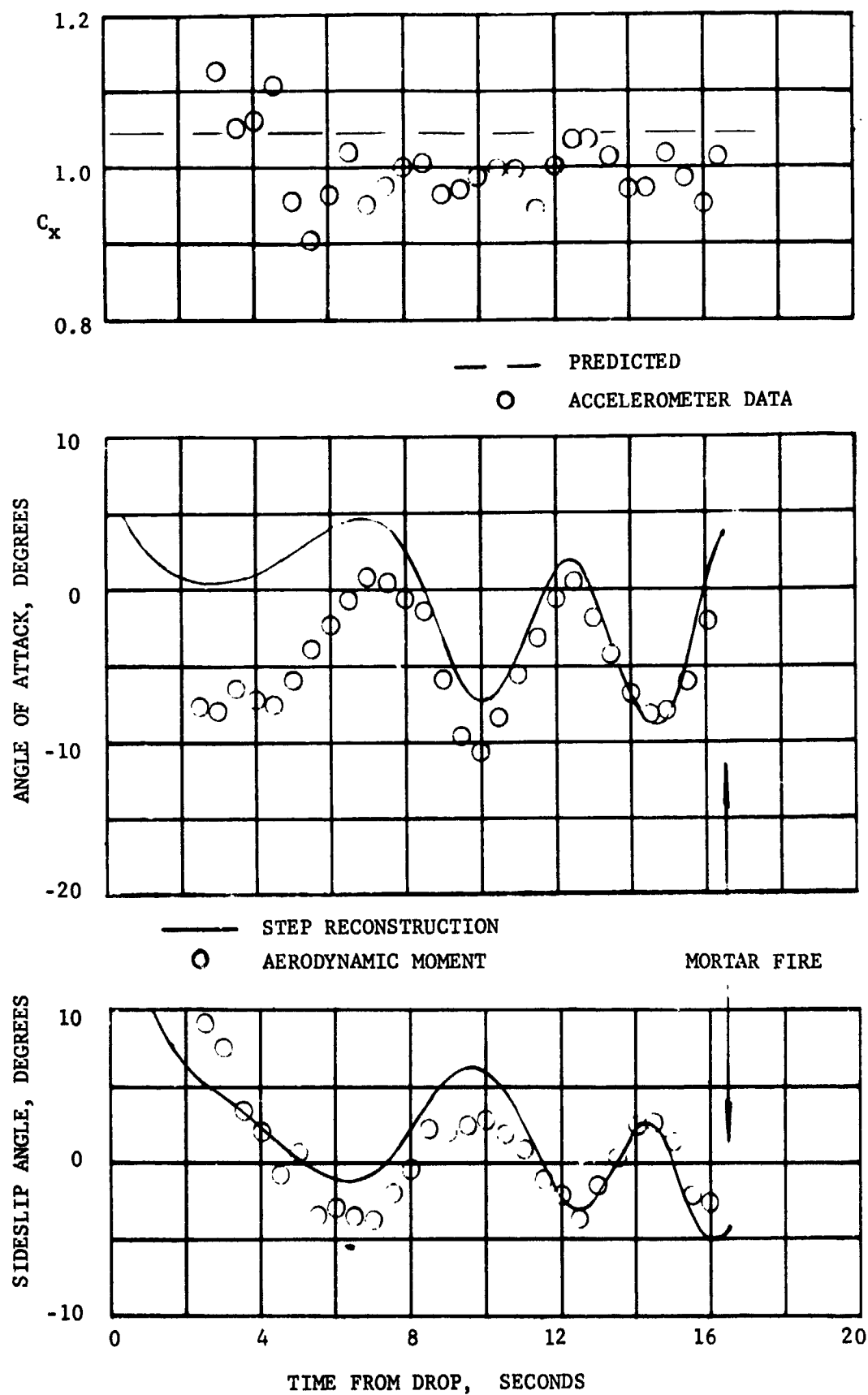


FIGURE VI-14 ANGLES OF ATTACK, SIDESLIP AND AXIAL  
FORCE COEFFICIENT AT MORTAR FIRE

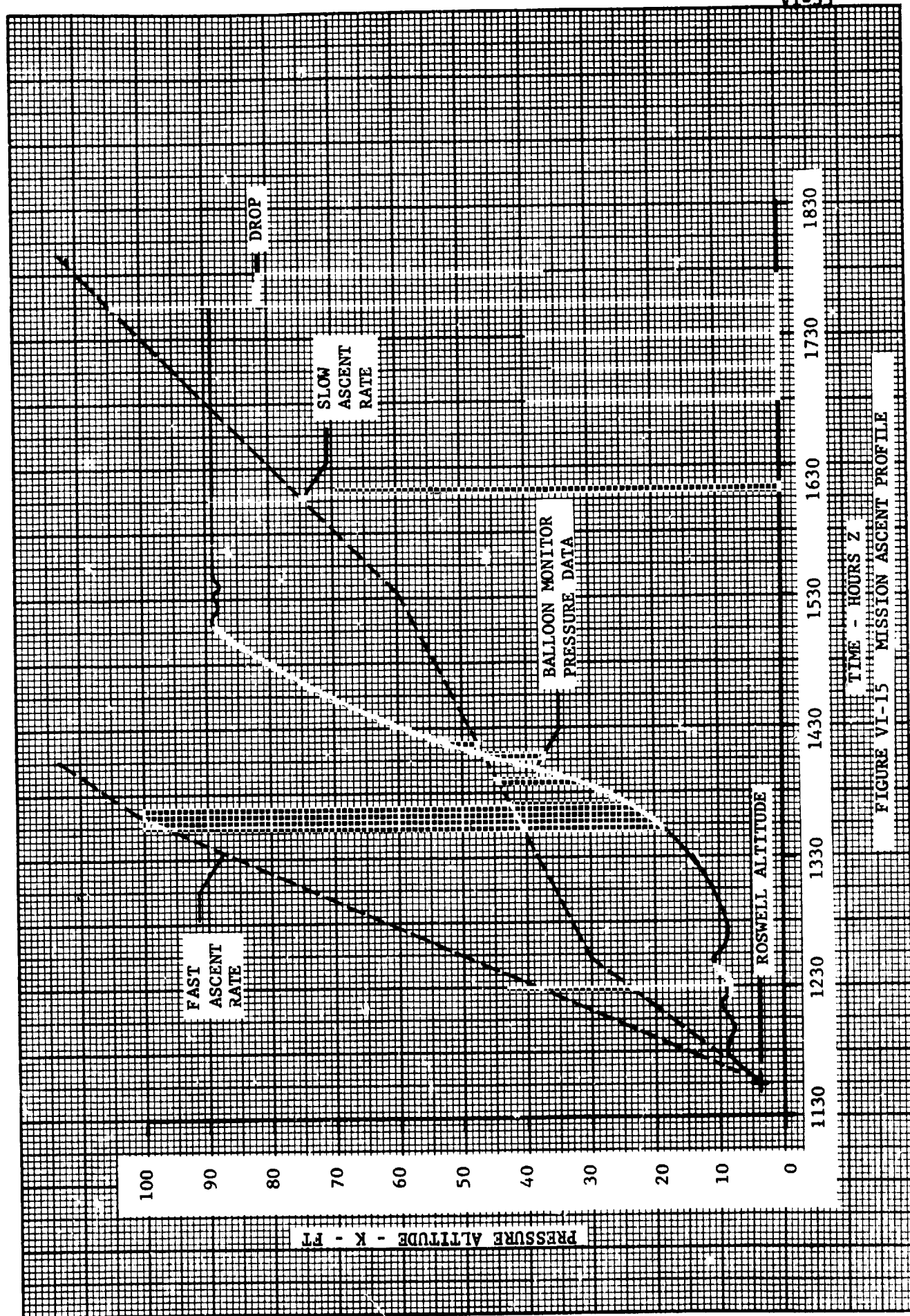


FIGURE VI-15 MISSION ASCENT PROFILE

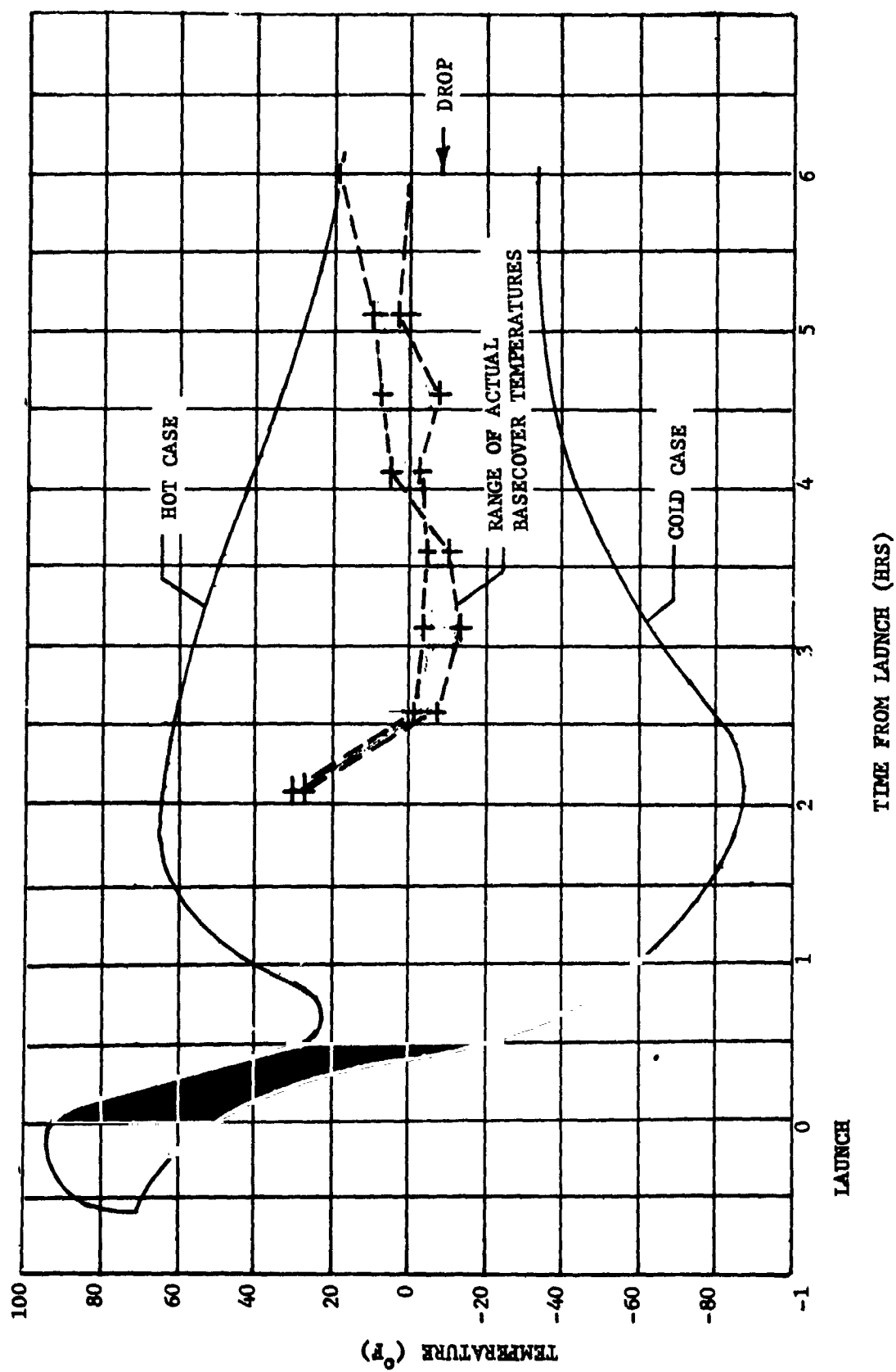


FIGURE VI- 16 BASECOVER TEMPERATURE HISTORY

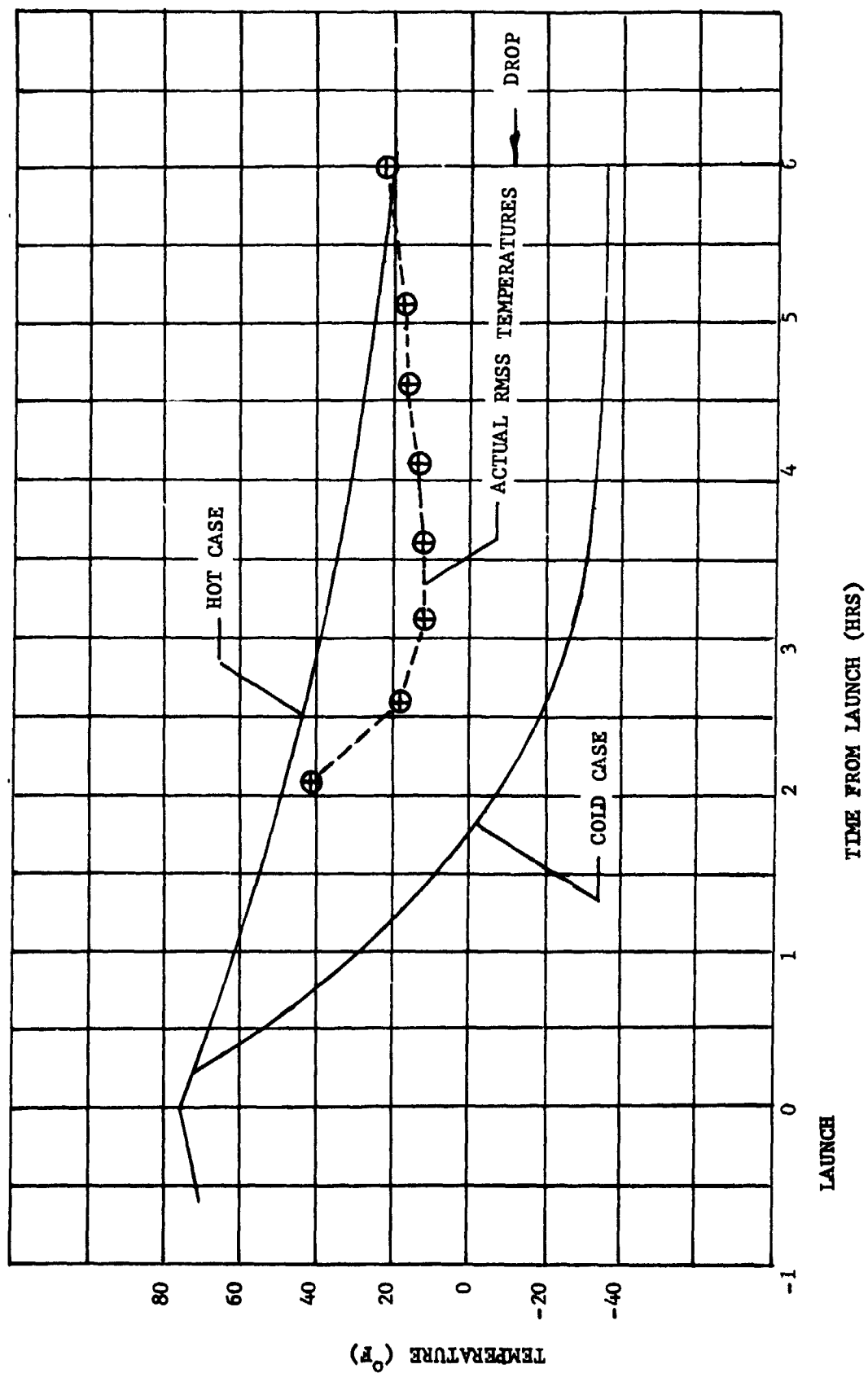


FIGURE VI-17 ROCKET MOTOR SUPPORT STRUCTURE TEMPERATURE HISTORY

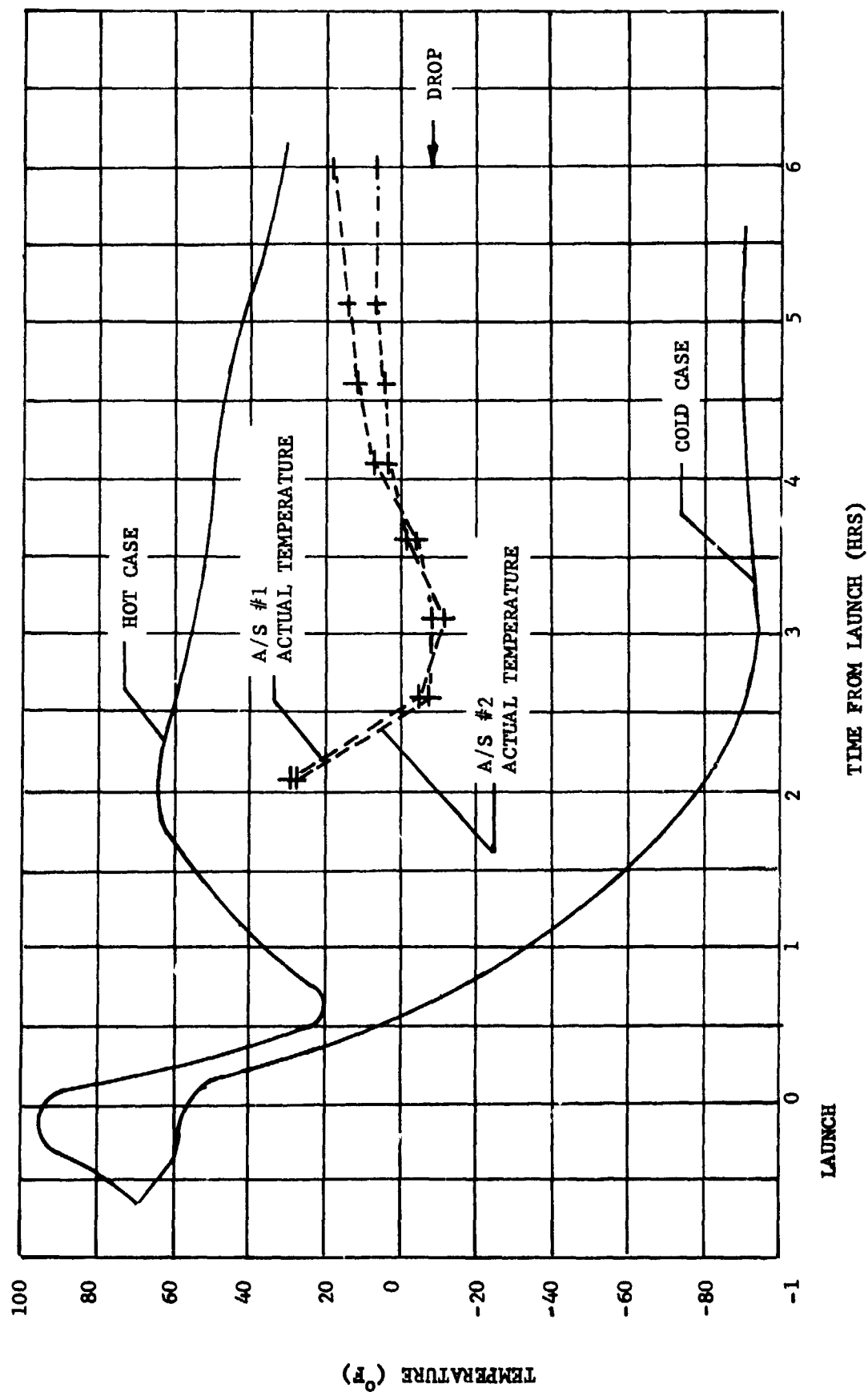


FIGURE VI - 18 AEROSHELL TEMPERATURE HISTORY



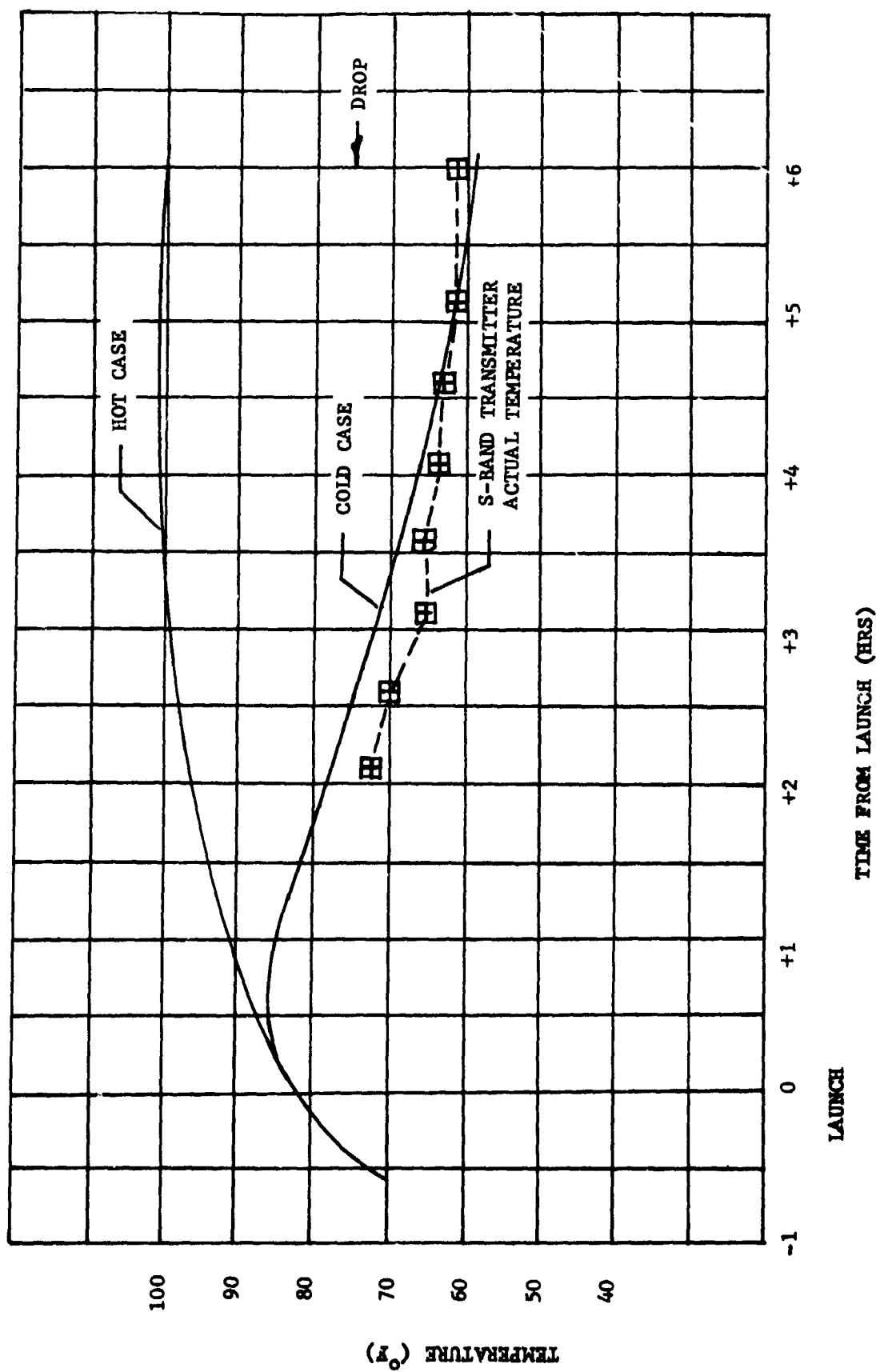


FIGURE VI-19 S-BAND TRANSMITTER TEMPERATURE HISTORY

VII. CONCLUSIONS

The conclusions reached from the in-depth analysis of the AV-3 mission data and films are:

A. The flight of the vehicle was as programmed and within the predicted dispersions.

B. The vehicle velocity and dynamic pressure at mortar fire and peak load easily fell within the required performance box (See Figure II-1). The remaining BLDT requirements which were also met are:

Resultant angle of attack (Deg)      < 21

Residual spin rate (deg/sec)      < 100

Decelerator Temperature ( $^{\circ}$ F)      < 80

C. The balloon ascent for this flight was slower than normal because an unexpected rain storm occurred shortly after launch. Water and ice on the airborne camera lenses reduced the quality of the parachute deployment film data, but had no effect on the successful qualification of the decelerator.

D. The decelerator performed as predicted with no damage sustained. This constitutes successful qualification of the decelerator at the subsonic conditions.

E. The aeroshell separation function more than adequately met the requirement for 50 feet of separation in 3 seconds.

VIII. REFERENCES AND OTHER DATA SOURCESA. References

1. MMC RD-3720247, Parachute Test Objectives and Requirements for BLDT Program, Dated March 29, 1972.
2. MMC TR-3720052, Viking Vehicle Dynamics Data Book, Rev. F, July 6, 1972.
3. MMC TK-3720074, Volume I, Transonic Aerodynamic Characteristics and Pressure Distributions on 8 Percent Scale Models of the Viking Lander Capsule, Aeroshell and Lander plus Base Cover, February 1971.
4. MMC TR-209014, Viking Aerodynamics Data Book, Rev. C, June 1972.
5. GAC GER 15215, Rev. A, Viking Decelerator Design Analysis Report, March 20, 1972.
6. NASA TND-5296, Inflation and Performance of Three Parachute Configurations from Supersonic Flight Tests in a low Density Environment, July 1969.
7. MMC TR-3720181, Scale Model Test Results of the Viking Parachute System at Mach Numbers from 1 through 2.6, November 1971.
8. MMC Memorandum 8943-72-116, Viking Parachute Swivel Loads and Pull-Off Angles from Dynamic Simulation, R. D. Moog, 10 May 1972.
9. NASA CR-1482, Statistical Trajectory Estimation Programs (STEP), Volumes I and II.
10. Users Guide No. 837L7041032, BLDT Six Degrees of Freedom Trajectory Program, dated February 1972.
11. TN-3770115, Aerothermodynamics Analysis of the BLDT Vehicle (CDR Configuration) dated July 1971.
12. GAC GER-15397, Low Altitude Drop Test (LADT) of Viking Decelerator System, February 8, 1972.

B. Abbreviations

A/B	Airborne
AGC	Automatic Gain Control
A/S	Aeroshell
AV	BLDT Flight Vehicle Designator
BLDT	Balloon Launched Decelerator Test
B/U	Backup
Cg	Center of Gravity
CST	Combined System Test
CW	Clockwise
CCW	Counter Clockwise
DGB	Disk-Gap-Band
DEG	Degree
Deg/Sec	Degree/Second
fps	Feet per second
FRT	Flight Readiness Test
FT	Feet
GAC	Goodyear Aerospace Corporation
g's	Gravitational acceleration = $32.2 \text{ FPS}^2$
IRIG	Inter Range Instrumentation Group
K	1000
KHz	Kilohertz
LADT	Low Altitude Drop Test
MMC	Martin Marietta Corporation
NASA	National Aeronautics and Space Administration
NOP	North Oscura Peak
P	Roll Rate

PSF	Pounds per Square Foot
PSI	Pounds per Square Inch
PEPP	Planetary Entry Parachute Program
q	Dynamic Pressure
Q	Pitch Rate
R	Yaw Rate
RAOB	Radiosonde Observation Balloon
RF	Radio Frequency
RMSS	Rocket Motor Support Structure
RTDS	Real Time Data System
s	Aerodynamic Reference Area
SCO	Subcarrier Oscillation
S/N	Serial Number
STEP	Statistical Trajectory Estimation Program
T	Time
TDC	Telemetry Data Center
TM	Telemetry
VLC	Viking Lander Capsule
V	Time Rate of Change of Velocity
WSMR	White Sands Missile Range
Z,Zulu	Greenwich Mean Time

APPENDIX A

DESCRIPTION OF

BALLOON LAUNCHED DECELERATOR

TEST VEHICLE

## APPENDIX A

## DESCRIPTION OF BALLOON LAUNCHED DECELERATOR TEST VEHICLE

The BLDT Vehicle utilized for the high altitude qualification tests of the Viking Mars Lander Decelerator consisted of six (6) major subsystems which were:

- o Structural Subsystem
- o Electrical Subsystem
- o Instrumentation Subsystem
- o R. F. Subsystem
- o Propulsion/Pyrotechnic Subsystem
- o Thermal Control Subsystem

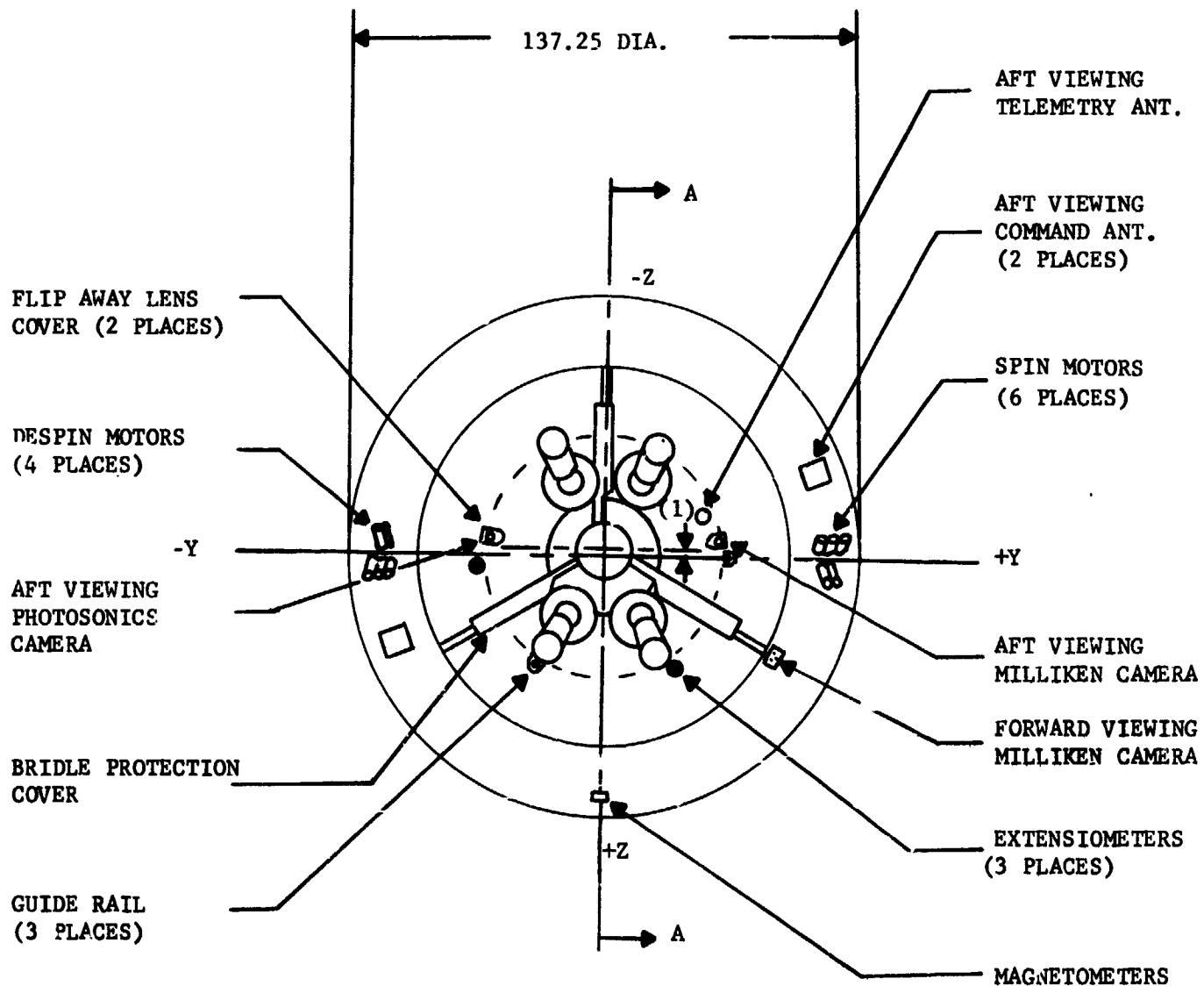
The BLDT vehicles are designed to be flown as supersonic, transonic and free fall vehicles in order to simulate the various anticipated Mars entry conditions for decelerator deployment.

#### A. Structural Subsystem

The vehicle structural configuration provides an external envelope which simulates the Viking Lander Capsule in order to qualify the Decelerator in the wake of a blunt body similar to the actual Mars VLC. The general configuration of the BLDT vehicle is shown in Figures A-1 through A-7.

At the initiation of the BLDT vehicle design, the test bed was to match the Mars VLC Cg and mass properties at decelerator deploy command, insofar as practical. The requirement was for the BLDT vehicle to have a weight of 1888 pounds with a Cg offset of 1.41 inches in the -Z direction at the time of decelerator mortar fire command. The final mass properties

(1) -Z AXIS Cg OFFSET =  $1.41'' \pm 0.030''$



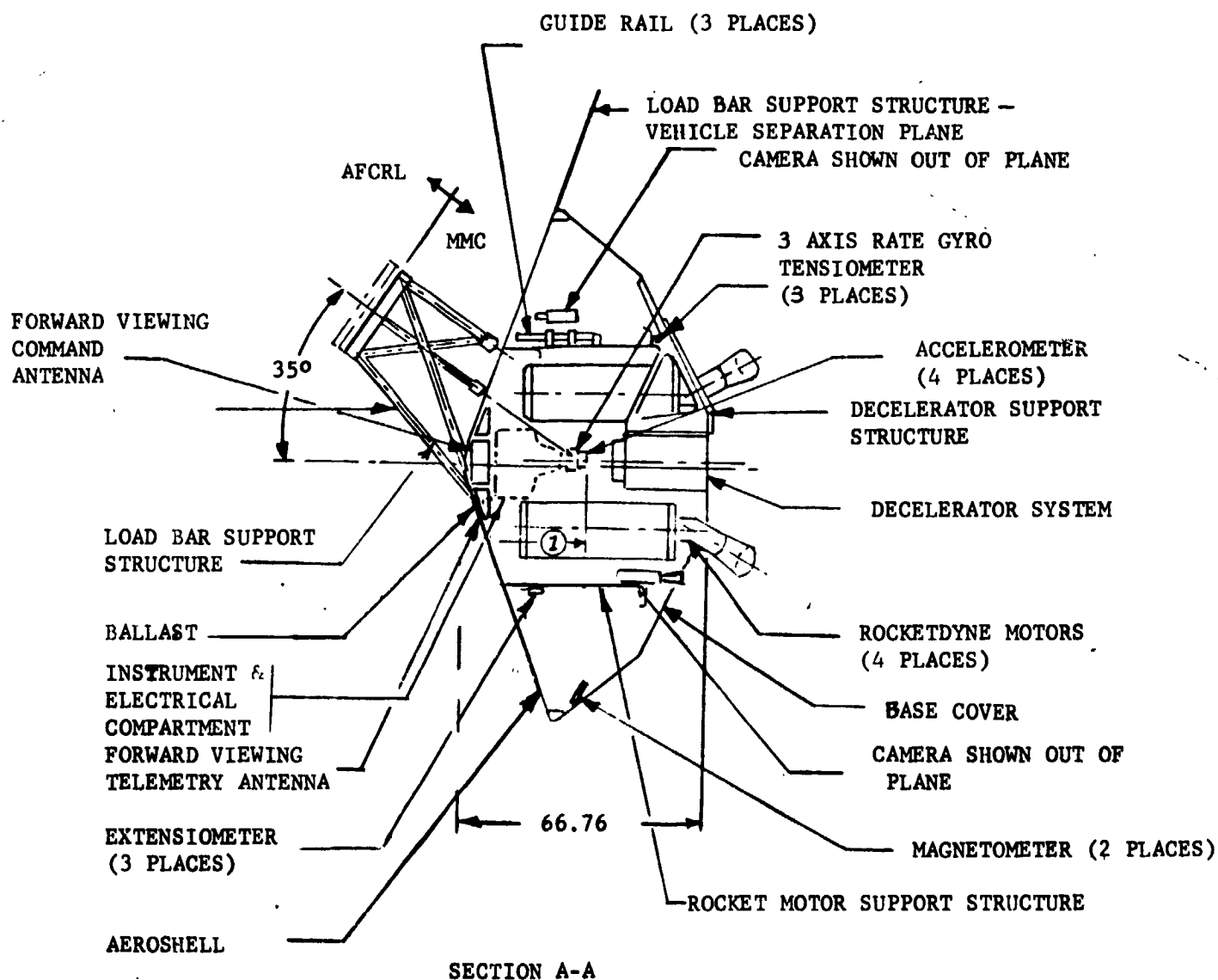
VIEW LOOKING AT AFT END  
OF VEHICLE

BLDT SUPERSONIC VEHICLE CONFIGURATION

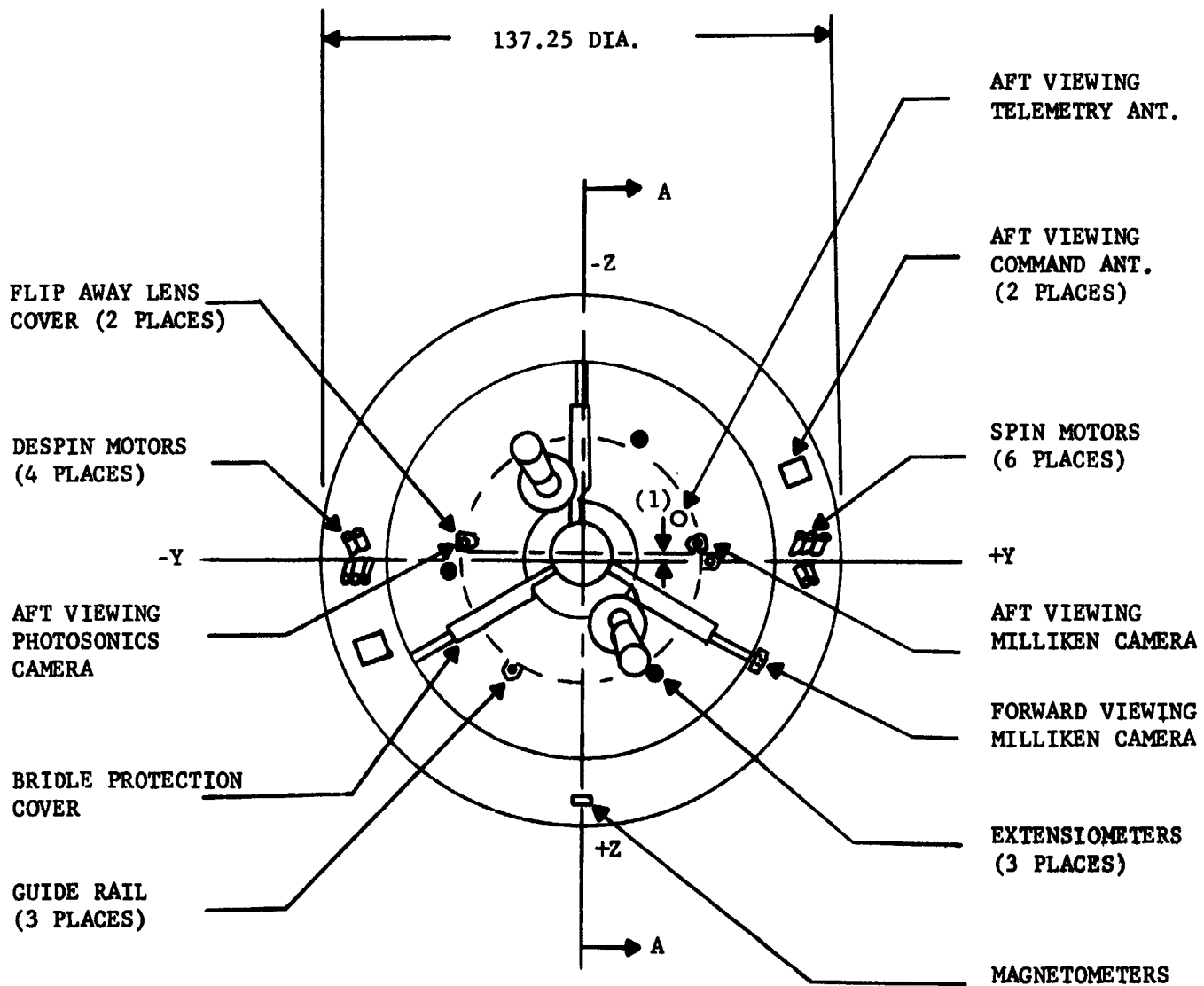
FIGURE A-1



(1) X AXIS Cg AT MORTAR FIRE = 31.7" to 33.7"



(1) -Z AXIS Cg OFFSET =  $1.41'' \pm 0.030''$

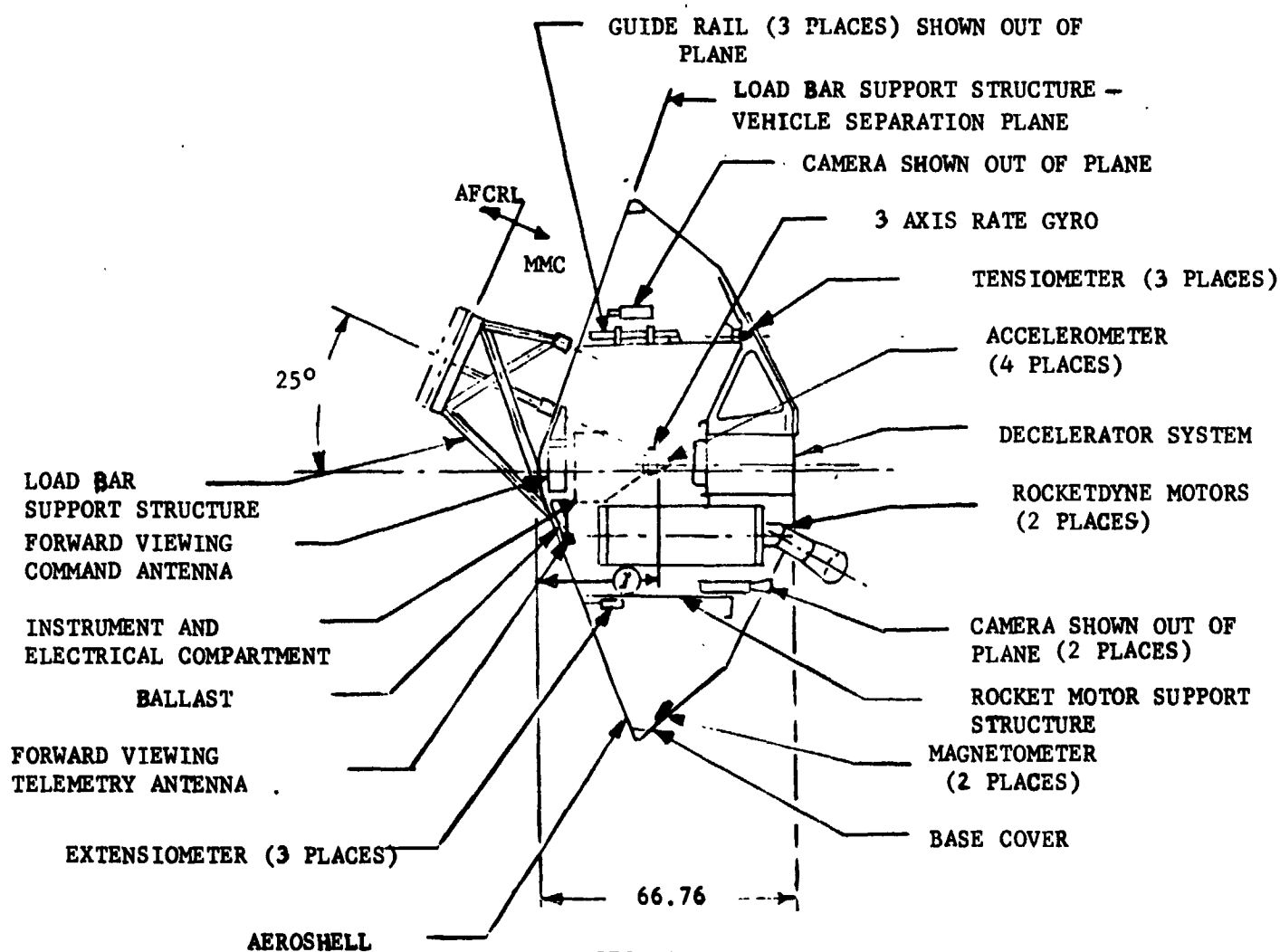


VIEW LOOKING AT AFT END  
OF VEHICLE

BLDT TRANSONIC VEHICLE CONFIGURATION

FIGURE A-3

(1) X AXIS Cg AT MORTAR FIRE = 31.7" to 33.7"

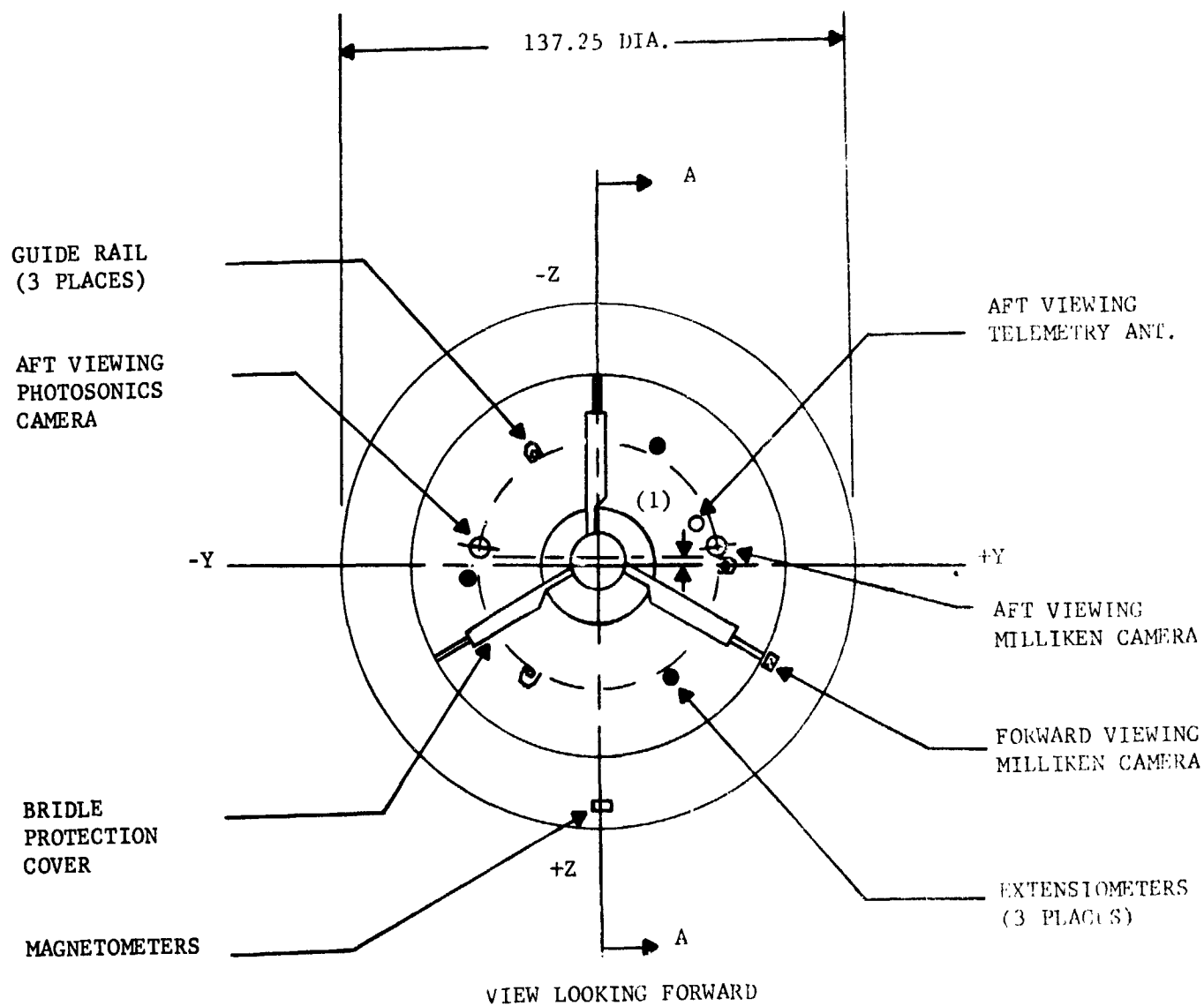


SECTION A-A

BLDT TRANSONIC VEHICLE CONFIGURATION

FIGURE A-4

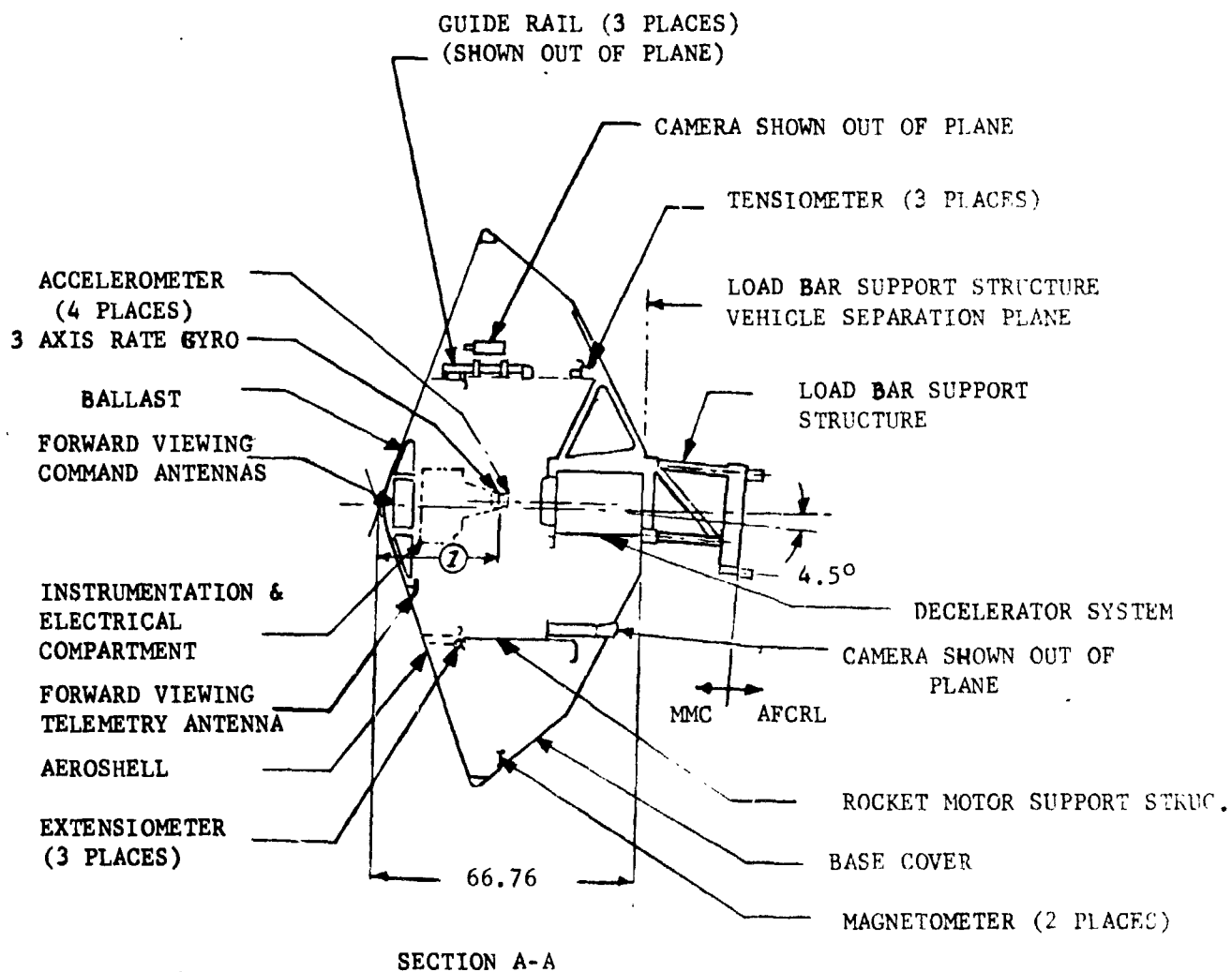
(1) -Z AXIS Cg OFFSET = 1.41"  $\pm$  0.030"



BLDT SUBSONIC VEHICLE CONFIGURATION

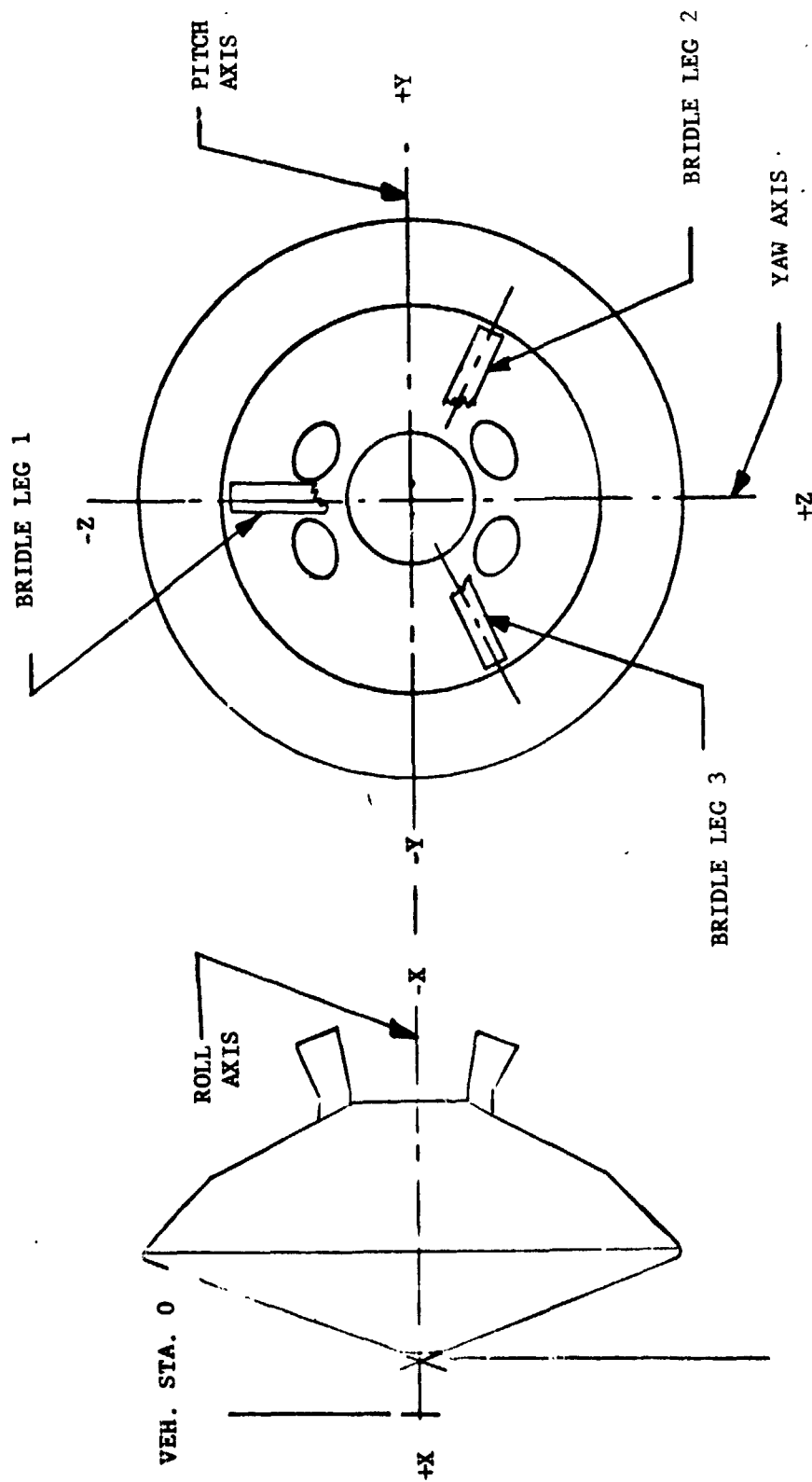
FIGURE A-5

(1) X AXIS  $C_g$  AT MORTAR FIRE = 31.7" to 33.7"



BLDT SUBSONIC VEHICLE CONFIGURATION

FIGURE A-6



VEH. STA.  
+3.183

BLDT COORDINATE SYSTEM  
FIGURE A-7

for each vehicle, included in the individual reports, indicates the revisions which were made to the mass properties subsequent to the BLDT vehicle design.

The structural subsystem consisted of six (6) major components as follows:

1. Rocket Motor Support Structure

The rocket motor support structure is a cylindrical component, approximately 64 inches in diameter, which provides the major vehicle internal longitudinal support structure as well as providing the motor mounts for the supersonic and transonic vehicles.

2. Instrument Beam

The instrument beam is a structural beam which was tied to the forward surface of the RMSS and ran symmetrically along the Y, -Y axis. It also contained an aft facing pylon to mount the accelerometers and rate gyros at or near the vehicle longitudinal Cg.

3. Base Cover

The base cover is a lightweight external shell providing an aft configuration similar to the Mars VLC.

4. Decelerator Support Structure

The decelerator support structure is a three leg structure, similar to the Mars VLC decelerator support structure, with a cylindrical center section for mounting of the decelerator cannister parallel to the BLDT longitudinal centerline. The decelerator support structure assembled into the base cover to provide an intermediate assembly.

### 5. Aeroshell

The Aeroshell which is the forward surface of the vehicle provides a conical blunt aerodynamic surface approximately 11.5 feet in diameter with a  $140^{\circ}$  included angle. The aeroshell provides a forward configuration similar to the Mars VLC.

### 6. Load Bar Support Structure

The load bar support structure is a tubular structural member which provides the interface with the Air Force Cambridge Research Laboratory (balloon) load bar as well as providing the correct hanging pitch attitude.

## B. Electrical Subsystem

The electrical subsystem provides the flight power, cabling and switching/sequencing devices required to properly sequence and activate the various functions. The electrical subsystem is shown schematically in Figure A-8.

The vehicle is powered by five (5) silver zinc batteries as follows:

#### 1. Main Battery - 60 AH - MMC P/W PD94S0026

Provides power for telemetry, command system A and A/B heaters.

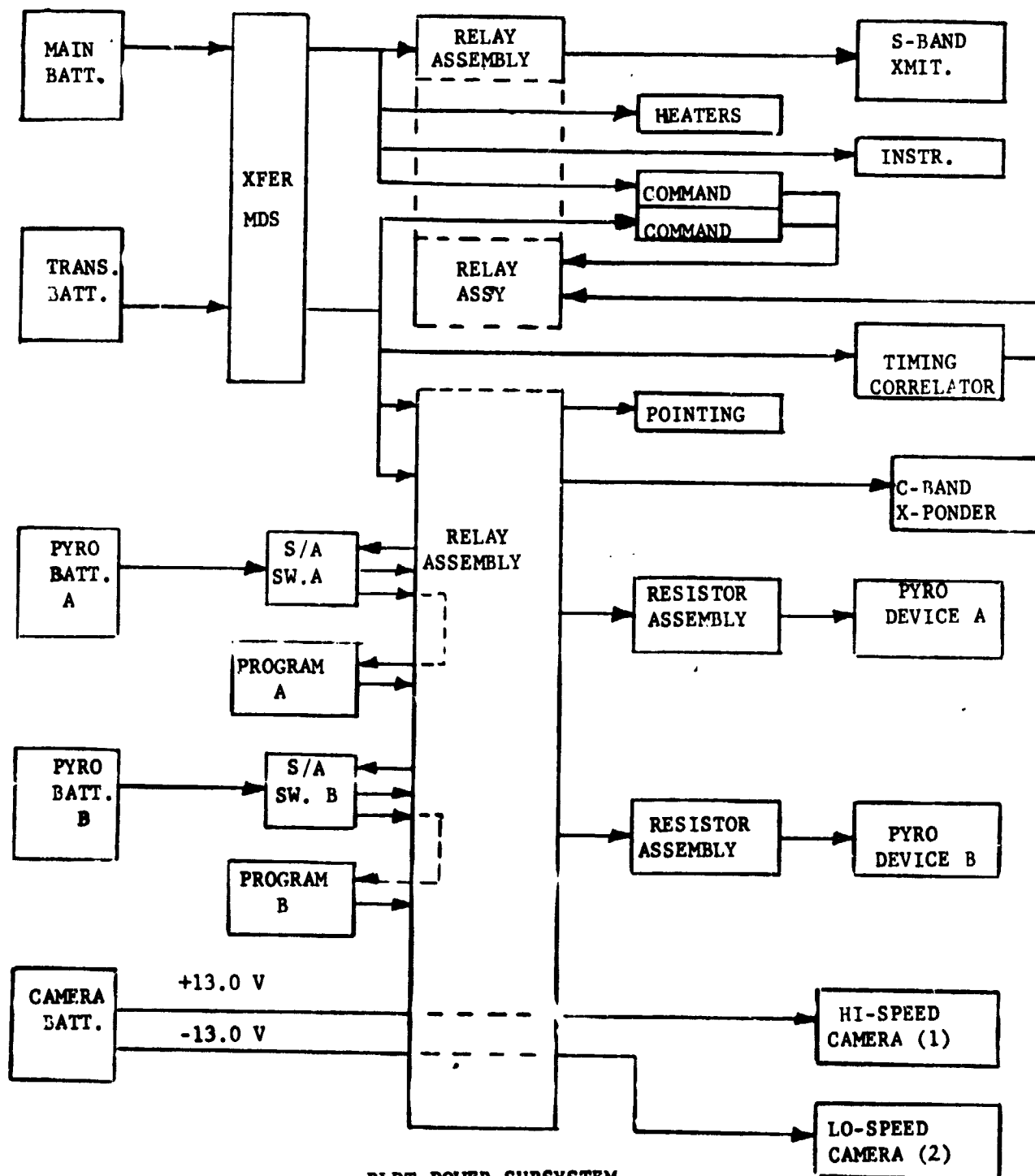
#### 2. Transient Battery - 16 AH Engle Pitcher Model 4332

Provides power for timing correlator, C-band transponder and command system B.

#### 3. Pyro Battery A - 1.0 AH - ESB Model 392

Provides power to all pyro A circuit ordnance devices and airborne programmer A.





BLDT POWER SUBSYSTEM  
BLOCK DIAGRAM

FIGURE A-8

4. Pyro Battery B - 1.0 AH - ESB Model 392

Provides power to all Pyro B circuit ordnance devices and airborne programmer B.

5. Camera Battery - 1.0 AH - ESB Model 393 (Similar to model 392 except tapped at 9 cells and 18 cells).

Provide +13 volts power to onboard high speed cameras.

The electrical subsystem provides completely redundant airborne sequencing programmers and completely redundant pyrotechnic circuits.

In addition, the electrical subsystem provides all power switching relays, motor driven switches, power limiting resistors and airborne heaters.

C. Instrumentation Subsystem

The BLDT Instrumentation subsystem provides for the real time measurement and conditioning of the parameters listed in Table A-1 and provides timing correlation for the real time measurements and airborne camera. The instrumentation subsystem utilizes a PAM/FM/FM configuration as shown schematically in Figure A-9.

Additionally, the instrumentation subsystem provides the following photographic coverage:

1. Aft Looking Photosonics

Approximately 450 frames/second to record the decelerator deployment sequence.

2. Aft Looking Milliken

Sixty-four frames/second to record the decelerator deployment sequence.

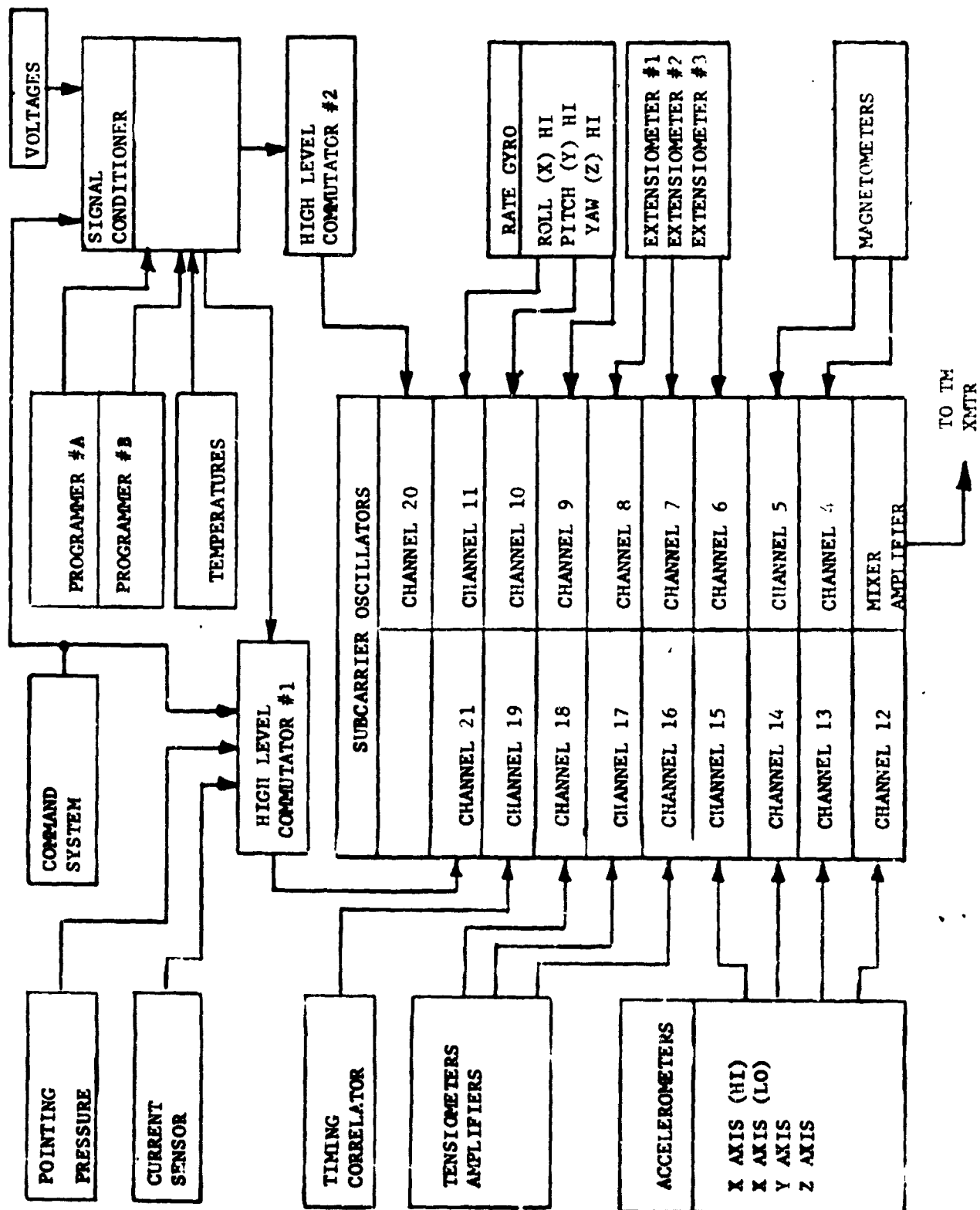


FIGURE A-9 BLDT INSTRUMENTATION SYSTEM

### 3. Forward Looking Milliken

Thirty-two frames/second to record the Aeroshell separation sequence and obtain a time/distance history.

## D. R. F. Subsystem

The R. F. Subsystem consists of the TM transmitter, the C-Band transponder and the redundant command receiver/decoders with all of the required antenna systems.

### 1. TM Transmitter

The telemetry transmitter provides for the FM transmission of the composite FM data from the Instrumentation Subsystem mixer amplifier. The transmitter provides 5 watts power output in the C-Band (2285.5 MHz) range. The TM transmitter and antenna system is shown schematically in Figure A-10.

### 2. C-Band Tracking Transponder

The GFE tracking transponder was provided by White Sands Missile Range and is compatible with tracking radar AN/FPS-16 utilized at WSMR. The transponder and antenna system is shown schematically in Figure A-10.

### 3. Command Receiver/Decoder

The vehicle command system, including antenna, multicoupler, receivers and decoders, is shown schematically in Figure A-11.

The redundant receiver/decoders operate on an assigned frequency of 541 MHz and provide a 28 volt nominal decoder output for command inputs with seven command tones selected from IRIG-103-61 channels 1 through 20.

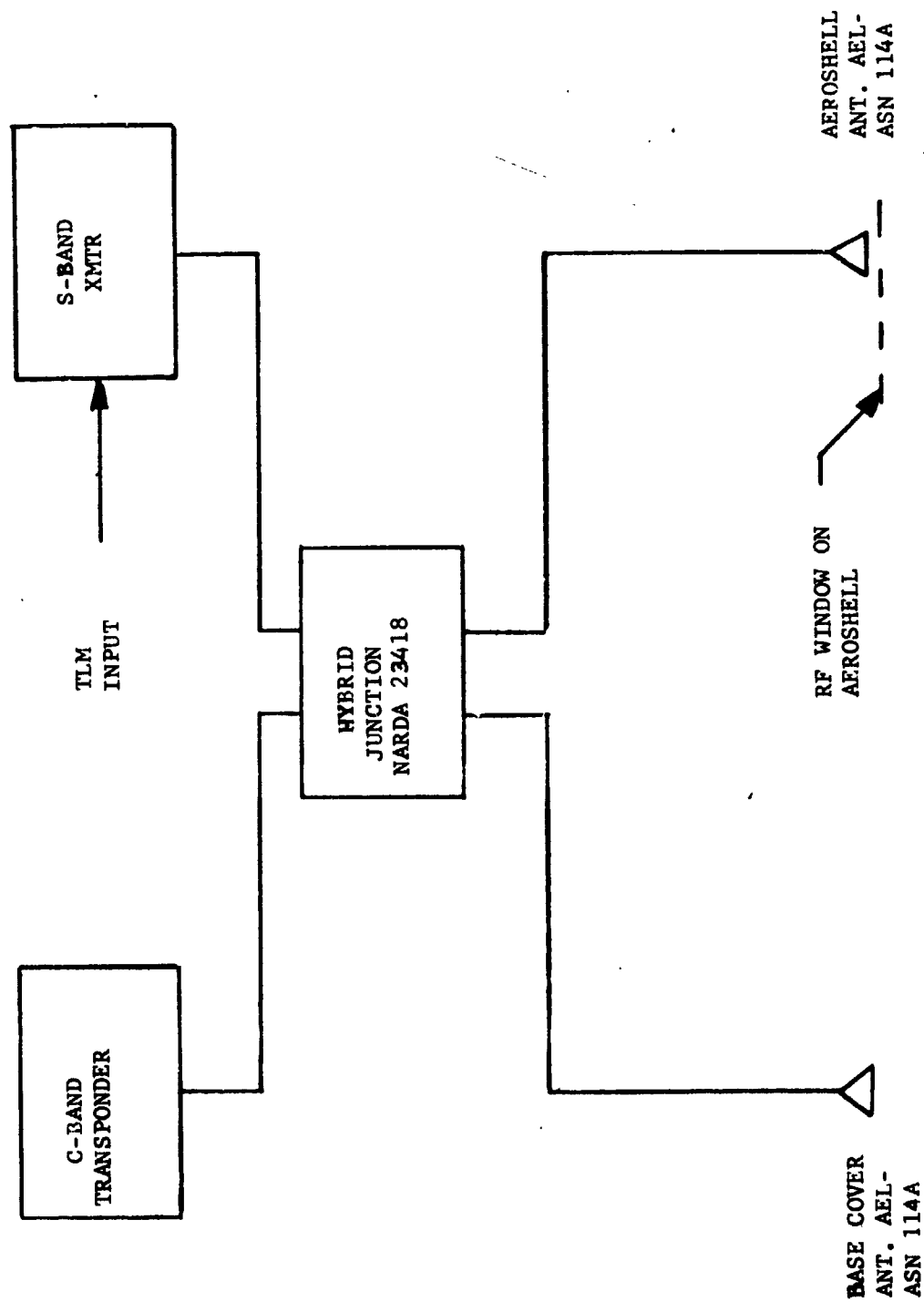


FIGURE A-10 TRACKING &amp; TELEMETRY ANTENNA SYSTEM

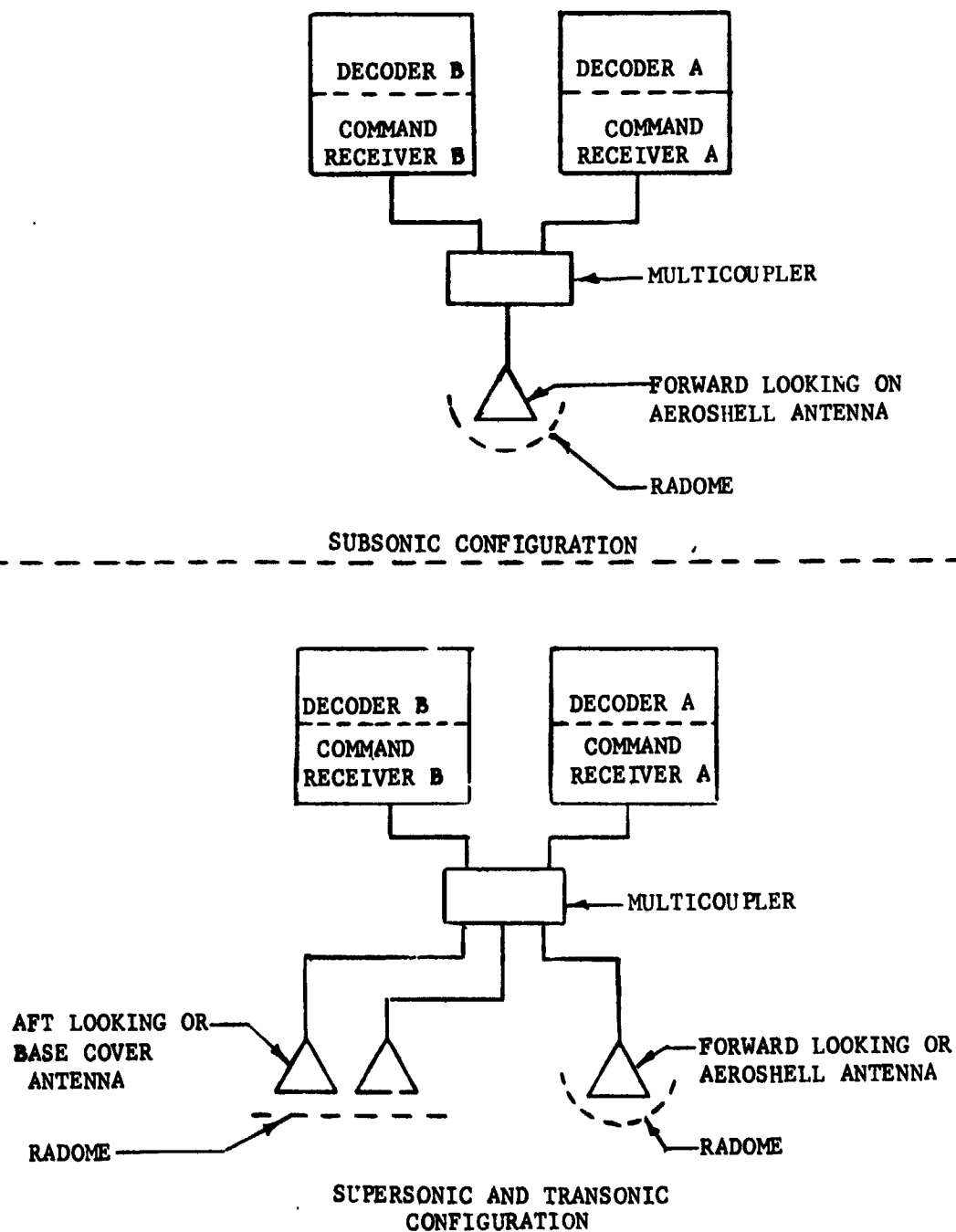


FIGURE A-11

The system coding is such that triple tone ground commands result in the following airborne functions:

<u>Function</u>	<u>Commands</u>		
	<u>Primary</u>	<u>Backup</u>	<u>Redundant</u>
Release from load bar	X		X
Mortar Fire	X		X
Arm Ordnance Bus	X		X
Safe Ordnance Bus	X	X	
Turn RF on	X		
Turn RF off	X		
Pointing, Clockwise	X	X	
Pointing, Counterclockwise	X	X	

#### E. Propulsion/Pyrotechnic Subsystem

The propulsion/pyrotechnic subsystem consists of the solid rocket motors required on the supersonic and transonic vehicles, the azimuth pointing system required on the supersonic and transonic vehicles and the pyrotechnic devices required on all three configurations.

The main propulsion assembly consists of a set of Rocketdyne RS-B-535 solid propellant rocket motors each having the following characteristics:

	<u>Nominal</u>	<u>3 <math>\sigma</math> Variation</u>
Total Impulse, lbf-sec	Classified	0.6%
Burn Time Avg. Thrust, lbf	Classified	1.9%
Nozzle Cant Angle, deg	35	0.1
Thrust Vector Alignment, deg**		0.2
Ignition Interval, msec	49	+27, -17
Burn Time, sec	Classified	1.8%
Loaded Weight, lbm	461.2	0.25***
Burnout Weight, lbm	91.7	3.7****

The supersonic configuration vehicles are provided with 4 of the above motors with the transonic vehicle containing 2.

The spin/despin system is required to reduce trajectory dispersions during booster burn and despin after burnout. Spin Motors having the following characteristics are used:

	<u>Nominal*</u>	<u>3 <math>\sigma</math> Variation</u>
Total Impulse, lbf-sec	76.5	3.0%
Burn Time Avg. Thrust, lbf	86.2	8.0%
Ignition Interval, msec	10.0	+10.0, -5.0
Burn Time, sec	0.87	+11.0%
Loaded Weight, lbm	1.2	0.1
Burnout Weight, lbm	0.9	0.1

\* Vacuum Conditions, 70°F

\*\* Alignment with respect to nozzle geometric centerline.

\*\*\* Actual weighing tolerance.

\*\*\*\* Variation from predicted value.

The supersonic and transonic vehicles utilized 6 each of the above motors for spin-up and 4 each of the above for despin.

Other pyromechanical and pyrotechnic functions included in the vehicle are:

<u>Function</u>	<u>Supersonic</u>	<u>Transonic</u>	<u>Subsonic</u>
Aeroshell Sep. Nuts	3	3	3
Load Bar Release Nuts	0	0	3
Tension Rod Separator	1	1	0
Cable Cutters	2	2	0
Decelerator Mortar*	1	1	1

\* Part of Decelerator System



Also included in the propulsion subsystem is an azimuth pointing system which is used to orient the supersonic and transonic vehicle azimuth at drop in order to assure impact within the White Sands Missile Range in the event of a complete decelerator failure.

The pointing system is comprised of a gaseous nitrogen thruster system located on the balloon load bar. The system provides paired clockwise or counterclockwise rotational moments in response to ground commands. The azimuth pointing system is shown schematically in Figure A-12.

#### F. Thermal Control Subsystem

The thermal control subsystem consists of those passive and active components required to maintain vehicle components within the required temperature levels. These components were generally:

1. Internal and external blankets,
2. Active heaters,
3. Base cover ablative material.

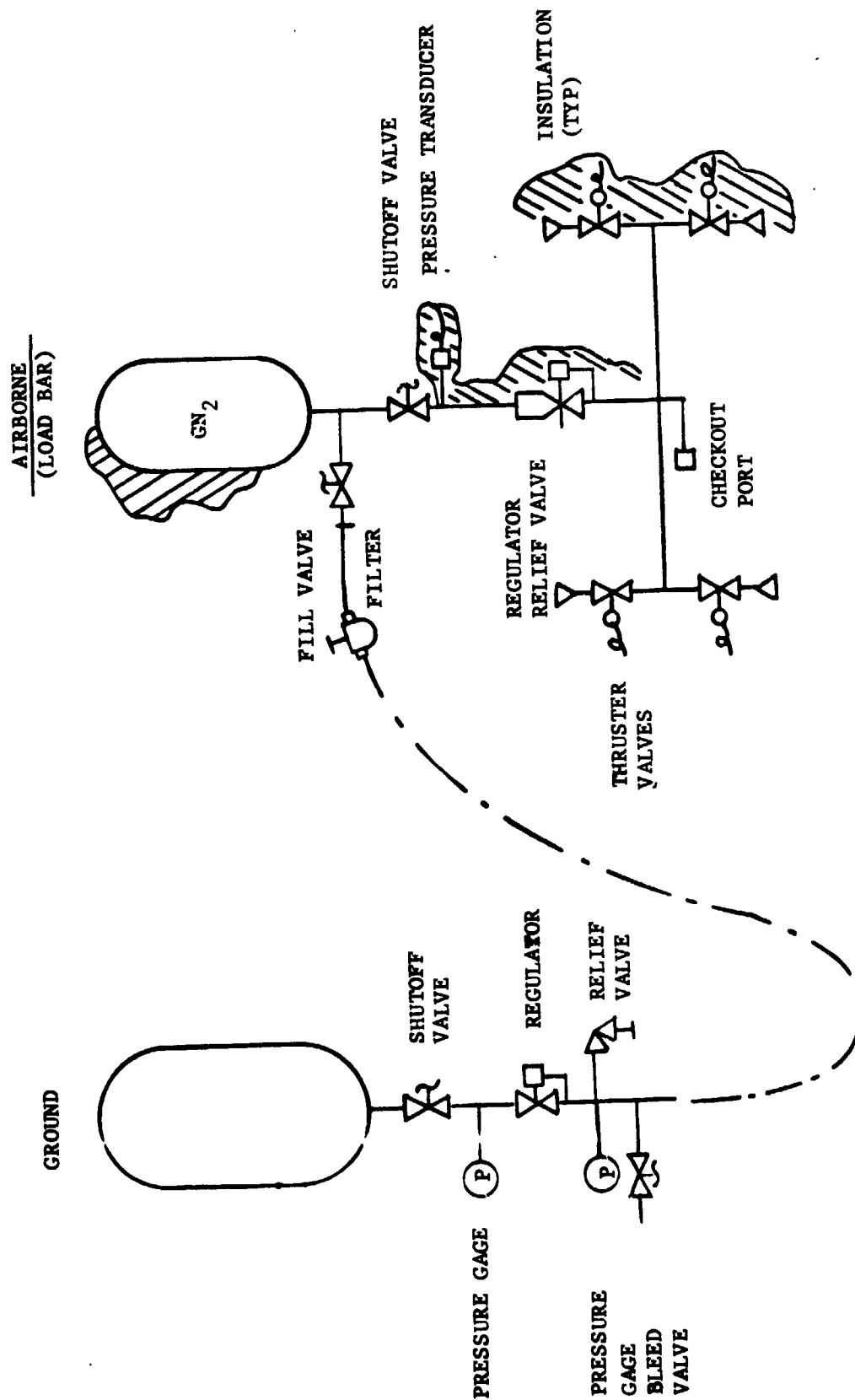


FIGURE A-12 BLDT POINTING SYSTEM

TABLE A-1

## BLDT Telemetry Measurement List

No.	Measurement	Range	Accuracy End-to-End	Resolution	Response	Remarks
1	Accel. X Axis	-2,+5g * -2,+3g **	5%	0.07g 0.05g	100 Hz	Low Range
2	Accel. X Axis	-15, 1g * -7, +1g **	5%	0.16g 0.08g	100 Hz	High Range
3	Accel. Y Axis	+1.0g	5%	0.01g	100 Hz	
4	Accel. Z Axis	+1.0g	5%	0.01g	100 Hz	
5	Heading	360 deg.	+5 deg.	1 deg.	5 Hz	Magnetometer No. 1
6	Heading	360 deg.	+5 deg.	1 deg.	5 Hz	Magnetometer No. 2
7	Rate Gyro, X Axis	+300°/sec.	5%	3.0°/sec	20 Hz	
8	Rate Gyro, Y Axis	+300°/sec.	5%	3.0°/sec	20 Hz	
9	Rate Gyro, Z Axis	+300°/sec.	5%	3.0°/sec	20 Hz	
10	Strain Link	0 to 12,000 lbs. ***	5%	120 lbs.	100 Hz	Parachute Linkage No. 1

\* Supersonic Flight

\*\* Transonic and Subsonic Flight

\*\*\* Amplifier will be adjusted to read 18,000 pounds full scale for supersonic flight only.

TABLE A-1 (CONTINUED)  
BLDT Telemetry Measurement List

No.	Measurement	Range	Accuracy End-to-End	Resolution	Response	Remarks
11	Strain Link	0 to 12,000 lbs. *	5%	120 lbs.	100 Hz	Parachute Linkage No. 2
12	Strain Link	0 to 12,000 lbs. *	5%	120 lbs.	100 Hz	Parachute Linkage No. 3
13	Timing Pulse	25 PPS, 0 to 1.25 VDC	1%	ON/OFF	125 Hz	Camera Correlation
14	Temperature	+25 to +150°F	5%	1.5F	10 Hz	Mortar Breech, Temp. Commuted at 30 SPS
15	Voltage	5 VDC	5%	0.05 VDC	10 Hz	Commutator #1 Full Scale Calibration at 30 SPS
16	Voltage	0 VDC	5%	0.05 VDC	10 Hz	Commutator #1 Zero Scale Calibration at 30 SPS
17	Voltage	0 to 36 VDC	5%	0.36 VDC	10 Hz	Main Battery, Commuted at 30 SPS
18	Current	0 to 16A	5%	0.16 A	10 Hz	Main Battery, Commuted at 30 SPS
19	Voltage	0 to 37 VDC	5%	0.37 VDC	10 Hz	Pyro Battery A Commuted at 30 SPS
20	Event, Cont.	0 to 14 VDC Step Change	± 50ms	(HI/LO)	10 Hz	Prog. A Reset Commuted at 30 SPS

\* Amplifier will be adjusted to read 18,000 pounds full scale for supersonic flight only.

TABLE A-1 (CONTINUED)  
BLDT Telemetry Measurement List

No.	Measurement	Range	Accuracy End-to-End	Resolution	Response	Remarks
21	Event, Pulse	0 to 14 VDC 0.1 sec Duration	$\pm$ 50 ms	(ON/OFF)	10 Hz	Prog. A TM Chan. Commuted at 30 SPS
22	Event, Pulse	0 to 14 VDC 0.1 sec Duration	$\pm$ 50 ms	(ON/OFF)	10 Hz	Prog. B TM Chan. Commuted at 30 SPS
23	Event, Cont.	0 to 4 VDC Step Change	$\pm$ 50 ms	(HI/LO)	10 Hz	CW Point. Valve Signal Commuted at 30 SPS
24	Event, Cont.	0 to 4 VDC Step Change	$\pm$ 50 ms	(HI/LO)	10 Hz	CCW Point. Valve Signal Commuted at 30 SPS
25	Event, Cont.	0 to 4 VDC Step Change	$\pm$ 50 ms	(HI/LO)	10 Hz	Safe/Arm Sw. A Arm Position Comm. at 30 SPS
26	Event, Cont.	0 to 4 VDC Step Change	$\pm$ 50 ms	(HI/LO)	10 Hz	Safe/Arm Sw. A Safe Position Comm. at 30 SPS
27	Pressure	0-2500 psia	5%	25 psi	10 Hz	Pointing system, Pressure Commuted at 30 SPS
28	Extensometer	0 to 12"	5%	0.12"	5 Hz	#1 Aeroshell Sep. Dist.
29	Extensometer	0 to 12"	5%	0.12"	5 Hz	#2 Aeroshell Sep. Dist.
30	Extensometer	0 to 12"	5%	0.12"	5 Hz	#3 Aeroshell Sep. Dist.
31	Voltage	0 to 37 VDC	5%	0.37 VDC	10 Hz	Pyro Battery B Commuted at 30 SPS
32	Voltage	0 to 33.5 VDC	5%	0.33	10 Hz	Transient Battery Commuted at 30 SPS

TABLE A-1 (CONTINUED)

## RLDT Telemetry Measurement List

No.	Measurement	Range	Accuracy End-to-End	Resolution	Response	Remarks
33	Event, Cont.	0 to 4 VDC Step Change	$\pm 50$ ms	(HI/LO)	10 Hz	Safe/Arm Sw. B. Arm Position Comm. at 30 SPS
34	Event, Cont.	0 to 4 VDC Step Change	$\pm 50$ ms	(HI/LO)	10 Hz	Safe/Arm Sw. B Safe Position Comm. at 30 SPS
35	Event, Cont.	0 to 14 VDC Step Change	$\pm 50$ ms	(HI/LO)	10 Hz	Programmer B Reset Commu- tated at 30 SPS
36	Deleted					
37	Temperature	-90 to +210°F	5%	3.0°F	10 Hz	Bridle Temp. #1 Commutated at 30 SPS
38	Temperature	-90 to +210°F	5%	3.0°F	10 Hz	Bridle Temp. #2 Commutated at 30 SPS
39	Temperature	-90 to +210°F	5%	3.0°F	10 Hz	Bridle Temp. #3 Commutated at 30 SPS
40	Temperature	-90 to +210°F	5%	3.0°F	10 Hz	Cannister Temp. #1 Commu- tated at 30 SPS
41	Temperature	-90 to +210°F	5%	3.0°F	10 Hz	Cannister Temp. #2 Commu- tated at 30 SPS
42	Temperature	0 to +125°F	5%	1.5°F	10 Hz	Instr. Beam Temp. #1 Commutated at 30 SPS
43	Temperature	0 to +175°F	5%	2.0°F	10 Hz	Main Battery Temp. Commutated at 30 SPS

TABLE A-1 (CONTINUED)  
BLDT Telemetry Measurement List

No.	Measurement	Range	Accuracy End-to-End	Resolution	Response	Remarks
44	Temperature	-100 to +150°F	5%	2.5°F	10 Hz	Rocket Mtr. Supp. Strt. Temp. Commutated at 30 SPS
45	Event	0 or 5 VDC	± 50 ms	HI/LO	10 Hz	Command Tone #1 Commu- tated at 30 SPS
46	Event	0 or 5 VDC	± 50 ms	HI/LO	10 Hz	Command Tone #2 Commu- tated at 30 SPS
47	Event	0 or 5 VDC	± 50 ms	HI/LO	10 Hz	Command Tone #3 Commu- tated at 30 SPS
48	Event	0 or 5 VDC	± 50 ms	HI/LO	10 Hz	Command Tone #4 Commu- tated at 30 SPS
49	Event	0 or 5 VDC	± 50 ms	HI/LO	10 Hz	Command Tone #5 Commu- tated at 30 SPS
50	Event	0 or 5 VDC	± 50 ms	HI/LO	10 Hz	Command Tone #6 Commu- tated at 30 SPS
51	Event	0 or 5 VDC	± 50 ms	HI/LO	10 Hz	Command Tone #7 Commu- tated at 30 SPS
52	Voltage	0 to 4 VDC	5%	0.04 VDC	10 Hz	Command Receiver A Signal Level Commutated at 30 SPS
53	Event	0 or 28 VDC 0.1 sec duration	± 50 ms	ON/OFF	10 Hz	Mortar Fire Commutated at 30 SPS
54	Temperature	+25 to 150°F	5%	1.5°F	10 Hz	Mortar Breech Flange Temp. Commutated at 30 SPS

TABLE A-1 (CONTINUED)  
BLDT Telemetry Measurement List

No.	Measurement	Range	Accuracy End-to-End	Resolution	Response	Remarks
55	Temperature	0 to +175°F	5%	2.0°F	10 Hz	S-Band Transmitter Temp. Commuted at 30 SPS
56	Temperature	-100 to +150°F	5%	2.5°F	10 Hz	Aeroshell Temp. #1 Commuted at 30 SPS
57	Temperature	-100 to +150°F	5%	2.5°F	10 Hz	Aeroshell Temp. #2 Commuted at 30 SPS
58	Temperature	0 to +175°F	5%	2.0°F	10 Hz	Equipment Ballast Temp. Commuted at 30 SPS
59	Temperature	0 to +125°F	5%	1.5°F	10 Hz	Instrument Beam (#2) Temp. Commuted at 30 SPS
60	Temperature	0 to +125°F	5%	1.5°F	10 Hz	Gyro Temp. Commuted at 30 SPS
61	Temperature	-100 to +150°F	5%	2.5°F	10 Hz	Boost Motor #1 Temp. Commuted at 30 SPS
62	Temperature	-100 to +150°F	5%	2.5°F	10 Hz	Boost Motor #2 Temp. Commuted at 30 SPS
63	Voltage	0 to 4 VDC	5%	0.04 VDC	10 Hz	Command RCVR B Signal Level Commuted at 30 SPS
64	Voltage	5 VDC	5%	0.05 VDC	10 Hz	Commulator #2 Full Scale Calibration at 30 SPS
65	Voltage	0 VDC	5%	0.05 VDC	10 Hz	Commulator #2 Zero Scale Calibration at 30 SPS



**APPENDIX B**

**DESCRIPTION OF BLDT**

**SYSTEM MISSION**

## APPENDIX B

A. Description of BLDT System Mission1. Purpose of the System

The BLDT System is designed to subject the Viking Decelerator System to Qualification Test Requirements at simulated Mars Entry atmospheric conditions.

2. System Requirements

The Viking Decelerator System earth atmospheric test conditions which result from consideration of the variation in probable Mars atmospheres are:

	<u>Supersonic Case 1</u>	<u>Supersonic Case 2</u>	<u>Transonic Case</u>	<u>Subsonic Case</u>
Peak Load Mach No.	$2.17 \pm 0.17$	$2.06 \pm 0.16$	$1.15 \pm 0.10$	$0.46 \pm 0.03$
Peak Load Dyn. Press. (PSF)	$10.09 \pm 0.57$	$9.39 \pm 0.55$	$4.52 \pm 0.30$	$6.46 \pm 0.80$
Angle of Attack at M/F (Degrees)	$\leq 17$	$\leq 17$	$\leq 20$	$\leq 17$

The design of the BLDT test bed is constrained by the Viking Lander Capsule design to the following:

- o Vehicle weight at mortar fire - 1888 pounds.
- o Cg offset in minus Z direction - 1.41 inches.
- o Vehicle external envelope similar to VLC (See Appendix A)
- o Decelerator Temperature at mortar fire -  $80^{\circ}\text{F}$

### 3. System Description

The BLDT System design which evolved from the above test requirements provides for a large volume, high lift balloon system capable of floating the BLDT Vehicles at altitudes from which the test conditions can be achieved with reduced or no propulsion capability. The predicted test altitudes and balloon lift capability involved in the system design are:

	<u>Supersonic Case 1</u>	<u>Supersonic Case 2</u>	<u>Transonic Case</u>	<u>Subsonic Case</u>
* Balloon Float Altitude (FT)	119,000	119,000	120,500	92,000
* Decelerator Mortar Fire Alt. (FT)	147,800	148,600	137,500	89,300
BLDT Vehicle Launch Weight (LBS)	3,550	3,550	2,800	2,050

The system concept provides for the launch of the balloon/flight vehicle system from the Roswell Industrial Air Center, Roswell, New Mexico with the system ascending to float altitude during the approximately 100 mile westward flight to the White Sands Missile Range. Once over the range, the flight vehicle is released from the balloon load bar to complete its flight sequence.

For the powered flight tests, the vehicle concept provides for spin rotation of the vehicle prior to solid rocket motor boost to minimize thrust dispersion effects. Following the boost phase, the vehicle is despun and allowed to coast to the correct dynamic pressure condition. For the subsonic case, the vehicle is released from the load bar and allowed to free fall until the correct velocity is attained.

---

\* USS62 Pressure Altitude

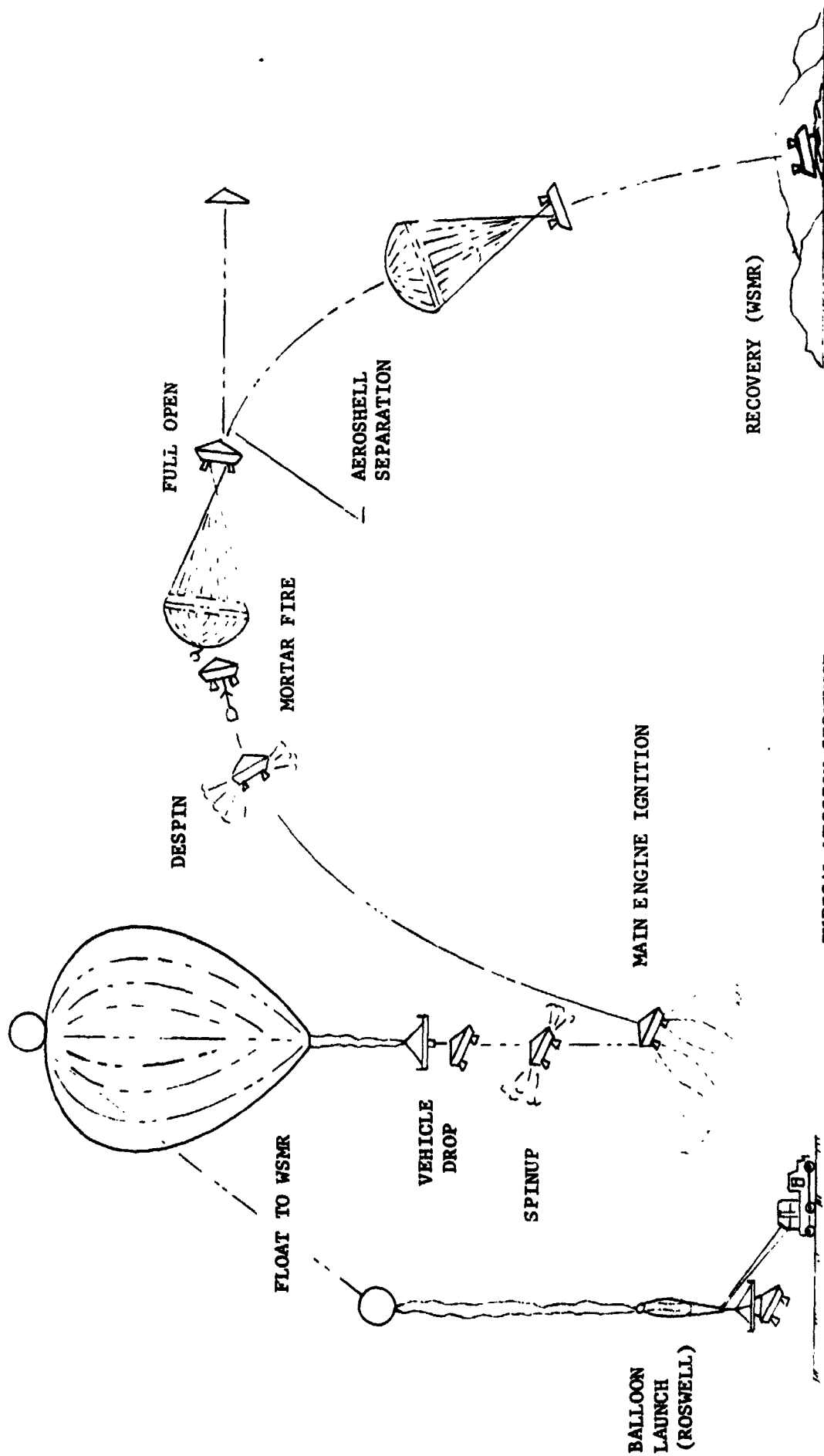
At the White Sands Missile Range, a ground computer system is programmed to receive tracking data which when integrated with predicted meteorological parameters provides the intelligence for the computer to issue a mortar fire command at the required test dynamic pressure for the powered flights. For the non-powered flight, the computer issues a timed mortar fire command following a delay for the correct velocity test conditions to be attained. In both powered and non-powered flights the vehicle incorporates an on-board programmer which provides a backup mortar fire command. Figure B-1 and B-2 depicted a typical powered and non-powered flight.

The system design includes all of the handling, checkout and control equipment necessary for prelaunch checkout, flight control and recovery of the system components.

#### 4. Operations Description

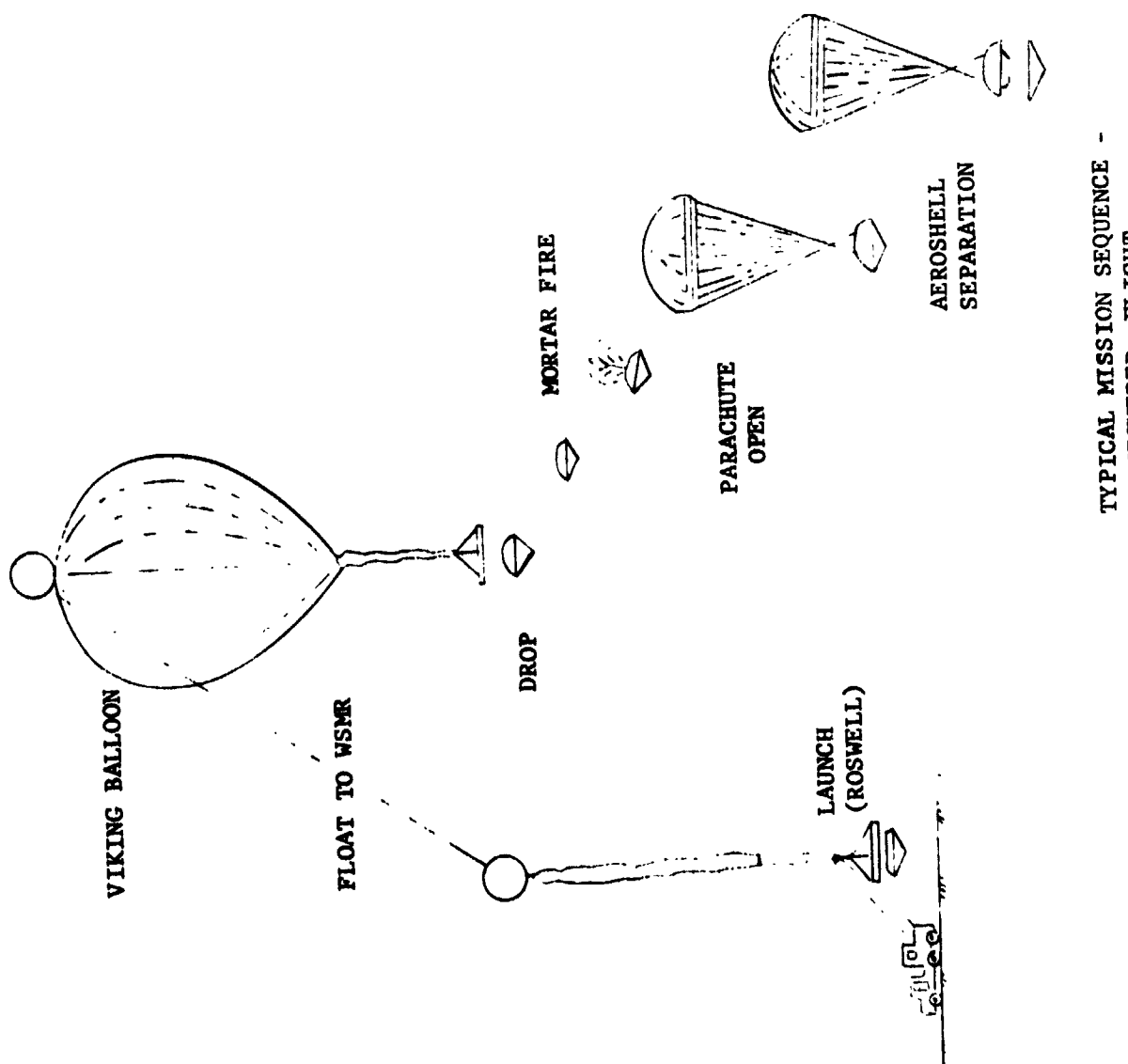
A typical sequence flow of the mission operations from assembly and checkout at Roswell, New Mexico through vehicle flight and recovery at WSMR, is shown in Figure B-3. Each of the sequence events is described below:

a. BLDT Vehicle Assembly and Checkout - This phase of the mission operation encompasses the assembly and checkout of the various system components. The ELDT vehicle, while connected to ground electrical power and in partially assembled condition, is subjected to subsystem and combined system testing in a close loop and open loop mode. The vehicle is then assembled including airborne batteries and subjected to a full flight readiness test on airborne power and in an open loop mode.



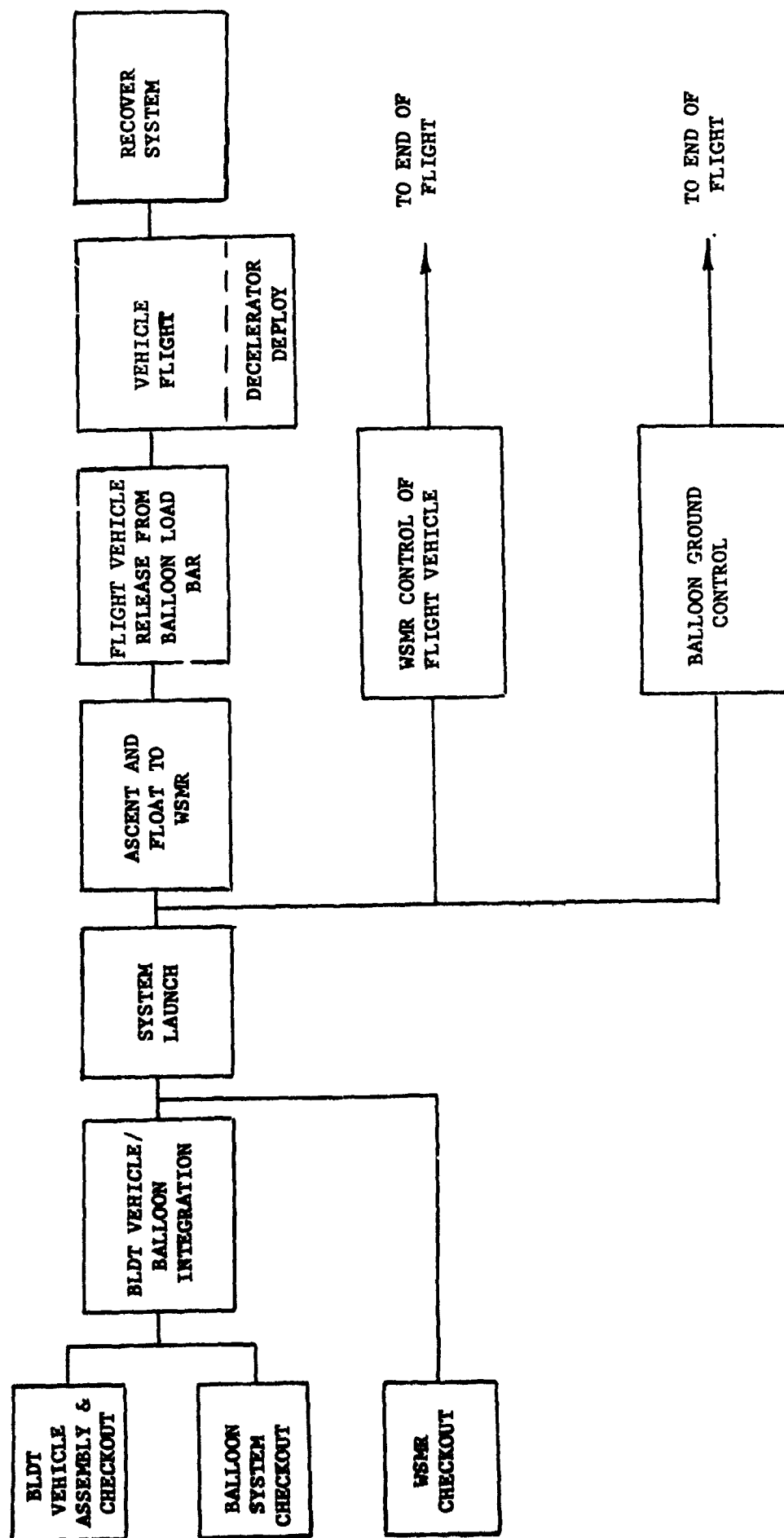
TYPICAL MISSION SEQUENCE -  
POWERED FLIGHT

FIGURE B-1



TYPICAL MISSION SEQUENCE -  
UNPOWERED FLIGHT

FIGURE B-2



TYPICAL OPERATIONS SEQUENCE

FIGURE B-3

While the flight vehicle is undergoing checkout and assembly, the balloon system is also being partially assembled and subjected to flight readiness testing. These checkout and assembly events were performed at the Roswell Industrial Air Center.

Coincident with the checkout of the flight system, the ground control system at the White Sands Missile Range is readied for the mission by assuring that:

- 1) The flight TM data is routed to the correct terminal data stations.
- 2) The ground command system is capable of transmitting acceptable commands.
- 3) The communications links are correctly activated.
- 4) The command station personnel are prepared to accept vehicle control.

b. BLDT Vehicle/Balloon Integration - When the prerequisite flight vehicle balloon system and WSMR Control Center checkout are completed and the meteorological constraints at the launch site and WSMR (Launch winds, float winds, local weather, etc.) are satisfactory, the flight vehicle and balloon systems are moved from the checkout hanger to the launch runway where system integration and final checkout is made.

The flight vehicle is connected to ground power and final subsystem testing is completed to assure all subsystems are functioning. The vehicle ordnance is electrically connected and the vehicle access panels are installed. In this time period the launch balloon and float balloon are layed-out and integrated with the flight vehicle, the abort recovery cargo chutes, the balloon winch and the launch crane.



When the system integration is completed, the launch stand is removed from the flight vehicle leaving the flight vehicle suspended from the balloon load bar which in turn is suspended from the launch crane. Also, the launch balloon is filled with a precisely metered quantity of helium.

c. System Launch - Following the integration of the flight vehicle and balloon into the BLDT system, the system is ready for launch.

The launch process begins with a ground winching operation in which the launch balloon is permitted to rise and which upon rising takes the float balloon (uninflated) and the cargo abort chutes from a horizontal attitude to a vertical attitude above the launch crane. Once the system is in the vertical attitude, the winch cable is separated from the balloon system through the use of an ordnance device. At this point, the two balloons with the abort cargo chutes are floating above and tethered to the launch crane with the balloon load bar and flight vehicle suspended from the crane beneath the tethered balloon. At this point, the total system for a powered flight extend from ground level to approximately 1000 feet above ground level (800 feet for a non-powered flight).

With all of the preceeding operations complete, it only remains to release the flight system from the launch crane. To do this, the launch crane is driven down wind at a velocity necessary to position the crane approximately under the balloon at which point the crane release device is actuated and the balloon floats free of the ground system taking with it the balloon load bar and flight vehicle.

d. Ascent and Float Phase - During the ascent and float phase, the balloon system, floating freely, responds to the wind directions and velocities encountered as it ascends to the design float altitude. Generally, once clear of low altitude wind influence, the balloons float in a westerly direction intersecting the WSMR at about mid-range.

As the system ascends, the helium which was loaded in the launch balloon is forced down into the float balloon which slowly inflates the float balloon and causes the system to ascend. This process continues until the float balloon becomes fully inflated at which point no further lift can be obtained. The balloon ascent to float altitude is rapid enough to arrive at the float altitude prior to intersecting the WSMR.

The balloon ascent and direction is somewhat controllable through the use of ballast dumping operations to control floating altitude and rise rates in order to take advantage of winds at the upper levels. The control of the balloon during the ascent and float phase is from the Air Force Cambridge Research Laboratory control center at Holloman Air Force Base, Alamogordo, New Mexico.

When the ascending system passes through approximately 30 K feet, the WSMR tracking radar, command networks and TM receiving stations are able to acquire the flight vehicle and start checkout. Part of the float checkout assures operation of the command nets by sending commands which do not change vehicle configuration (i.e. safe ordnance circuits, turn R.F. on, etc.) and verifying receipt of the commands through flight vehicle TM data being received at the control center.

e. Vehicle Release from Load Bar - Once the BLDT system reaches the proper float altitude and intersects the range, the vehicle ordnance circuits are armed, the vehicle flight azimuth is attained using a cold gas pointing system and the vehicle release from the load bar is commanded. All of these functions occur as a result of ground commands issued by the flight vehicle control crew at WSMR.

f. Vehicle Flight - The vehicle flight events are a function of the type of mission being flown. Table B-1 presents a sequence of

events and event times for the Supersonic, Transonic and Subsonic missions. All of the event times in Table B-1 are times from release of the flight vehicle from the balloon load bar with the exception of the ground mortar fire command for the powered flights. This command is time variable and is issued by the ground computer during the vehicle coast following despin when the vehicle achieves the correct dynamic pressure.

For the powered flights following release of the vehicle from the load bar, the vehicle is under control of the redundant airborne programmers with the exception of the issuance of the decelerator mortar fire. The vehicle functions provide a flight profile as shown in Figures B-1 and B-2.

During the vehicle powered flights, the vehicle is tracked by the WSMR tracking devices to provide the ground computer with the intelligence for issuing the mortar fire command. For all flights, tracking devices provide data for post flight analysis and to support vehicle recovery operations.

For the non-powered, free fall mission, the vehicle functions are commanded by the on-board redundant programmers except for the mortar fire which is issued as a timed output from the ground computer.

g. Recovery Operations - During this phase of the mission, all of the system components are located and moved to WSMR facilities for post flight inspection. Also during this phase the various system cameras are recovered and the film processed for post flight analysis.

TABLE B-1  
VEHICLE FLIGHT SEQUENCE OF EVENTS

<u>SUPERSONIC</u>		<u>TRANSONIC</u>		<u>SUBSONIC</u>	<u>FUNCTION</u>	<u>SOURCE</u>
<u>CASE 1</u>	<u>CASE 2</u>					
$T_D - 30 \text{ min.}$	$T_D - 30 \text{ min.}$	Drop - 30 min.	Drop - 30 min.		Attain Float Altitude	--
$T_D - 10 \text{ min.}$	$T_D - 10 \text{ min.}$	$T_D - 10 \text{ min.}$	$T_D - 10 \text{ min.}$	--	Start Azimuth Pointing	Ground Command
$T_D - 5 \text{ min.}$	$T_D - 5 \text{ min.}$	$T_D - 5 \text{ min.}$	$T_D - 5 \text{ min.}$	$T_D - 5 \text{ min.}$	Arm Ordnance Bus	Ground Command
$T_D - 10 \text{ sec.}$	$T_D - 10 \text{ sec.}$	$T_D - 10 \text{ sec.}$	$T_D - 10 \text{ sec.}$	--	Confirm Drop Azimuth	A/B T/M
$T_D$	$T_D$	$T_D$	$T_D$	$T_D$	Drop from Load Bar. Initiate A/B Programmer.	Ground Command
$T_D + 1 \text{ sec.}$	$T_D + 1 \text{ sec.}$	$T_D + 1 \text{ sec.}$	$T_D + 1 \text{ sec.}$	--	Ignite Spin Motors/ Enable Boost Motor	A/B Programmer
$T_D + 2 \text{ sec.}$	$T_D + 2 \text{ sec.}$	$T_D + 2 \text{ sec.}$	$T_D + 2 \text{ sec.}$	--	Ignite Boost Motors	A/B Programmer
--	--	--	--	$T_D + 12 \text{ sec.}$	Start AFT Looking Camera, Enable Mortar	A/B Programmer
--	--	--	--	$T_D + 16 \text{ sec.}$	Initiate Mortar Fire/ Start AFT Hi-Speed Camera	Ground Command
--	--	--	--	$T_D + 18 \text{ sec.}$	Initiate M/F Backup	A/B Programmer
--	--	--	--	$T_D + 30 \text{ sec.}$	Separate Aeroshell	A/B Programmer
$T_D + 33 \text{ sec.}$	$T_D + 33 \text{ sec.}$	$T_D + 33 \text{ sec.}$	$T_D + 33 \text{ sec.}$	--	Ignite Despin Motors/ Release Camera Lens Covers/Start AFT Camera Enable Mortar	A/B Programmer
$T_D$ (s cond. correct)	$T_D$ (q cond. correct)	$T_D$ (q cond. correct)	$T_D$ (q cond. correct)	--	Initiate Decelerator Mortar Fire/Start AFT Hi-Speed Camera	Ground Command
$T_D + 37 \text{ sec.}$	$T_D + 38 \text{ sec.}$	$T_D + 39 \text{ sec.}$	$T_D + 39 \text{ sec.}$	--	Initiate M/F Backup	A/B Programmer
$T_D + 47.6 \text{ sec.}$	$T_D + 47.6 \text{ sec.}$	$T_D + 47 \text{ sec.}$	$T_D + 47 \text{ sec.}$	--	Separate Aeroshell	A/B Programmer

APPENDIX C

GAC POST-TEST INSPECTION

## APPENDIX C

## GAC POST-TEST INSPECTION

EXCERPTS FROM GAC REPORT NO. RSE-20927-21

The Viking decelerator system S/N 17 was flown as BLDT 4 (AV-3). This system incorporated S/N 18 parachute. The following constitutes the post-flight inspection report.

Chute Canopy

The damage chart is present in Figure C-1. As noted on the chart, there are 4 black smudges on gore 25 in the band area. There are random brown spots on the disk. One of the brown spots was accompanied by a small bug. There was no physical damage to the canopy.

Suspension Lines - No damage.

Deployment Bag

There are 4 small cuts located between 5" and 8" from the bottom of the bag. Two of the cuts are near an imprint of the swivel bolt. The bag is blackened on the outside surface.

Buffer

The quartz facing of the buffer is torn (approximately 1 inch) at each of the tie locations. The facing in the center of the buffer is torn at the points where the filler block is attached.

Filler Block - The filler block is missing.

Bridle Legs

The bridle legs are undamaged. Some of the basting stiches are broken. The bridle legs are blackened.

Cover Thermal Protection

Some random ruptures of the quartz facing are in evidence. The segments are blackened.

Bridle Leg Covers - The covers are blackened. No apparent damage.

Mortar

The inside of the mortar tube is blackened. The straps at the top of the mortar are all intact. The choker cord is fused to one of the straps. There is no apparent damage to the mortar.

Sabot

The sabot is blackened on the outer surface. The Teflon and stainless steel discs are still attached. The sabot retention straps are blackened but intact.

- x BROWN SPOTS  
⊗ BROWN SPOT ACCOMPANIED  
BY SMALL BUG

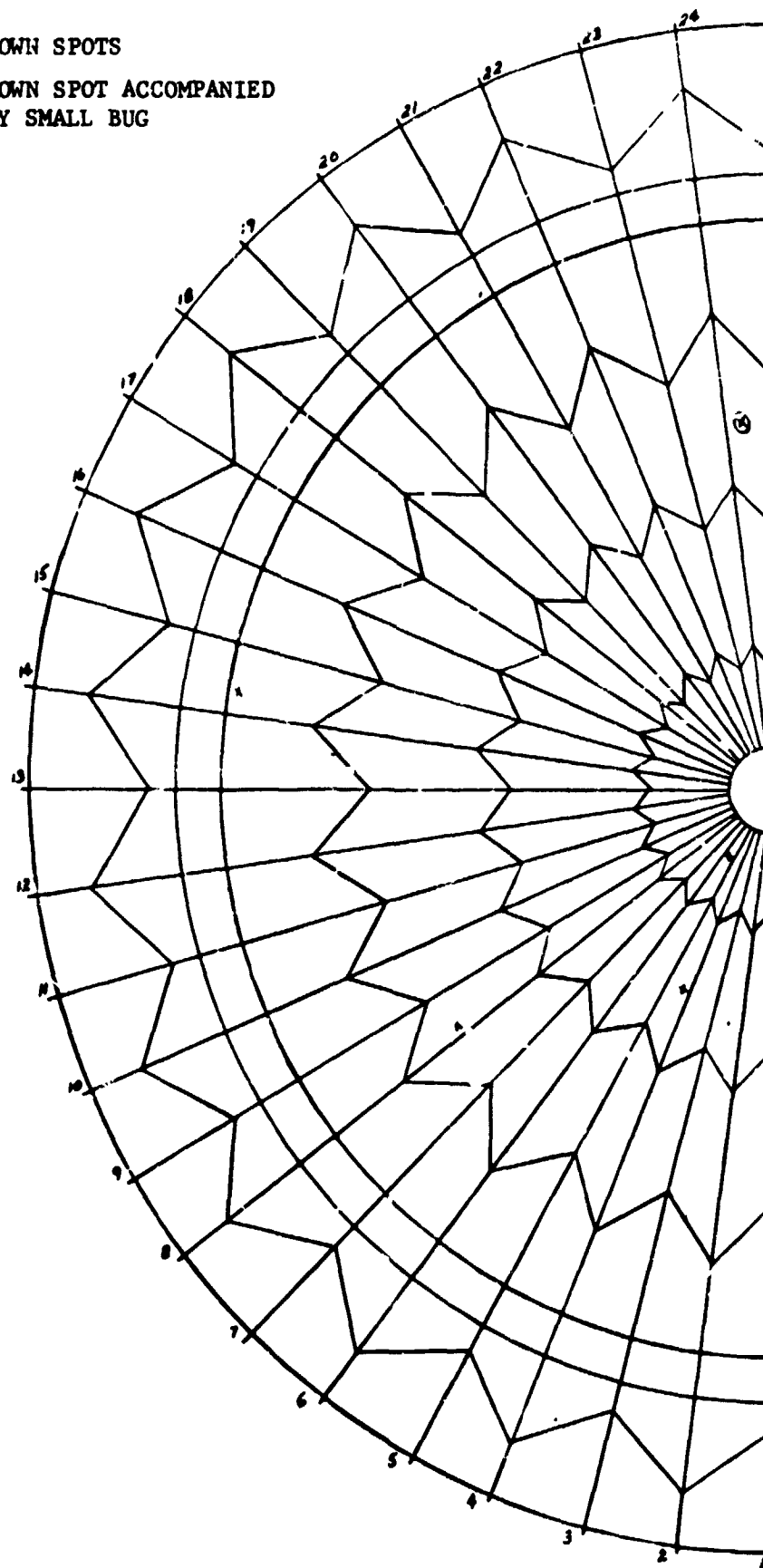


FIGURE C-1 PARACHUTE DAMAGE CHART



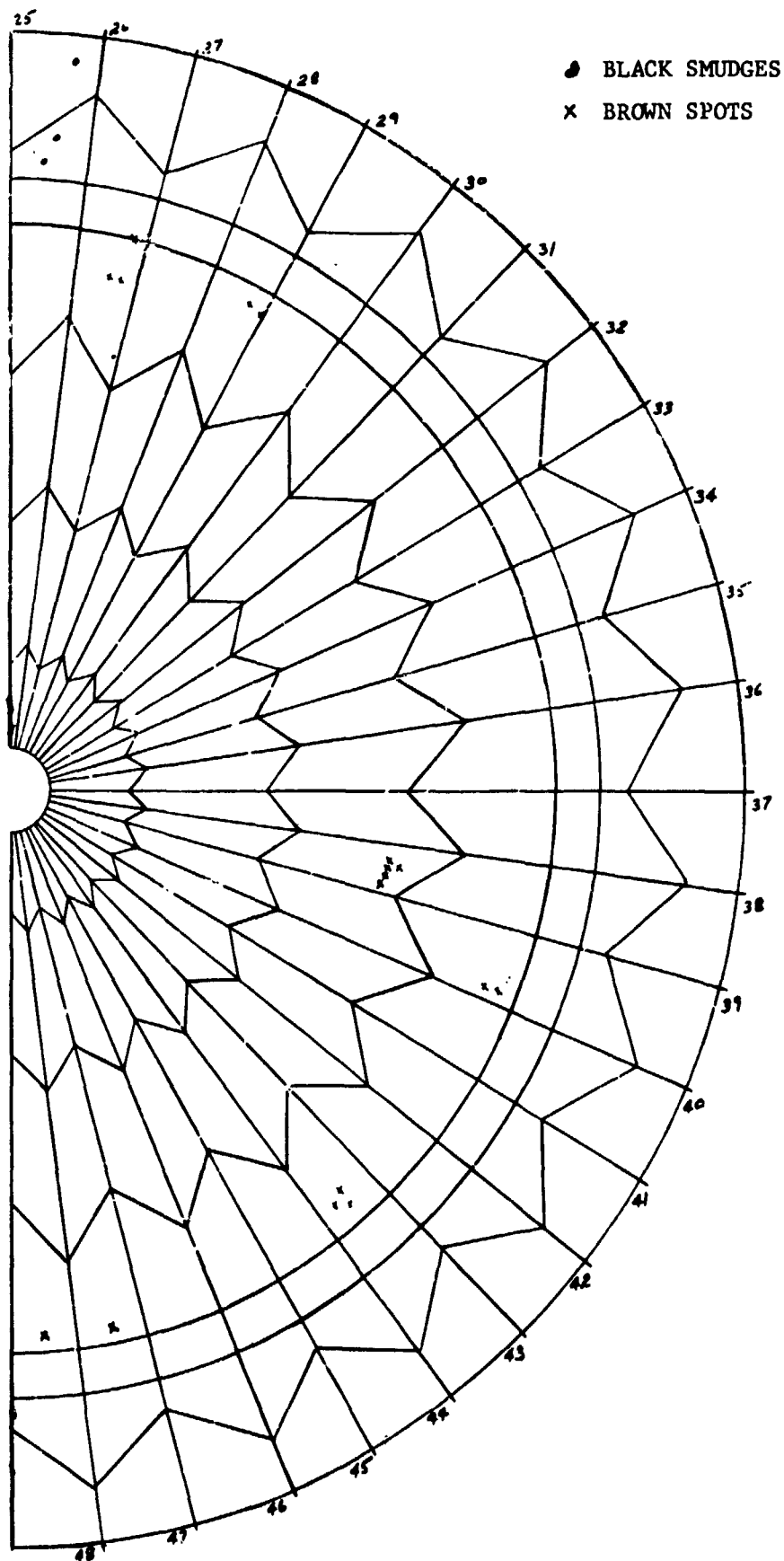


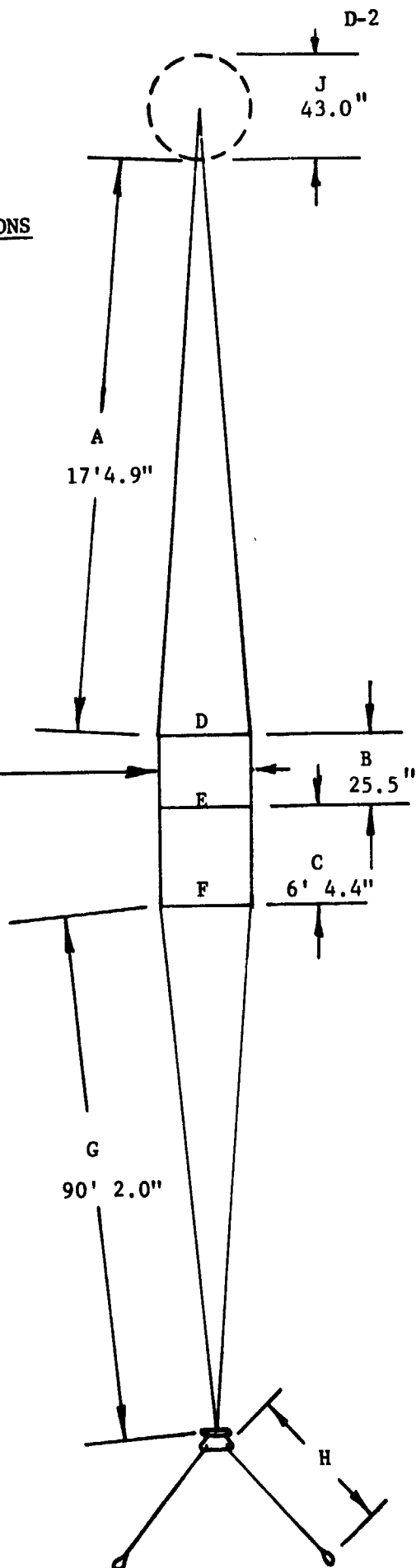
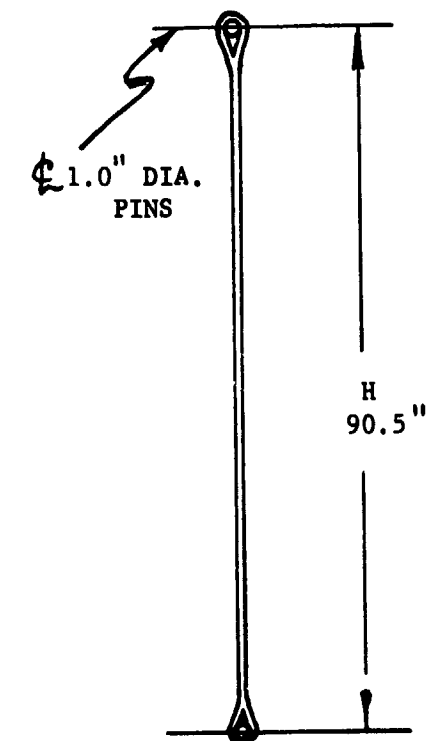
FIGURE C-1 (CONTINUED)

APPENDIX D  
PARACHUTE DIMENSIONAL SURVEY

# APPENDIX D

## PARACHUTE DIMENSIONS

30.3" D-DISK  
E-BAND  
F-BAND  
BETWEEN RADIAL SHOWN  
AND NEXT HIGHER NO.



## PRE-FLIGHT AV-3

<u>RADIAL NO.</u>	<u>A(DISC) FT-INCHES</u>	<u>B(GAP) INCHES</u>	<u>C(BAND) INCHES</u>	<u>D(DISK) INCHES</u>	<u>E(BAND) INCHES</u>	<u>F(BAND) INCHES</u>	<u>G(SUSP) FT-INCHES</u>
1	17 - $3\frac{1}{2}$	$25\frac{5}{16}$	$75\frac{1}{8}$	$30\frac{1}{2}$	$30\frac{1}{16}$	$30\frac{1}{4}$	90 - $2\frac{1}{2}$
2	$4\frac{1}{2}$	$\frac{1}{4}$	$\frac{1}{4}$	$\frac{1}{8}$	$\frac{1}{2}$	$\frac{1}{2}$	2
3	5	$\frac{5}{16}$	$\frac{3}{16}$	$\frac{1}{4}$	$\frac{7}{16}$	$\frac{1}{2}$	2
4	5	$\frac{1}{4}$	$\frac{5}{16}$	$\frac{3}{8}$	$\frac{7}{16}$	$\frac{5}{8}$	$1\frac{3}{4}$
5	$5\frac{1}{8}$	$\frac{1}{4}$	$\frac{1}{8}$	$\frac{1}{4}$	$\frac{1}{4}$	$\frac{1}{4}$	2
6	$4\frac{3}{4}$	$\frac{5}{16}$	$\frac{1}{4}$	$\frac{5}{16}$	$\frac{1}{2}$	$\frac{3}{8}$	$1\frac{1}{2}$
7	$4\frac{3}{4}$	$\frac{3}{16}$	0	$\frac{1}{4}$	$\frac{1}{4}$	$\frac{3}{8}$	$1\frac{1}{4}$
8	$4\frac{3}{8}$	$\frac{1}{4}$	$\frac{3}{8}$	$\frac{1}{4}$	$\frac{1}{2}$	$\frac{1}{2}$	$1\frac{1}{4}$
9	$4\frac{1}{4}$	$\frac{3}{16}$	$\frac{5}{16}$	$\frac{3}{8}$	$\frac{3}{8}$	$\frac{1}{2}$	2
10	$4\frac{1}{4}$	$\frac{3}{16}$	$\frac{1}{8}$	$\frac{1}{4}$	$\frac{1}{4}$	$\frac{3}{8}$	$1\frac{3}{4}$
11	4	$\frac{3}{16}$	0	$\frac{3}{8}$	$\frac{1}{4}$	$\frac{5}{16}$	$1\frac{1}{2}$
12	$3\frac{3}{4}$	$\frac{1}{4}$	$74\frac{13}{16}$	$\frac{1}{4}$	$\frac{1}{2}$	$\frac{5}{8}$	$1\frac{1}{4}$
13	$3\frac{3}{4}$	$\frac{1}{4}$	0	$\frac{1}{2}$	$\frac{1}{2}$	$\frac{1}{2}$	$1\frac{1}{4}$
14	$4\frac{1}{4}$	$\frac{3}{8}$	$\frac{3}{16}$	$\frac{3}{16}$	$\frac{1}{4}$	$\frac{3}{8}$	$1\frac{1}{4}$
15	$4\frac{3}{4}$	$\frac{5}{16}$	$\frac{5}{16}$	$\frac{3}{16}$	$\frac{7}{16}$	$\frac{1}{2}$	$1\frac{1}{2}$
16	$4\frac{3}{8}$	$\frac{1}{4}$	$\frac{3}{16}$	$\frac{1}{4}$	$\frac{3}{8}$	$\frac{1}{4}$	$1\frac{1}{4}$
17	$4\frac{1}{4}$	$\frac{1}{4}$	$\frac{3}{8}$	$\frac{1}{4}$	$\frac{3}{8}$	$\frac{7}{16}$	$1\frac{1}{4}$
18	4	$\frac{7}{16}$	$\frac{5}{16}$	$\frac{1}{4}$	$\frac{1}{2}$	$\frac{1}{4}$	$1\frac{3}{4}$
19	$4\frac{1}{2}$	$\frac{1}{4}$	$\frac{1}{4}$	$\frac{1}{2}$	$\frac{1}{2}$	$\frac{3}{4}$	$1\frac{1}{4}$
20	$4\frac{1}{2}$	$\frac{1}{4}$	$\frac{1}{8}$	$\frac{3}{16}$	$\frac{5}{16}$	$\frac{3}{8}$	$1\frac{1}{4}$
21	$4\frac{1}{4}$	$\frac{5}{16}$	$\frac{1}{4}$	$\frac{3}{16}$	$\frac{5}{16}$	$\frac{3}{4}$	$1\frac{1}{2}$
22	$4\frac{3}{8}$	$\frac{5}{16}$	$\frac{5}{16}$	$\frac{7}{16}$	$\frac{1}{2}$	$\frac{5}{16}$	$1\frac{1}{2}$
23	$4\frac{1}{2}$	$\frac{5}{16}$	$\frac{1}{4}$	$\frac{1}{16}$	$\frac{7}{16}$	$\frac{5}{16}$	$1\frac{1}{4}$
24	$4\frac{1}{2}$	$\frac{5}{16}$	$\frac{7}{16}$	$\frac{1}{4}$	$\frac{9}{16}$	$\frac{3}{4}$	$1\frac{1}{4}$

## PRE-FLIGHT AV-3 (CONTINUED)

<u>RADIAL NO.</u>	<u>A(DISC) FT-INCHES</u>	<u>B(GAP) INCHES</u>	<u>C(BAND) INCHES</u>	<u>D(DISK) INCHES</u>	<u>E(BAND) INCHES</u>	<u>F(BAND) INCHES</u>	<u>G(SUSP) FT-INCHES</u>
25	17 - $4\frac{3}{4}$	$25\frac{5}{16}$	$75\frac{3}{8}$	$30\frac{1}{4}$	$30\frac{1}{4}$	$30\frac{5}{8}$	90 - $1\frac{1}{4}$
26	$4\frac{1}{2}$	$5/16$	$1/4$	$1/8$	$3/4$	$3/16$	$1\frac{1}{4}$
27	4	$1/4$	$1/16$	$3/8$	$5/8$	$5/8$	$1\frac{3}{4}$
28	4	$5/16$	0	$3/16$	$5/8$	$1/2$	$1\frac{1}{4}$
29	$4\frac{1}{4}$	$1/4$	$1/16$	$7/16$	$1/2$	$1/2$	$1\frac{1}{4}$
30	$3\frac{7}{8}$	$5/16$	$3/8$	$3/16$	$1/2$	$1/2$	$1\frac{1}{2}$
31	$4\frac{1}{4}$	$3/8$	$5/8$	$3/16$	$1/2$	$1/2$	$1\frac{1}{4}$
32	$4\frac{1}{8}$	$5/16$	$7/16$	$3/16$	$7/16$	$1/2$	$1\frac{3}{4}$
33	4	$1/4$	$7/16$	$3/8$	$7/16$	$5/16$	$1\frac{1}{4}$
34	$3\frac{1}{2}$	$1/4$	$3/16$	$1/8$	$5/8$	$5/8$	$1\frac{3}{4}$
35	4	$5/16$	$5/16$	$3/16$	$1/2$	$9/16$	$1\frac{3}{4}$
36	$3\frac{3}{4}$	$5/16$	$3/16$	$1/16$	$1/2$	$5/8$	$1\frac{3}{4}$
37	$4\frac{3}{4}$	$1/4$	$1/4$	$5/8$	$1/4$	$3/8$	2
38	$4\frac{3}{4}$	$3/8$	$3/16$	$1/8$	$5/8$	$1/2$	$1\frac{1}{2}$
39	$4\frac{3}{4}$	$1/4$	$1/4$	$3/8$	$1/2$	$1/2$	$1\frac{1}{4}$
40	$4\frac{3}{8}$	$3/8$	$1/4$	$1/16$	$3/8$	$1/2$	$1\frac{1}{2}$
41	$4\frac{1}{8}$	$5/16$	$5/16$	$3/8$	$1/4$	$3/16$	$1\frac{3}{4}$
42	$4\frac{1}{4}$	$1/4$	$1/4$	$3/8$	$1/2$	$3/4$	$1\frac{1}{2}$
43	$4\frac{1}{2}$	$5/16$	$3/8$	$3/16$	$5/8$	$1/4$	$1\frac{1}{2}$
44	$4\frac{1}{4}$	$3/8$	$3/8$	$1/8$	$1/4$	$1/4$	$1\frac{1}{2}$
45	$4\frac{1}{2}$	$1/4$	$5/16$	$7/16$	$5/8$	$3/8$	$1\frac{1}{2}$
46	$4\frac{1}{2}$	$5/16$	$3/8$	$1/4$	$5/8$	$1/2$	$1\frac{1}{4}$
47	$4\frac{1}{2}$	$1/4$	$3/8$	$1/8$	$1/2$	$1/2$	$1\frac{1}{4}$
48	$4\frac{1}{2}$	$3/8$	$3/8$	$3/8$	$1/2$	$7/16$	$1\frac{1}{4}$

## PRE-FLIGHT AV-3 (CONTINUED)

BRIDLE LEG	H	-	INCHES	RADIAL	J	-	INCHES
S/N 52	90 <sup>3</sup> / <sub>16</sub>			1/25	42 <sup>1</sup> / <sub>2</sub>		
S/N 53	90 <sup>1</sup> / <sub>2</sub>			7/31	42 <sup>1</sup> / <sub>8</sub>		
S/N 54	90 <sup>3</sup> / <sub>16</sub>			13/37	42 <sup>3</sup> / <sub>8</sub>		
				19/43	42 <sup>1</sup> / <sub>4</sub>		

## POST-TEST AV-3

<u>RADIAL NO.</u>	<u>A(DISC) FT-INCHES</u>	<u>B(GAP) INCHES</u>	<u>C(BAND) INCHES</u>	<u>D(DISK) INCHES</u>	<u>E(BAND) INCHES</u>	<u>F(BAND) INCHES</u>	<u>G(SUSP) FT-INCHES</u>
1	17 - 5 <sup>1</sup> / <sub>4</sub>	25 <sup>3</sup> / <sub>8</sub>	75 <sup>1</sup> / <sub>2</sub>	30 <sup>1</sup> / <sub>2</sub>	30-0	30 <sup>3</sup> / <sub>16</sub>	88 - 4
2	6	1/ <sub>4</sub>	3/ <sub>4</sub>	1/ <sub>8</sub>	5/ <sub>8</sub>	7/ <sub>16</sub>	3
3	6 <sup>1</sup> / <sub>4</sub>	3/ <sub>8</sub>	3/ <sub>4</sub>	1/ <sub>8</sub>	3/ <sub>8</sub>	1/ <sub>2</sub>	4
4	5 <sup>3</sup> / <sub>4</sub>	3/ <sub>8</sub>	3/ <sub>4</sub>	3/ <sub>8</sub>	3/ <sub>8</sub>	5/ <sub>8</sub>	2 <sup>3</sup> / <sub>4</sub>
5	5 <sup>3</sup> / <sub>4</sub>	1/ <sub>4</sub>	5/ <sub>8</sub>	1/ <sub>4</sub>	1/ <sub>4</sub>	1/ <sub>4</sub>	3 <sup>1</sup> / <sub>2</sub>
6	5 <sup>3</sup> / <sub>4</sub>	5/ <sub>16</sub>	5/ <sub>8</sub>	1/ <sub>4</sub>	5/ <sub>8</sub>	3/ <sub>8</sub>	3
7	6	5/ <sub>16</sub>	5/ <sub>8</sub>	1/ <sub>8</sub>	1/ <sub>4</sub>	3/ <sub>8</sub>	1
8	5 <sup>3</sup> / <sub>4</sub>	3/ <sub>8</sub>	7/ <sub>8</sub>	3/ <sub>8</sub>	9/ <sub>16</sub>	1/ <sub>2</sub>	1 <sup>1</sup> / <sub>2</sub>
9	5 <sup>5</sup> / <sub>8</sub>	3/ <sub>8</sub>	7/ <sub>8</sub>	1/ <sub>2</sub>	5/ <sub>8</sub>	1/ <sub>2</sub>	3 <sup>1</sup> / <sub>4</sub>
10	5 <sup>1</sup> / <sub>4</sub>	3/ <sub>8</sub>	3/ <sub>4</sub>	1/ <sub>8</sub>	3/ <sub>8</sub>	3/ <sub>8</sub>	2 <sup>1</sup> / <sub>2</sub>
11	5 <sup>1</sup> / <sub>2</sub>	1/ <sub>4</sub>	3/ <sub>4</sub>	3/ <sub>8</sub>	3/ <sub>8</sub>	3/ <sub>8</sub>	1
12	5 <sup>1</sup> / <sub>2</sub>	1/ <sub>4</sub>	5/ <sub>8</sub>	1/ <sub>4</sub>	7/ <sub>16</sub>	3/ <sub>4</sub>	0 <sup>1</sup> / <sub>2</sub>
13	4 <sup>5</sup> / <sub>8</sub>	5/ <sub>16</sub>	1/ <sub>2</sub>	1/ <sub>8</sub>	7/ <sub>16</sub>	7/ <sub>16</sub>	0
14	5 <sup>1</sup> / <sub>4</sub>	3/ <sub>8</sub>	5/ <sub>8</sub>	1/ <sub>4</sub>	1/ <sub>4</sub>	5/ <sub>16</sub>	11 <sup>1</sup> / <sub>4</sub>
15	6	3/ <sub>8</sub>	3/ <sub>4</sub>	1/ <sub>4</sub>	9/ <sub>16</sub>	1/ <sub>2</sub>	11 <sup>1</sup> / <sub>2</sub>
16	5 <sup>1</sup> / <sub>2</sub>	3/ <sub>8</sub>	3/ <sub>4</sub>	3/ <sub>8</sub>	3/ <sub>8</sub>	5/ <sub>16</sub>	11
17	4 <sup>7</sup> / <sub>8</sub>	3/ <sub>8</sub>	3/ <sub>4</sub>	3/ <sub>8</sub>	1/ <sub>4</sub>	9/ <sub>16</sub>	11
18	4 <sup>1</sup> / <sub>2</sub>	1/ <sub>2</sub>	3/ <sub>4</sub>	1/ <sub>4</sub>	1/ <sub>2</sub>	1/ <sub>4</sub>	11 <sup>1</sup> / <sub>2</sub>
19	5 <sup>1</sup> / <sub>2</sub>	1/ <sub>4</sub>	3/ <sub>4</sub>	1/ <sub>2</sub>	5/ <sub>16</sub>	3/ <sub>4</sub>	11 <sup>1</sup> / <sub>2</sub>
20	5 <sup>1</sup> / <sub>4</sub>	1/ <sub>4</sub>	5/ <sub>8</sub>	5/ <sub>16</sub>	1/ <sub>4</sub>	3/ <sub>8</sub>	11
21	5 <sup>1</sup> / <sub>2</sub>	1/ <sub>4</sub>	7/ <sub>8</sub>	1/ <sub>4</sub>	1/ <sub>8</sub>	3/ <sub>4</sub>	11
22	5 <sup>1</sup> / <sub>2</sub>	7/ <sub>16</sub>	15/ <sub>16</sub>	1/ <sub>2</sub>	3/ <sub>8</sub>	1/ <sub>4</sub>	11 <sup>1</sup> / <sub>2</sub>
23	5 <sup>1</sup> / <sub>2</sub>	1/ <sub>2</sub>	3/ <sub>4</sub>	1/ <sub>8</sub>	5/ <sub>16</sub>	1/ <sub>4</sub>	6
24	5	1/ <sub>2</sub>	7/ <sub>8</sub>	3/ <sub>8</sub>	5/ <sub>8</sub>	3/ <sub>4</sub>	6

## POST-TEST AV-3 (CONTINUED)

<u>RADIAL NO.</u>	<u>A(DISC) FT-INCHES</u>	<u>B(GAP) INCHES</u>	<u>C(BAND) INCHES</u>	<u>D(DISK) INCHES</u>	<u>E(BAND) INCHES</u>	<u>F(BAND) INCHES</u>	<u>G(SUSP) FT-INCHES</u>
25	17 - 5	25 <sup>1</sup> / <sub>2</sub>	75 <sup>5</sup> / <sub>8</sub>	30 <sup>3</sup> / <sub>8</sub>	30 <sup>1</sup> / <sub>4</sub>	30 <sup>9</sup> / <sub>16</sub>	88 - 6 <sup>1</sup> / <sub>2</sub>
26	5 <sup>1</sup> / <sub>4</sub>	7/16	1/2	1/4	7/8	0	6 <sup>1</sup> / <sub>2</sub>
27	4 <sup>3</sup> / <sub>4</sub>	5/16	1/2	3/8	3/8	3/4	7
28	4 <sup>7</sup> / <sub>8</sub>	3/8	3/8	1/4	1/2	1/2	6 <sup>1</sup> / <sub>2</sub>
29	5 <sup>1</sup> / <sub>8</sub>	3/8	1/4	1/2	3/8	1/2	6 <sup>1</sup> / <sub>2</sub>
30	5	3/8	5/8	1/4	3/8	1/2	8
31	4 <sup>3</sup> / <sub>4</sub>	1/2	3/4	1/4	1/2	1/2	6 <sup>1</sup> / <sub>2</sub>
32	4 <sup>3</sup> / <sub>4</sub>	3/8	3/4	1/4	5/16	3/8	6 <sup>1</sup> / <sub>4</sub>
33	4 <sup>3</sup> / <sub>4</sub>	1/4	3/4	1/2	3/8	1/4	6 <sup>1</sup> / <sub>2</sub>
34	4 <sup>1</sup> / <sub>4</sub>	1/4	1/2	1/4	1/2	1/2	6 <sup>3</sup> / <sub>4</sub>
35	5 <sup>1</sup> / <sub>4</sub>	1/4	3/4	1/4	1/2	1/2	7
36	5 <sup>1</sup> / <sub>2</sub>	3/8	76-0	1/8	3/8	5/8	6 <sup>1</sup> / <sub>2</sub>
37	5 <sup>1</sup> / <sub>2</sub>	3/8	75 <sup>1</sup> / <sub>2</sub>	3/4	1/4	3/8	9
38	5 <sup>1</sup> / <sub>2</sub>	3/8	1/2	3/16	5/8	3/8	8 <sup>1</sup> / <sub>4</sub>
39	5 <sup>3</sup> / <sub>4</sub>	3/8	3/4	7/16	5/16	9/16	9
40	5	3/8	1/2	1/8	3/8	7/16	8 <sup>1</sup> / <sub>2</sub>
41	5 <sup>1</sup> / <sub>4</sub>	1/2	5/8	3/8	1/4	3/8	9 <sup>1</sup> / <sub>4</sub>
42	5	1/4	76-0	3/8	9/16	7/8	9
43	5 <sup>1</sup> / <sub>2</sub>	3/8	75 <sup>7</sup> / <sub>8</sub>	1/4	5/8	3/16	8 <sup>1</sup> / <sub>4</sub>
44	5	3/8	3/4	1/8	1/4	5/16	8 <sup>1</sup> / <sub>2</sub>
45	5	1/4	3/4	3/8	5/8	3/8	8 <sup>1</sup> / <sub>4</sub>
46	5 <sup>1</sup> / <sub>2</sub>	1/4	76-0	1/4	5/8	9/16	8
47	5 <sup>3</sup> / <sub>4</sub>	1/2	75 <sup>3</sup> / <sub>4</sub>	1/16	1/2	1/2	7 <sup>1</sup> / <sub>2</sub>
48	5 <sup>3</sup> / <sub>4</sub>	1/2	76-0	1/4	1/2	7/16	7 <sup>1</sup> / <sub>2</sub>



## POST-TEST AV-3 (CONTINUED)

BRIDGE	LEG	H	-	INCHES	RADIAL	J	-	INCHES
S/N	52	90	<sup>7</sup> / <sub>8</sub>		1/25	42	<sup>1</sup> / <sub>2</sub>	
S/N	53	91	<sup>1</sup> / <sub>8</sub>		7/31	42	<sup>1</sup> / <sub>2</sub>	
S/N	54	90	<sup>7</sup> / <sub>8</sub>		13/37	42	<sup>5</sup> / <sub>8</sub>	
					19/43	42	<sup>1</sup> / <sub>2</sub>	

APPENDIX E

BLDT COMPUTER SOFTWARE

## I. PURPOSE

The control of the Balloon Launch Decelerator Test Flights at WSMR was aided through computer predictions and operations. It was the responsibility of WSMR (RTDS) personnel to develop computer software necessary to fulfill operational requirements imposed by MMC and constraints imposed by Range Safety. The purpose of this appendix is to discuss the real time computer software needed at WSMR for the BLDT mission and, in particular, describe the software furnished by MMC. The major software functions were to:

- Predict impact of flight/payload components
- Issue a precision, real time decelerator mortar fire command
- Generate real time flight information

In support of the above requirements, the following computer programs were developed by MMC for WSMR implementation:

- Vehicle Flight Azimuth Program
- Vehicle Impact Prediction Program
- Decelerator Mortar Fire Command Program

## II. VEHICLE FLIGHT AZIMUTH PROGRAM

The vehicle azimuth was not controlled during the subsonic drop test. The vehicle flight azimuth program, which was developed for the powered flight, was not operational on this flight.

### III. IMPACT PREDICTION PROGRAM

#### A. Program Requirement

As previously discussed in IIA, it is a requirement to provide impact information to Range Safety in order to select a drop point and corresponding flight azimuth. Additionally, the impact data are used to select the best impact area to expedite recovery of the spent hardware and to direct the recovery crew to the predicted impact area.

The program is required to operate in two modes as follows:

1. A static mode in which drop parameters are selected and impact analysis are performed using range intersect predictions.
2. A dynamic mode in which real time drop parameters are used and real time impact predictions are derived.

The mode of operation is manually selected and requires only a change in the source of input data.

#### B. Program Implementation

The Impact Prediction Program is based upon a nominal trajectory (perturbed by current wind conditions), latitude and longitude of drop and vehicle heading at drop.

The software reflects two modes of flight; accelerated flight (powered flight and decelerator transients); and equilibrium descent, where the aerodynamic drag is nearly equal to the system weight and the rate of descent is a direct function of the atmospheric density. The point of impact is obtained by first computing the wind effect to the nominal, zero wind, accelerated flight trajectory and then adding the wind drift effect of the equilibrium descent.

### 1. Accelerated Flight Mode

The vehicle position, at the completion of accelerated flight, is computed by adding wind corrections to a nominal zero wind trajectory which is represented by a nominal range (R) for each vehicle configuration and a nominal azimuth shift ( $\Delta A_Z$ ) which occurs because of vehicle spin. The time equivalents of the nominal trajectory and wind velocities are tabulated as functions of altitude at intervals of 5000 feet. The position corrections due to wind are computed by multiplying the wind velocity ( $W_1$ ) by the time ( $t_1$ ) required to transverse each of the 5000 foot intervals of altitude.

The position ( $X_a, Y_a$ ) at the completion of accelerated flight is given by the equations:

$$(4) \quad X_a = X_D + R \sin (A_Z + \Delta A_Z) + \sum_{i=1}^N t_i (W_{x_i})$$

$$(5) \quad Y_a = Y_D + R \cos (A_Z + \Delta A_Z) + \sum_{i=1}^N t_i (W_{y_i})$$

where:  $A_Z$  is the drop heading  
 $X_D, Y_D$  is the range drop position.

The position location ( $X_a, Y_a$ ) is the starting location for the equilibrium descent portion of the computation which follows.

### 2. Equilibrium Descent

During equilibrium descent, the vehicle weight counterbalances aerodynamic drag as shown in the relationship:

$$(6) \text{ Weight} = \text{Drag}$$

$$\begin{aligned} wt &= q C_D A \\ &= 1/2 \rho \left( \frac{dh}{dt} \right)^2 \end{aligned}$$

where:  $q$  is dynamic pressure

$C_D$  is aerodynamic drag coefficient

$\rho$  is atmospheric density

$\frac{dh}{dt}$  is rate of descent

It is noted that the atmospheric density ( $\rho$ ) is considered constant over each altitude interval.

Rearranging equation (6), the time spent during any altitude interval can be computed as:

$$(7) \Delta t_i = \left( \frac{\rho C_D A}{2 wt} \right)^{1/2} \cdot 5000$$

The summation of the displacements obtained by multiplying the  $\Delta t$  by the corresponding wind velocity for each 5000 feet altitude interval gives the increment of vehicle displacement ( $X_b, Y_b$ ) for the equilibrium descent portion of the impact prediction. This summation is represented by:

$$(8) X_b = \sum_{i=1}^N \Delta t_i (W_{x_i})$$

$$(9) Y_b = \sum_{i=1}^N \Delta t_i (W_{y_i})$$

The displacements given by equations (8) and (9) are added to the position computed by the accelerated flight operations to obtain the impact position ( $X_p, Y_p$ ). The equations for this operation are:

$$(10) X_p = X_a + X_b$$

$$(11) Y_p = Y_a + Y_b$$

The impact prediction is computed separately for each of the possible flight conditions which are:

- o Powered flight followed by payload decelerated descent to impact.
- o Powered flight followed by aeroshell descent to impact.
- o Powered flight without decelerator deployment (abort mode).

The impact prediction program drove an XY plotted which displayed impact locations of the above flight articles superimposed on a map of the White Sands Missile Range. During the dynamic mode of operation, where the heading angle was fed directly to the impact prediction program from the azimuth program, the impact prediction was displayed continuously for the abort mode which was the most critical case due to its extended trajectory. This continuous impact display provided assurance to Range Safety that the overall azimuth control operation was adequate and stable and since the display was for the worst case (abort), Range Safety was assured that all flight articles would impact within an acceptable area.



#### IV. DECELERATOR MORTAR FIRE PROGRAM

##### A. Program Requirement

The Airborne Command receiver was used to allow the ground computer to fire the decelerator mortar at the proper flight conditions. The dual vehicle programmers were set to open a time window for this signal to prevent inadvertent mortar fire and also to backup the ground command in the event this command link failed.

##### B. Program Implementation

The drop command was used to start a count-down clock in the computer which transmitted the mortar fire command when it timed out. No provisions were included to change this time due to the predictable nature of the gravitation acceleration of the vehicle.